SYNTHESIS AND CHARACTERIZATION OF DENDRIMER-BASED
NITRIC OXIDE DELIVERY SYSTEMS

by
Nathan Allan Stasko

A dissertation submitted to the faculty of the University of North Carolina at Chapel Hill in partial fulfillment of the requirements for the degree of Doctor of Philosophy in the Department of Chemistry.

Chapel Hill
2007

Approved by

Professor Mark H. Schoenfisch

Professor Maurice S. Brookhart

Professor Jeffery S. Johnson

Professor Malcolm D.E. Forbes

Professor Linda L. Spremulli

ABSTRACT

NATHAN ALLAN STASKO: Synthesis and Characterization of Dendrimer-Based
Nitric Oxide Delivery Vehicles
(Under the direction of Mark H. Schoenfisch)

Nitric oxide (NO) has garnered much attention as a therapeutic due to its multifaceted role in human physiology. However, NO is a highly reactive radical, making its chemical storage and controlled release extremely challenging. Although several small molecule NO donors have been reported in the literature, the limited NO storage and the inability to target NO to a specific site of action have seriously hindered the clinical utility of NO donors. To address these limitations, my research has focused on the synthesis of macromolecular NO-releasing dendrimers that store large quantities of NO (1–5 µmol NO/mg). Herein, the synthesis and characterization of two systems are presented employing the two most common small molecule NO donors: *N*-bound diazeniumdiolates and *S*-nitrosothiols. Decomposition of the diazeniumdiolate NO donor was proton initiated under aqueous conditions with the NO release being highly influenced by the local dendritic environment. *S*-nitrosothiol dendrimer conjugates were subject to decomposition by various triggers of NO release (e.g., copper and light) and also shown to directly transfer NO to proteins via transnitrosation. The systems described in this thesis represent two of the highest NO-releasing nanoparticle NO donors reported to date. Additionally, studies investigating the cytotoxicity of multifunctional dendrimer conjugates and the physiological activity of dendrimer derived nitric oxide are presented.

To my parents,

Who made all of this possible through their encouragement to keep it simple while never forgetting to look behind the white line.

"The competitive fire burns inside us all,

some more brightly than others."

- NAS, 1998

ACKNOWLEDGEMENTS

I am extremely grateful for all of the support that I have received throughout my entire educational experience in chemistry. None of my accomplishments would have been possible without the love and prayers of my family, who constantly pushed me until I learned how to never quit pushing myself. I always had a passion for chemistry which was fostered early on by Dr. Clemente and then nurtured by Dr. Sipe and all of my professors at Hampden-Sydney College. I also want to thank my committee members at the University of North Carolina-Chapel Hill for their individual contributions to my doctoral education and for giving me the opportunity to receive a doctorate in this wonderful field of science.

There were many contributors along the way that deserve special thanks. Thank you Dr. Schoenfisch for allowing me to run with my visions and for providing a research environment that fosters excellence. I would also like to extend a special thank you to all of my fellow lab members who either directly contributed to my research or provided support when morale was low. Especially Evan, Jae, and Carri, without you guys it would not have been possible. Also thanks to the undergraduates that I had the privilege of working with Bryce, Dan, and Julia. The entire lab provided the "team-like" feel that I personally needed to keep my feet moving. I was just one contributor on an excellent team of scientists that is pushing the frontier of biomaterials and nano-drug delivery research. We all have bright futures and for those still earning their degrees or as I like to say "FOR THOSE ABOUT TO ROCK," I salute you.

TABLE OF CONTENTS

LIST OF TABLES

LIST OF SCHEMES

LIST OF FIGURES

LIST OF ABBREVIATIONS AND SYMBOLS

^{o}C	degree(s) Celsius
%	percentage(s)
±	statistical margin of error or tolerance
[...]	concentration
·	radical
ε	extinction coefficient
μL	microliter(s)
μm	micrometer(s)
μmol	micromole(s)
Ac	acetamide group
AEAP3	*N*-(2-aminoethyl)-3-aminopropyltrimethoxysilane
AHAP3	*N*-(6-aminohexyl)aminopropyltrimethoxysilane
Al	aluminum
aq	aqueous
Ar	argon gas
atm	atmosphere(s)
BSA	bovine serum albumin
Ca^{2+}	calcium ion
cfu	colony forming unit(s)
CH_3	methyl
Cl^-	chloride ion

cm	centimeter(s)
cm^2	square centimeter(s)
CO_2	carbon dioxide gas
Cu	copper
Cu^{2+}	copper ion
CuZnSOD	copper-zinc superoxide dismutase
d	day(s)
DAB	diaminobutane core
DDE	2-acetyldimedone
DMF	dimethylformamide
DMR	dendrimer
DMSO	dimethylsulfoxide
DTPA	diethylenetriamine-pentaacetic acid
EDTA	ethylenediamine-tetraacetic acid
e.g.	for example
et al.	and others
etc.	and so forth
EtOH	ethanol
Fe	iron
FITC	fluorescein isothiocyanate
fmol	femtomole(s)
g	gram(s)
G4	generation 4

GSH	glutathione
GSNO	S-nitrosoglutathione
h	hour(s)
H^+	hydrogen ion
H_2O	water
H_2O_2	hydrogen peroxide
HCl	hydrochloric acid
HNO	nitroxyl
HUVEC	human umbilical vein endothelial cells
i.e.	that is
IPA/NO	sodium-1-(isopropylamino)diazene-1-ium-1,2-diolate
k	kinetic coefficient
K	kelvin
K^+	potassium ion
KCl	potassium chloride
KRH	Krebs-Ringer-Hepes buffer
L	liter(s)
M	molar concentration
MeOH	methanol
mg	milligram(s)
min	minute(s)
mL	milliliter(s)
mM	millimolar concentration

mm	millimeter(s)
mmol	millimole(s)
mol	mole(s)
N	number of samples
N-	nitrogen bound
N-diazeniumdiolate	1-amino-substituted diazen-1-ium-1,2-diolate
N_2	nitrogen gas
N_2O_3	dinitrogen trioxide
Na^+	sodium ion
NaCl	sodium chloride
NHAc	N-acetyl group
nm	nanometer(s)
nM	nanomolar concentration
NMR	nuclear magnetic resonance
N_2O	nitrous oxide
NO	nitric oxide
NO^-	nitroxyl anion
NONOate	*N*-diazeniumdiolate moiety
NO_2	nitrogen dioxide
NO_2^-	nitrite
NO_3^-	nitrate
O_2	oxygen gas
O_3	ozone

OEt	ethoxy group
OH$^-$	hydroxide ion
OMe	methoxy group
ONOO$^-$	peroxynitrite
PAMAM	polyamidoamine dendrimer
PBS	phosphate-buffered saline
PDMS	poly(dimethylsiloxane)
PEG	poly(ethylene glycol)
pH	-log of proton concentration
PI	propidium iodide
pmol	picomole(s)
ppb	part(s) per billion
ppm	part(s) per million
PRP	platelet enriched plasma
PVC	poly(vinyl chloride)
R, R', R$_1$, R$_2$	organic functional group
RSNO	*S*-nitrosothiol
S-	sulfur bound
s, sec	second(s)
SEC	size exclusion chromatography
Si	silicon
SNAC	*S*-nitroso-*N*-acetyl-L-cysteine
SNAP	*S*-nitroso-*N*-acetyl-D,L-penicillamine

t	time
TEOS	tetraethyl orthosilicate
THF	tetrahydrofuran
Ti	titanium
TMRM	tetramethylrhodamine
TMOS	tetramethyl orthosilicate
Trt	trityl protecting group
TSB	tryptic soy broth
UV	ultraviolet
V	volts
v:v	volume/volume
Vis	visible
vs.	versus
W	watt(s)
Zr	zirconium

Chapter 1

Macromolecular Nitric Oxide Delivery Systems

1.1 Introduction

Nitric oxide (NO), a simple diatomic free radical synthesized by the human body, has vast potential as a therapeutic agent in medicine. Since Ignarro, Furchogtt, and Murad's Nobel Prize winning discovery that NO is the vascular endothelial derived relaxation factor (VEDRF), an extensive number of physiological pathways that utilize NO and/or are regulated by NO have been discovered.[1-5] The list of bioregulatory processes includes vasodilation,[4, 6] angiogenesis,[7, 8] neurotransmission,[9, 10] macrophage destruction of foreign pathogens,[11] gastrointestinal motility,[12] and muscle contractility.[13, 14] Endogenously, NO is produced by the enzyme nitric oxide synthase (NOS) which catalyzes the conversion of bioavailable L-arginine to L-citrulline and NO.[15, 16] Three forms of NOS exist, including the two constitutive endothelial (eNOS) and neuronal (nNOS) enzymes, and the inducible (iNOS) enzyme which responds to physiological stimuli and produces NO according to demand. [17, 18]

Due to its integral role in human physiology, deficiencies in NO biosynthesis or the overproduction of NO have been linked to a number of disease states ranging from Parkinson's disease to cancer.[19-22] Thus, the pharmacological regulation of NO synthesis has become a major target of drug discovery. Significant strides have been made toward developing lead compounds that modulate NOS activity as therapies to mediate disease

progression.[23, 24] In some cases, utilizing the cellular machinery for NO production is insufficient, and higher, more prolonged doses of NO are required. In response, small-molecule NO donors have been synthesized. These compounds effectively store and release NO according to donor specific stimuli. *N*-bound diazeniumdiolates, *S*-nitrosothiols, organic nitrates, hydroxylamine, and transition metal complexes are representative classes of the NO donors recently reviewed (Figure 1.1).[5, 25, 26] These synthetic NO-releasing compounds have been used to unravel some of the mysteries of NO in physiology and proposed as potential therapeutics for disease states requiring NO therapy. Numerous reports have detailed the therapeutic efficacy of NO donors, including their toxicity toward cancerous cells,[27, 28] broad spectrum antimicrobial activity,[29-32] cardioprotective effects during ischemia/reperfusion injury,[33-35] and use as anti-thrombotic agents.[36-41]

Despite the promising therapeutic potential of "small-molecule NO donors," the inability to carefully modulate NO-release at a specific site of action and the rapid systemic clearance associated with small drug molecules have seriously hindered the clinical development of NO-releasing therapeutics. In response, macromolecular NO storage and delivery systems have been devised to obtain highly tunable NO-release scaffolds and expand the areas for NO treatment. These macromolecules focus on the "delivery" of NO to sites of need and aim to eliminate the problems associated with poor biodistribution, limited solubility, lack of tissue specific targeting, and undesirable small-molecule NO donor toxicity. In this Introduction chapter, I will set the stage for my research by reviewing the field of NO-releasing macromolecules. Specifically, two classes of NO donor chemistry will be reviewed: *N*-diazeniumdiolate and *S*-nitrosothiol conjugates. The syntheses of the macromolecular NO donors is discussed as it pertains to storing NO. Obvious challenges arise when preparing NO donor conjugates with macromolecular properties due to environmentally sensitive NO

donor structures. For example, the NO-release properties of the macromolecular NO donors may exhibit different behaviors than the analogous small molecule NO donors. A number of macromolecular scaffolds have been employed to date including proteins, polymeric matrices, and inorganic nanoparticles all of that have led to the evolution of next-generation NO-releasing devices.

1.2 *N*-Diazeniumdiolate Modified Macromolecules

1.2.1 Diazeniumdiolate formation and nitric oxide release characteristics

Diazeniumdiolate NO donors, first reported by Drago and Paulik in the 1960's, are formed via the reaction of amines with high pressures (5 atm) of NO.[42, 43] As shown in Scheme 1.1, a nucleophilic amine substrate attacks the uncharacteristically electrophilic nitrogen atom of NO and the resulting radical species reacts rapidly with an additional NO to form a zwitterionic intermediate. Efficient diazeniumdiolate formation requires the presence of a second basic residue, either an unreacted amine substrate or in recent synthetic procedures an added alkoxide base to deprotonate the backbone amine forming the stable *N*-diazeniumdiolate structure. Secondary amine substrates are preferred due to the enhanced electron density at the backbone nitrogen. Nevertheless, primary amine adducts have also been reported (e.g., isopropylamine diazeniumdiolate, IPA/NO).[44] The cation stabilized products are particularly attractive as NO donors because they dissociate spontaneously under physiological conditions (i.e., 37°C, pH 7.4) to yield two moles of NO per mole of NO donor.[25] The proton initiated decomposition has been demonstrated to exhibit first-order exponential decay for small molecule alkyl secondary amine diazeniumdiolates with rates governed by the pH of the solution.[45] Keefer and coworkers have reported the synthesis and characterization of a multitude of small molecule diazeniumdiolates whereby NO release rates are governed by the chemical structure of the amine precursor.[25, 45, 46] For example,

diazeniumdiolate derivatives of polyamines like diethylenetriamine, DETA/NO, exhibit lengthy durations of NO release with a half-life ($t_{1/2}$) approaching 60 h. In contrast, the diazeniumdiolate adduct of the amino acid proline, PROLI/NO, has a $t_{1/2}$ of only 5 s.[46]

The formation of carcinogenic nitrosamines on the amine backbone following NO release[47] has hindered the development of diazeniumdiolate NO donors as successful drug formulations. In addition to backbone toxicity, the lack of specificity of NO release has warranted the creation of macromolecular NO donors that covalently immobilize diazeniumdiolates to release NO more locally (at the site of action).

1.2.2 Polymeric diazeniumdiolate delivery vehicles

Following the discovery that NO was involved in blood pressure regulation and vasodilation, the concept of macromolecules capable of NO release was born via incorporating small molecule NO donors into polymeric matrices. Medical devices coated such anti-thrombotic polymers were hypothesized to improve a device's thromboresistivity by reducing platelet adhesion while maintaining device function.[48-50] Keefer and co-workers have reviewed the three possible methods for incorporating *N*-diazeniumdiolate NO donors into polymers.[51] The NO donor may be doped into the polymer matrix, covalently bound to the polymer sidechains, or integrated into the polymer backbone. Each methodology has made significant advancements in the field of NO-releasing macromolecules. Leaching of the small molecule diazeniumdiolates from polymer coatings warranted the covalent immobilization of the potentially toxic byproducts leading to the synthesis of diazeniumdiolate-modified polyethylenimine,[52] polyurethane,[53, 54] polymethylmethacrylate,[55] silicone rubber,[49] and xero-gel[56] polymers as scaffolds for NO release. The capacity for NO storage, duration of NO release, and biomedical applications of these polymeric macromolecules been reviewed previously.[50]

4

Organic Nitrates   S-nitrosothiols   Metal Complexes

N-bound Diazeniumdiolates

(DETA/NO)   (PROLI/NO)   (MAHMA/NO)
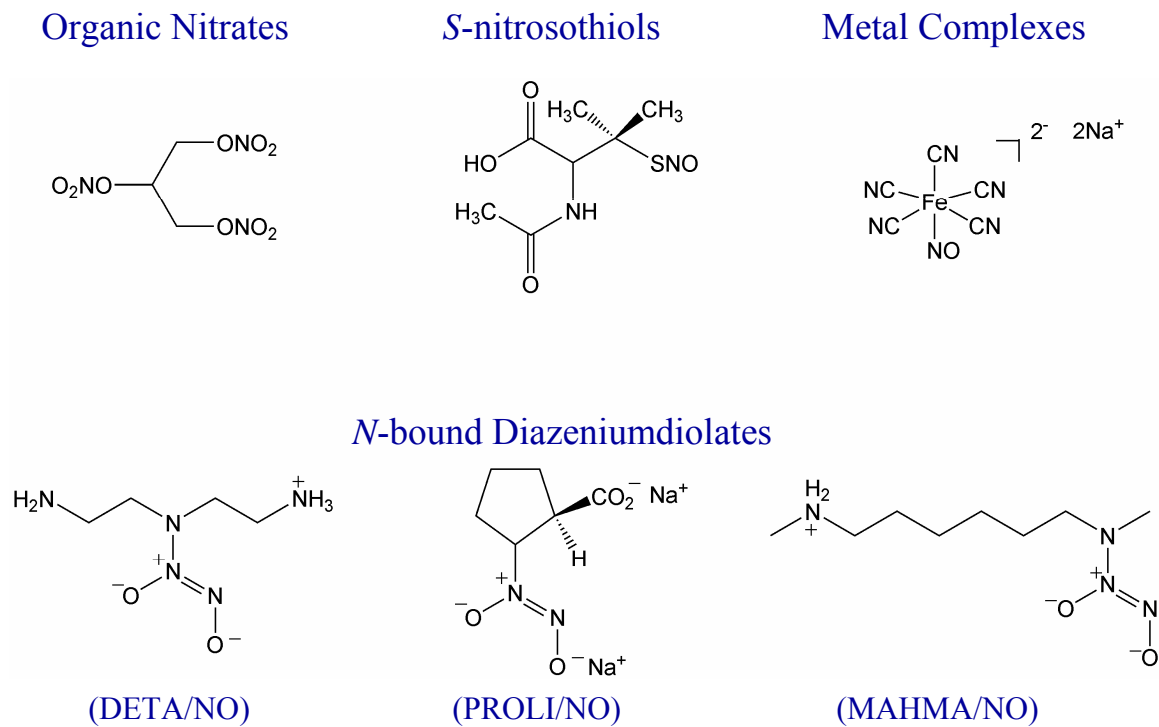
Figure 1.1   Small-molecule NO donors utilized for discovering the role of NO in biology and as therapeutic agents.
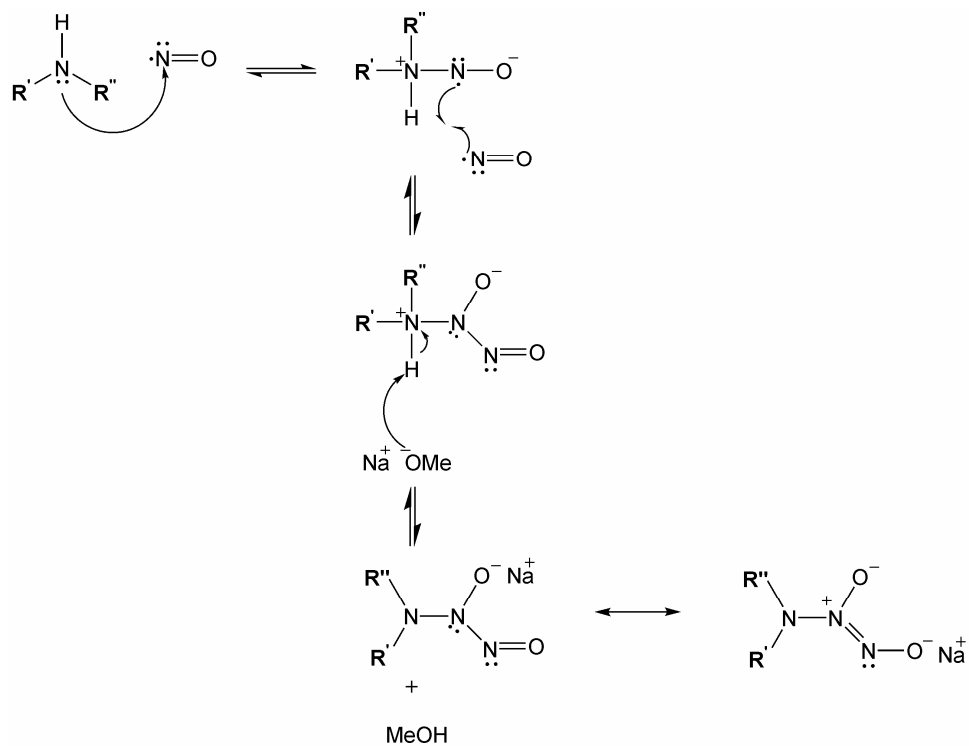
Scheme 1.1   Formation of *N*-bound diazeniumdiolate in the presence of NaOMe.

Although the majority of the NO-releasing polymers synthesized in the literature have been utilized as device coatings, several polymer conjugates have been employed as delivery vehicles to release NO in other biomedical areas of unmet need. For example, Pulfer et al. incorporated diazeniumdiolated polyethyleneimine microspheres (PEIX/NO) into vascular grafts as micron-sized NO storage reservoirs.[52] The polyethylenimine microspheres were formed using a water-in-oil emulsion and chemically crosslinked via a bis-epoxide. Conversion of interior amines to diazeniumdiolates resulted in particles with long NO-release half-lives due to the basicity of the local NO donor environment ($t_{1/2}$ = 66 h). The polydisperse particles (d = 10 – 50 μm) were doped into the pores of Gore-tex vascular grafts with a yield of 10 nmol NO/mg graft material. The PEI was also modified with fluorescein isothiocyanate (FITC) to allow particle leaching studies from the Gore-tex grafts. Of note, leaching was not observed following NO release and the PEIX/NO microspheres proved effective at preventing thrombosis in small diameter prosthetic grafts. This work represents the genesis of NO-releasing particle therapeutics. Zhou et al. employed a similar strategy with amine-modified water-soluble polyethylenimine conjugates to improve the NO-storage capacity (up to 4.15 μmol NO/mg) while maintaining the large macromolecular size for use in hemodialysis experiments.[57] The PEI derivatives remained in the dialysate solution while the NO evolved was able to diffuse across the membrane reducing platelet adhesion and the risk of thrombosis in the dialysis unit.

The concept of micron-sized diazeniumdiolate delivery vehicles was expanded by Jeh et al. who reported the encapsulation of PROLI/NO in biodegradable microparticles.[58] As described previously, PROLI/NO decomposes rapidly under aqueous conditions. Proline is a particularly attractive NO donor precursor due to the biocompatibility of the amino acid metabolite following NO release. Indeed, the nitrosamine adduct of proline had negligible

toxicity.[47] Delivery of NO to the alveolar region of the lungs requires both biocompatibility of the NO donor and biodegradability of the delivery vehicle. Encapsulation of PROLI/NO via polyethylene oxide-co-lactic acid (PELA) by double emulsion and solvent evaporation, followed by freeze-drying, led to PELA/NO microparticles capable of releasing 123 nmol NO/mg ($t_{1/2}$ = 4.1 min), extending the duration of NO release from PROLI/NO into time scales applicable for inhalation therapy. Of note, poly-lactic-co-glycolic acid (PLGA) required the addition of gelatin to the emulsion conditions resulting in PLGA/NO particles too large for inhalation therapy (d = 23.5 um). Although PELA/NO and PLGA/NO delivery vehicles possessed the necessary biodegradability, both were characterized by limited PROLI/NO encapsulation efficiency (~50%).

1.2.3 Proteins

Since diazeniumdiolate complexes decompose spontaneously at physiological pH, their administration in vivo present undesirable side effects at NO-sensitive sites throughout the body. Major challenges exist in both targeting NO to a specific site so that it will affect only that target, and in attaching diazeniumdiolates to delivery vehicles that will increase their retention in blood (i.e., biodistribution). By taking advantage of the reactivity of the diazeniumdiolate functionality, several strategies for preparing tissue-selective drugs have been proposed. For example, the terminal oxygen (O^2) of the diazeniumdiolates have been protected with environmentally labile protecting groups and are thus referred to as being O^2-protected.[59] This "prodrug" approach allows the diazeniumdiolate to move freely throughout the circulatory system without spontaneous dissociation until reaching a "site" of interest. Vinylated-diazeniumdiolates store NO until passing through the liver where epoxidation and hydrolysis of the diazeniumdiolate to NO occurs via catalysis by cytochrome P450 enzymes.[60] Further studies on O^2-protected diazeniumdiolates have resulted in esterase-

sensitive NO donors that exhibit in vitro antileukemic activity and peptide diazeniumdiolates that are specifically metabolized by prostate specific antigen and may prove useful for the selective treatment of prostate cancer.[61] Unfortunately, the small molecule diazeniumdiolates used in these studies have no barrier to renal clearance when administered systemically and produce potentially carcinogenic byproducts that have circumvented their clinical application.

Hrabie et al. utilized the pro-drug approach to attach a methoxy methylether (MOM)-protected piperazine diazeniumdiolate to bovine serum albumin (BSA) (Figure 1.2).[62, 63] Representing the first diazeniumdiolate derivatized protein, the PIPERAZI/NO-BSA conjugate possessed an extremely long half life of NO-release (56 h) due to the stability of the MOM protecting group that hydrolyzes slowly even under acidic conditions. The derivatization of BSA provides proof-of-concept for "pre-packaging" diazeniumdiolate NO donors and attaching them to biologically relevant drug delivery vehicles. Recent improvements in O^2-protection chemistries may be utilized in combination with the emerging techniques in nanotechnology to result in highly specialized NO-releasing medicines via diazeniumdiolate chemistry.[47, 64]

Bovine Serum Albumin

Lysine   Linker   MOM-PIPERAZI/NO
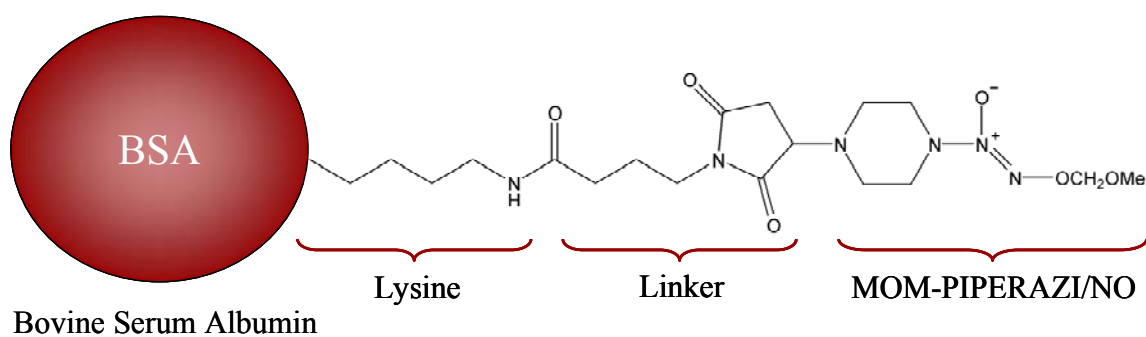
Figure 1.2   Diazeniumdiolate-modified bovine serum albumin (BSA) prepared from an O^2-methoxymethyl-protected diazeniumdiolated piperazine.

1.2.4 Nanoparticle-derived diazeniumdiolate NO-donors

Based on their unique size-dependent physical and chemical properties, nanoparticles have the potential to revolutionize the field of medicine.[65-69] Indeed, nanoscale materials have been under development for a number of biological and medical applications including drug and gene delivery,[70, 71] fluorescent biological labels,[26, 72, 73] pathogen and protein detectors,[74, 75] DNA structure probes,[76] tissue engineering,[77, 78] and MRI contrast agents.[79] Over the past several years, a number of diazeniumdiolate-modified nanoparticles have been created in the Schoenfisch Lab utilizing the drug delivery advantages of nanoparticles to fully harness the power of NO.

1.2.4.1 Monolayer protected gold clusters

Monolayer protected gold clusters (MPCs) may represent the most widely studied nanoparticles to date. The synthesis of MPCs (d = 1 – 5 nm) was first reported by Brust using alkanethiol protecting ligands surrounding a 2 nm gold core.[80] Since this report, several classes of gold MPC nanoparticles have been synthesized with a variety of stabilizing ligands, allowing for tunable physical properties and multiple functionalization options.[65, 81] As such, MPCs have obvious utility for drug delivery applications.[82] Their dense gold core allows for simple imaging with transmission electron microscopy (TEM), thus providing a built-in method for monitoring their cellular uptake.[83, 84]

Rothrock et al. synthesized the first reported nanoparticle-sized diazeniumdiolate modified MPC via gold-thiolate chemistry.[85] Hydrogen tetrachloroaurate salt was reacted with hexanethiol in the presence of sodium borohydride followed by functionalization with bromo-terminated alkanethiols via the place exchange method.[86, 87] The bromine-functionalized gold nanoparticles were dissolved in toluene or methylene chloride and reacted with ethylenediamine, butylamine, hexanediamine, or diethylenetriamine as NO donor precursors. Transmission

electron microscopy images confirmed the core diameter of the nanoparticles to be 2.1 ± 0.9 nm with constant size regardless of amine derivatization or diazeniumdiolate formation. The NO release for diazeniumdiolate-modified gold nanoparticles was tunable by varying the number and/or the chemical structure of the substituted amine ligands. Increasing the concentration of ethylenediamine ligand from 14 to 21%, led to a corresponding increase in total NO (t[NO]) (9.8 to 19.3 nmol NO/mg MPC) and $t_{1/2}$ (from 15 to 78 min). Increasing the length of the alkyl chain separating the amines from two to six methylene units led to an increase in the total amount of NO released (19.3 to 87.0 nmol NO/mg MPC for ethylenediamine- and hexanediamine-modified MPCs, respectively), but a decrease in the half-life, suggesting a NO release/diazeniumdiolate structure relationship. The modest NO release was attributed to inefficient conversion of the amine precursors to diazeniumdiolates. The low NO storage capacity and limited aqueous solubility thus restricts the use of alkanethiol MPCs as NO delivery vehicles for pharmaceutical applications.

Polizzi et al. expanded the previous work to impart water solubility and increase the NO-storage of the gold MPCs.[88] Tiopronin-stabilized MPCs[89] (d ~3 nm) were functionalized with polyamine ligands containing 1, 3, or 4 secondary amine sizes for conversion to diazeniumdiolates. Despite their aqueous solubility, proton-initiated decomposition of the diazeniumdiolate-modified polyamine Tio-MPCs resulted in only modest NO-release (0.023 µmol/mg) for short durations (<1.5 h). To increase the NO storage capacity of gold nanoparticles, the tiopronin linker was removed and the polyamines were used to stabilize gold clusters via a strategy reported by Schulz-Dobrick et al.[90] The polyamine-MPCs (d ~5 nm) exhibited significantly enhanced NO storage capacity following diazeniumdiolate formation (up to 0.386 µmol/mg) with NO release durations exceeding 16 h. The MPCs represent the smallest water-soluble NO-releasing nanoparticles to date (d = 3 − 5 nm).

Additionally, the polyamine-protected MPCs present a multivalent surface for use in subsequent delivery efforts. Functionalization of the nanoparticle exteriors with ligands for tissue-specific targeting or molecular probes for imaging may further facilitate the use of NO-releasing polyamine-protected MPCs for a wide range of pharmacological applications.

1.2.4.2 Silica nanospheres

The use of polyamines to store diazeniumdiolate NO donors originated from the early work by Hrabie et al. that demonstrated tunable properties of NO release based on the number of amines on the donor backbone as well as the distance between them.[45, 46] The kinetic differences in rates of NO release observed when using diamines as NO donor precursors has been utilized extensively by Schoenfisch and co-workers who have synthesized a variety of NO-releasing xerogel films via sol-gel chemistry.[56] The polymerization of aminoalkoxysilanes (e.g., *N*-(6-aminohexyl)-3-aminopropyltrimethoxysilane, AHAP3) with alkylalkoxysilanes (isobutyltrimethoxysilane, BTMOS) results in optically transparent films that store and release variable quantities of NO based on the type and percentage of aminoalkoxysilane polymerized in the network. Using a similar strategy, Meyerhoff and co-workers reported the synthesis of fumed silica particles with aminoalkoxysilanes grafted on the surface as substrates for diazeniumdiolate formation (200-300 nm).[91] As with the xerogel films, the storage and release of NO were mediated by the type of aminosilane grafted. For example, surface grafted silica particles prepared via this method released up to 0.56 μmol NO/mg with a $t_{1/2}$ = 43 min prepared with pendant hexane diamine structure (i.e., Sil-2N[6]-N_2O_2Na).[91] These NO-releasing silica particles were initially employed as fillers for preparing NO-releasing polyurethane extracorporeal circuits.[91] It was further shown that the resulting NO-releasing fumed silica particles could be embedded into polymer films to create thromboresistant coatings via the release of NO at

flufes that mimic healthy endothelial cells (EC). For example, a silicone rubber coating containing 20 wt% Sil-2N[6]-N_2O_2Na improved the surface thromboresistivity (compared to controls) when used to coat the inner walls of extracorporeal circuits (ECC) employed in a rabbit model for extracorporeal blood circulation.

The NO-releasing silica particles prepared by Zhang et al. solved the previous problem of NO-donor backbone leaching from hydrophobic polymer films through the creation of macromolecules embedded in the polymer matrix. The aminosilane-grafted fumed silica also released up to several hundred nmol NO/mg, a substantial reservoir for NO exceeding most other diazeniumdiolate-modified macromolecular scaffolds reported in the literature. However, these larger particles (d = 200-300 nm) only contained diazeniumdiolates grafted to the surface, hindering the storage capacity of the entire scaffold. Shin et al. improved the NO-storage on silica particles through direct co-condensation of aminoalkoxysilane and alkoxysilanes to uniformly distribute the NO-donor precursors throughout the entire silica network.[92] The amine functional groups in the silica structure were then converted to diazeniumdiolate NO donors via exposure to high pressures of NO (5 atm, 3 d) under basic conditions. The selection of the silane precursors (e.g., type and concentration) and specific reaction/processing conditions (e.g., solvent, catalyst, pH, and temperature) allowed for tremendous chemical flexibility in creating nanoparticles of diverse sizes and NO release properties (e.g., NO payload and kinetics). Changing the aminosilane functionality altered a range of NO release characteristics including the total amount of NO released (t[NO]), half-life of NO release ($t_{1/2}$), and the maximum value of NO release ($[NO]_m$). [92] The NO "payload" and corresponding release rates were easily tuned by varying both the percent composition and/or structure of the aminosilane used to prepare nanoparticles. The variety of

NO-releasing nanoparticles available enables a "toolbox" from which to select the desired NO-release characteristics for developing anti-infective/wound healing products.

Another advantage of the silane co-condensation process was the ability to control the size of the silica nanoparticle by varying the type and concentration of aminoalkoxysilane used. This property is of incredible importance for the systemic delivery and biodistribution of nanoparticle devices. The drug delivery potential of silica has received a great deal of attention because of its non-toxic nature and tunable size and porosity.[93, 94]. Indeed, mesoporous silica nanoparticles, prepared from silicon dioxide, have been explored extensively as carrier systems for drugs,[95-99] biocides,[100-102] genes,[103] and proteins.[104, 105] Recently, Shin et al. reported the synthesis of inorganic/organic hybrid silicia nanoparticles whereby the aminoalkoxysilanes are first modified as *N*-diazeniumdiolates and then co-condensed with the alkoxysilane backbone in the presence of an ammonia catalyst to form NO-releasing silica nanoparticles with unprecedented storage capacity.[106] Loading the NO donor before nanoparticle synthesis allowed for the incorporation of higher aminosilane percentages (10-75 mol%) increasing the diazeniumdiolate storage efficiency. A range of aminosilanes have been employed to synthesize NO delivery silica scaffolds with remarkably improved NO storage and release properties, surpassing all macromolecular NO donor systems reported to date with respect to NO payload (11.26 μmol NO/mg), maximum NO release (357 ppm NO/mg), NO release half-life (253 min), and NO release duration (101 h).[106]

1.3 *S*-Nitrosothiol Macromolecular NO Donor Systems

1.3.1 S-nitrosothiol formation and NO-release characteristics

In contrast to exogenously administered diazeniumdiolates, *S*-nitrosothiols (RSNO) are the endogenous transporters of NO and form the basis of a number of NO signaling

cascades.[2] It is well known that free NO inhibits platelet aggregation via a guanylyl-cyclase dependent mechanism[36] but the entire mechanism by which RSNO signaling occurs is more complex.[107] Transnitrosation, or transfer of the nitroso functional group from a nitrosothiol donor to a free thiol, provides a mechanism for direct cellular communication with membrane bound proteins.[108-111] *S*-nitrosoglutathione (GSNO), formed either via the reaction of glutathione with N_2O_3 or through a host of redox mechanisms involving metabolites of NO and transition metal centers, has shown the capacity to regulate several biological processes including vasodilation, platelet activation, neurotransmission, and tissue inflammation.[108, 112, 113] Nitrosated cysteine residues on albumin and other serum proteins account for a large portion of the 1.8 µM nitrosothiol concentration in blood, as protein RSNO carriers have improved stability compared to low molecular weight thiol derivatives.[114, 115]

Aside from the absence/presence of nitrosothiol versus diazeniumdiolate NO donors in physiology, several other properties clearly differentiate the two classes of NO donors. These properties are summarized in Table 1.1. Diazeniumdiolate NO donors undergo proton initiated NO-release under aqueous conditions. In contrast, *S*-nitrosothiols require an added trigger to spontaneously generate NO (Figure 1.3). For example, copper intiates RSNO decomposition via the Cu^+/Cu^{2+} redox couple or through copper containing enzymatic metal centers. Trace thiolate anion in solution reduces Cu^{2+} to Cu^+ which subsequently reduces RSNO compounds to initiate NO release.[108, 116, 117] Photoinitiated NO-release is another well-characterized mechanism of RSNO decomposition.[118] Irradiation of RSNO donors results in homolytic cleavage of the S-N bond to yield NO and a thiyl radical in a process that is approximately first-order.[118] Electron paramagnetic resonance spectra of spin-trapped thiyl radicals have been reported as concrete evidence for the photo-triggered homolysis of the S-N bond.[119] The synthetic procedures required for NO donor formation are also quite

16

different. Diazeniumdiolates are formed on amines under basic conditions and high pressures of NO, whereby S-nitrosothiols are formed on thiols in acidified solutions of sodium nitrite or through organic nitrite donors.[120] The photolytic and thermal stabilities, formation conditions, and environmental factors governing NO release must all be considered when selecting an appropriate NO donor for a desired biological application.

Nitrosothiols can also be made synthetically through the conversion of free thiols in acidified sodium nitrite solutions to the corresponding S-nitrosothiols. Donors including S-nitroso-N-acetyl-DL-penicillamine (SNAP) synthesized via this method have been employed as tools to better understand the many complicated roles of NO in regulatory biology. Their activity as anti-platelet agents,[36-41] toxicity toward cancerous cells,[27, 28] broad spectrum antimicrobial activity,[29-32] and protective effects in a number of cardiovascular applications have garnered nitrosothiol NO donors widespread recognition.[33-35] Despite the promising therapeutic potential of nitrosothiols, analogous to diazenimdiolate compounds, the inability to target NO to a specific site of action and the rapid systemic clearance associated with small drug molecules has seriously hindered the clinical development of nitrosothiol therapeutics. Similar to innovations made with N-diazeniumdiolates, a number of macromolecular drug delivery vehicles have been developed to circumnavigate the challenges associated with successful RSNO-based drugs.

Table 1.1   Comparison of *N*-diazeniumdiolate and *S*-nitrosothiol NO donors.

	N-diazeniumdiolates	*S*-nitrosothiols
Formation Conditions	Basic, high pressures of NO	Acidic or nitrosative conditions
Decomposition Triggers	H_3O^+	Light, Cu^{2+}, thiols
Thermal stability	Limited (store at -20 °C)	Limited (store at -20 °C)
NO-release kinetics	Highly tunable based on pH and lipophilicity	Dependent on Trigger Concentration
Toxicity of Metabolites	Yes, carcinogenic nitrosamines	None
Charged	Yes	No
Storage Capacity	2 mol NO / mol 2° amine	1 mol NO / mol thiol
Light Sensitive	No	Yes
Nature	Exogenous	Endogenous
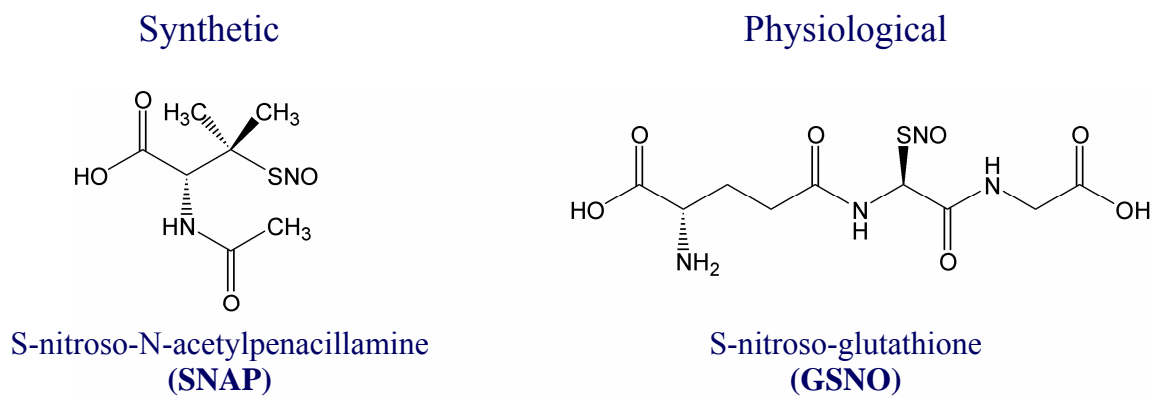
Synthetic   Physiological

S-nitroso-N-acetylpenacillamine   S-nitroso-glutathione
(SNAP)   **(GSNO)**

Synthetic

$$RSH + NaNO_2 + HCl \xrightarrow{\text{MeOH}} RSNO + NaCl + H_2O$$

Physiological

$$2NO^\bullet + O_2 \longrightarrow 2NO_2^\bullet$$
$$+$$
$$NO \rightleftharpoons N_2O_3$$

$$N_2O_3 + GSH \longrightarrow GSNO + NO_2^- + H^+$$
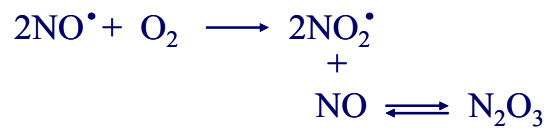
Figure 1.3   Representative structures for synthetic and physiological NO donors
and their pathways for nitrosothiol formation.

19
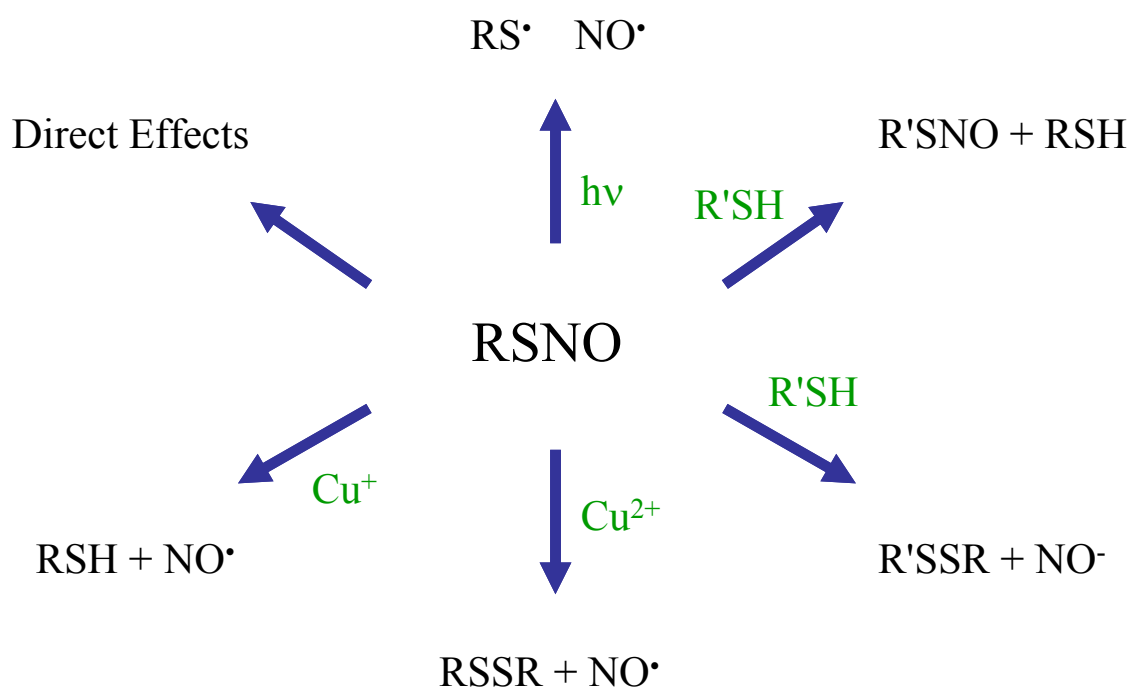
Figure 1.4   Mechanisms of *S*-nitrosothiol decomposition.

1.3.2 Protein-based RSNO delivery vehicles

Due to the physiological occurrence of protein-SNO adducts, protein-based nitrosothiol delivery vehicles have been extensively explored as a strategy to extend the systemic half-lives of exogenous RSNO donors and to aid in the treatment of circulation disorders.[121-124] Katsumi et al. reacted bovine serum albumin (BSA) with acidified nitrite to yield BSA-NO adducts possessing ~0.2 mol SNO/mol BSA with molecular weights near 67 kDa.[122] Nitrosation caused reversible changes in protein secondary structure and the modifications were not confined to cysteine residues as the number of modified amino groups also increased with increasing nitrosation conditions (i.e., nitrosamine formation). When administered intravenously to a rat at a dose of 100 mg/kg, BSA-NO induced a transient decrease in arterial blood pressure for 3 min and exhibited biodistribution properties similar to unmodified BSA.[122] Realizing the need for higher NO storage per unit of protein and prolonged NO release particularly when injected systemically, Hashida and co-workers synthesized PEG-polySNO-BSA conjugates capable of storing 10 mol NO/mol protein delivery vehicle (250 kDa) with half-lives of NO release 11 times longer than unpegylated BSA-NO and 108 times longer than small molecule SNAP.[123] The use of PEG chains decreased the aggregation of proteins formed during the synthesis of previous BSA-NO constructs[121, 124] and provided added thermal stability to the NO donors through "cage effects" reported previously by de Oliveira and co-workers.[125] Furthermore, the PEG microenvironment created a more compact solution structure increasing the frequency of geminate radical pair recombination following thermal decomposition and thus, slowing the rates of NO release at room temperature. As a result of the enhanced stability, the pegylated BSA-NO adduct prolonged the decrease in mean arterial blood pressure when compared to BSA-NO and classical small molecule NO donors (e.g., SNAP, GSNO).

Serum albumin-RSNO conjugates have been recently expanded to include human serum albumin (HSA). Ishima et al. nitrosated a genetic variant of HSA (R410C) possessing an additional free cysteine at position 410 to yield 1.25 mol SNO/mol protein.[126] Protein aggregation was not observed during synthesis and lyophilization, and R410C-SNO had excellent physicochemical stability with an approximate half-life of 20.4 min in a mouse. In addition to the cytoprotective effects observed in hepatic ischemia/reperfusion experiments, potent bactericidal activity was observed for the nitrosated protein. The concentration of R410C-SNO required reducing cell viability to 50% (IC_{50}) of *Salmonella typhimurium* was 0.6 μM compared to the 3300 μM dose required with the GSNO small molecule. These findings suggest that protein-based macromolecular delivery vehicles for nitrosothiols may afford unexpected biological activity due to their ability to interact preferentially with membrane proteins or other cellular targets for RSNO action. The authors also noted that Cys-410 in HSA is surrounded by acidic (Glu) and basic (Lys) residues which may constitute the acid-base motif necessary for formation, stability, and reactivity of protein-bound RSNO groups suggested by Stamler and colleagues.[127] Mechanistic interactions between nitrosothiols and other blood proteins (e.g., hemoglobin (Hb)) are currently being explored and will likely lead to stabilized structural and functional analogues (e.g., HbSNO) that serve as NO sources in the absence of red blood cells.[128-134]

1.3.3 Polymeric S-nitrosothiol conjugates

The documented effects of nitrosothiols on preventing platelet adhesion/aggregation and the early stages of thrombus formation have led to the creation of nitrosothiol-modified polymers as macromolecular delivery vehicles of NO, similar to diazeniumdiolate based NO donors. A number of hydrogels and liquid/solid polymeric matrices have been developed that stabilize small-molecule nitrosothiols and deliver NO at controlled rates for topical drug

delivery[135-138] and metallic device coatings.[139] However, doping nitrosothiols into polymeric materials faces two main limitations: 1) the solubility of the NO donor in the polymer matrix limits the vehicle's NO storage capacity; and, 2) diffusion of the donor into tissue is uncontrollable if the NO donor is water-soluble and not covalently bound to the polymer backbone.[138]

Several polymer conjugates containing covalently immobilized nitrosothiols have been synthesized to overcome these limitations and deliver nitrosothiols more effectively for cardiovascular and topical wound healing applications. Duan et al. modified polyurethane (PU) and polyethylene terephthalate (PET) polymers to contain cysteine residues as precursors for NO storage via RSNOs.[140] The polymer backbones were aminated with aminopropyltrimethoxysilane or ethylendiamine (PU and PET, respectively), reacted with glutaraldehyde to form the Schiffs base, and incubated in buffered cysteine solutions to covalently attach the amino acid RSNO precursor. The surfaces were converted to *S*-nitrosothiols following exposure to solutions of BSA-NO with the auspice that these polymers could serve as stable reservoirs for NO once implanted into the body after contact with the ~2 μM concentrations of BSA-NO in the blood. Indeed, the cysteine-modified polymers rapidly decreased BSA-NO levels in solution via transnitrosation. In separate experiments, CysNO modified surfaces were capable of reducing platelet aggregation >50% compared to glycine modified control PU and PET. Cysteine incorporation at 5 − 8 nmol/cm^2 was sufficient to provide haemocompatibility in vitro and the delivery of NO via transnitrosation from BSA-NO was a novel concept for NO donor formation on surfaces.[140]

West and co-workers developed a method to covalently immobilize *S*-nitrosocysteine (CysNO) in photo-polymerized hydrogels as a vehicle for the local delivery of NO after lifesaving cardiovascular procedures such as angioplasty and stenting.[141] *S*-nitrosothiols that

spontaneously generate NO at the site of vascular injury have been demonstrated to aid in the prevention of neointima formation and restenosis.[142] The N-hydroxysuccinimide ester of poly(ethylene glycol) monoacrylate was coupled to the free amines of cysteine residues and converted to PEG-CysNO with an acidified nitrite solution. The PEG-CysNO were photopolymerized with a PEG-diacrylate in aqueous solutions containing 2,2-dimethoxy-2-phenylacetophenone as a long wavelength photoinitiator of polymerization (solubilized via 0.15% N-vinyl pyrrolidone).[141] The RSNO-loaded hydrogels were formed in the perivascular space of a rat heart and delivered NO with a half-life of several hours post–surgery. Histological analysis two weeks later revealed significant attenuation of wall thickening in arteries treated with the NO-releasing hydrogels.[142]

1.3.4 Surface-grafted silica

Covalent attachment of nitrosothiols directly into poly(ethylene glycol) hydrogels and polyesters that possess amorphous structures has been successful for topical NO delivery.[138, 141, 142] However, this strategy may not be accessible for all biomedical grade polymers requiring a high level of structural uniformity for medical device fabrication. Alterations to the polymer backbone may change the chemical and mechanical properties (e.g., solubility, hardness, water uptake, permeability) and consequently result in the re-evaluation of these parameters and/or poor device performance. An alternative approach is the incorporation of macromoleculear NO donors into the already well-known biomedical grade polymer compositions. Previously, Meyerhoff and co-workers employed diazeniumdiolate-modified silica particles as polymer fillers that release NO and increase the biocompatibility of silicone rubber and poly(urethane).[91] Frost et al. also utilized fumed silica as a scaffold for *S*-nitrosothiol modification creating macromolecular-doped polymers capable of releasing NO rapidly when exposed to light.[143, 144] In a typical synthesis, the free silanol groups on the

surface of the fumed silica were modified with (3-aminopropyl)trimethoxysilane and the newly formed amine functionalities were reacted with the self-protected thiolactone of *N*-acetyl-DL-penicillamine (NAP). The thiol-derivatized surface was subsequently converted to the corresponding *S*-nitroso-*N*-acetyl-DL-penicillamine (SNAP-FS) by reaction with *tert*-butylnitrite. These derivatized fumed silica nanoparticles stored 0.138 μmol NO/mg with NO release rates precisely controlled through the duration and the intensity of the light used to initiate NO release.

The nanoparticles (d = 7 – 10 nm) served as large reservoirs of NO when incorporated into trilayer silicone rubber polymer films, effectively immobilizing the nitrosothiols inside a device coating without the leaching issues associated with small molecule dopants. Localizing NO release at the polymer/biological sample interface and maintaining photo-triggered control over the NO-release rates may enable fundamental studies on the minimum surface fluxes required to inhibit platelet and bacterial adhesion. Additionally, the light initiated release of NO from nanoparticle devices opens the gateway to utilizing NO as a therapeutic in photodynamic therapy treatments of cancerous cells. Frost et al. proposed incorporating the SNAP-FS particles into silicone rubber material at the end of a fiber optic probe for direct insertion into a tumor mass. Upon illumination of the fiber, NO would be released in controllable doses based on the duration, intensity, and wavelength of light.[144] Future work enabling the synthesis of nitrosothiol-modified silica in combination with photosensitizers used in typical photodynamic therapy treatments[145] may lead to devices capable of releasing NO with the longer wavelengths of light necessary for effective tissue penetration.[146]

1.4 Inorganic/organic Hybrid Systems and Photo-triggered Nitric Oxide Donors

Since the first report by Rothrock et al. of NO-releasing nanoparticles synthesized from diazeniumdiolate-modified gold cores,[85] several other inorganic/organic hybrid nanoparticles have been synthesized to store and release NO. These systems do not employ diazeniumdiolate or nitrosothiol chemistry but are excellent examples of recent advancements in materials science that may lead to the next generation of NO-releasing devices. Morris and co-workers created transition metal-exchanged zeolites that store up to 1 μmol NO/mg.[147] The NO was adsorbed both reversibly or irreversibly to the zeolite scaffolds through physisorption or chemisorption. Water was used as a nucleophile to displace the irreversibly adsorbed NO ($t_{1/2}$ = 340 s of NO-release). Experiments with human platelets confirmed that NO released from cobalt-exchanged zeolite-A reduced platelet activation and aggregation illustrating the anti-thrombotic potential of the NO-loaded xeolite scaffold.[147] Furthermore, the kinetics of NO-release were tunable by controlling the amount of water contacting the zeolite through incorporation into mixtures of powdered poly(tetrafluoroethylene) (PTFE) or poly(dimethylsiloxane) (PDMS). Pressed disks made from the powdered mixtures resulted in increased half-lives of 509 s and 3076 s (PTFE and PDMS, respectively), demonstrating control over NO-release fluxes from the disc surface albeit at the expense of NO storage capacity.[147] Similar gas adsorption experiments were carried out on copper benzene tricarboxylate metal-organic frameworks, HKUST-1.[148] The metal framework had a large adsorption capacity for NO at 298 K (1 bar), 3 μmol NO/mg, but the quantities released when exposed to aqueous physiological conditions plateaued at ~1 nmol NO/mg. Despite the inability to recover all of the adsorbed NO, these low levels of NO release were sufficient to reduce platelet aggregation in platelet rich plasma.[148]

Water is a simple trigger that initiates NO release from diazeniumdiolates and zeolite complexes, but recent studies have explored using light as a stimulant for site-selective NO release from inorganic macromolecules. As described above, photo-triggered NO release provides an attractive avenue for using NO in the photodynamic therapy of cancerous tissue and other areas of medicine requiring localized NO therapy. Caruso et al. reported the synthesis of monolayer-protected platinum nanoparticles capable of delivering NO upon exposure to visible light (λ_{max} = 386 nm).[149] Water soluble, carboxy-terminated platinum nanoparticles were partially modified with a thiol derivatized photoactive NO donor through a phase-exchange reaction to yield MPCs containing 6 flutamide derivatives per platinum cluster (ca. 1 nm). Photolysis of the nitroaromatic anticancer drug flutamide leads nitro-to-nitrite photo-rearrangement followed by rupture of the O-N bond to generate a phenoxy radical and NO.[150] The platinum MPCs exhibited an on/off triggered release profile dependent on the light source with a release rate of 1.5 pmol s^{-1}.

The phototriggered release of NO from transition metal nitrosyl and nitrito complexes incorporated into stable matrix formulations have also been pursued as light-responsive NO donors.[151-153] Due to low extinction coefficients and absorption maxima residing in the UV-visible range, metal complexes have seen little utility for in vivo biomedical applications. For example, *trans*-Cr(cyclam)(ONO)$_2$$^+$ (cyclam = 1,4,8,11-tetraazacyclotetradecane) is photoactive toward cleavage of the CrO-NO bond to release NO, but the dinitrito complex is weakly absorbing at near-UV and visible wavelengths. Recently, Neuman et al. reported the use of CdSe/ZnS core/shell quantum dots as antennas to harness light energy and promote electron transfer to the NO donor precursor to initiate NO release.[154] Quantum dots were prepared by a three-step procedure involving synthesis of the CdSe cores, growth of the ZnS shell, and surface ligand exchange with dihydrolipoic acid to impart water solubility.

Formation of an electrostatic assembly between the cationic *trans*-Cr(cyclam)(ONO)$_2^+$ complex with the negatively charged quantum dot surface resulted in particles with an average CdSe core diameter of 3.8 nm. Excitation with a Hg arc lamp (320-390 nm band-pass filter) resulted in much faster NO release in the presence of the quantum dot antennas than photolysis of the metallic complex alone, indicating indirect photosensitization of the chromium complex to spontaneously release NO.

The works reported by Neuman and Caruso bring the field of nanomedicine one step closer to utilizing photoactive transition-metal-based prodrugs for NO delivery.[149, 154] Quantum dots and platinum MPCs hold considerable promise as site-specific agents for the photochemical delivery of NO because their surface ligands may be utilized to tether additional functionalities to the nanoparticle surface. These modifications may alter vehicle solubility as well as impart specificity to the photo-initiated NO prodrug carrier. The formation of metallic nanoparticles typically yields monodisperse populations but the control over ligand coverage and surface modifications can vary widely from batch to batch. Scaffolds that have a uniform number of surface groups and less dense core structures may result in macromolecular NO donors with enhanced NO storage.

1.5 Dendrimers as Drug Delivery Vehicles

The macromolecular NO donors described above have made significant advancements in the chemical storage and controlled release of NO for a number of biomedical applications. Ultimately, limitations to the quantity of NO on each macromolecular scaffold and the failure to deliver NO to a specific cell or tissue of interest has prevented their widespread clinical application.[5, 26, 155] A particular macromolecular drug delivery scaffold that has received a lot of attention in the literature but not yet been integrated with NO donor chemistry is dendrimers. Dendrimers are hyper-branched or "tree-like" polymers that possess precisely

defined molecular structures with a multivalent exterior (Figure 1.5). Dendrimers have garnered significant attention as a new class of drug delivery vehicles due to their ability to achieve high drug payloads per unit of drug carrier.[156]. These branched molecules also exhibit dynamic solution behavior and adopt globular conformations similar to proteins that minimize hydrophobic interactions and separate charge along the dendritic backbone. A number of biocompatible dendrimers have been synthesized based on polyether, polyarylether, polyamine, and polypeptide networks.[157] The multivalent exterior of dendrimers can be used to attach multiple functionalities on one molecular scaffold, making them extremely useful for targeting drugs to specific tissue types or for imaging drug biodistribution.[158] For example, Baker and co-workers have functionalized polyamidoamine (PAMAM) dendrimers with multiple copies of the anticancer drug methotrexate, folic acid for targeting cancerous tissue, and fluorophores for tracking dendrimer distribution in an animal model.[159] These multifunctional dendrimer delivery vehicles selectively target epithelial cancer in rat animal models with no drug accumulation in healthy tissues.[159] Overall, drug-loaded dendrimers have exhibited enhanced cellular delivery and more rapid pharmacological responses than therapeutic agents administered without the hyperbranched delivery vehicles. The improved efficacy of dendrimer-based drugs has lead to their widespread application in many areas of bioscience including anti-cancer, antimicrobial, and antiviral drug research.[156, 157, 160, 161]

1.6 Overview of Dissertation Research

The goals of my research sought to overcome the obstacles impeding targeted NO delivery through the development of NO-releasing dendrimers. Their highly functionalizable exterior and reproducible molecular structure of dendrimers make them attractive as NO storage devices. Commercially available starting materials like polypropylenimine (PPI) and

polyamidoamine (PAMAM) dendrimers contain a large number of exterior amine precursors which can be modified to then serve as NO donor storage sites (Figure 1.5, 1.6). The number of NO donor precursor sites may be further manipulated by selecting dendrimers with different generations of growth. For example generation 5 dendrimer (DAB-Am-64) has 64 amines at its exterior compared to just 16 for generation 3 polypropylenimine dendrimer (DAB-Am-16). The capacity to pack a large density of NO donors on a loosely branched structure may afford unprecedented storage reservoirs for bioavailable NO.   Extensive research has been reported on the derivatization of the amine exteriors with a variety of functionalities, ranging from lipophilic groups to enhance the hydrophobicity[162, 163] to ligands required for targeting dendrimer delivery vehicles to proteins on the surface of cancerous cells.[159, 164] To date, no chemistry has been elucidated to chemically store NO via either *N*-diazeniumdiolate or *S*-nitrosothiol chemistry on a dendrimer scaffold. The specific aims of my research included:

1) the synthesis and characterization of secondary amine dendrimer conjugates for modification with *N*-diazeniumdiolate NO donors;

2) the creation of hydrophobic and hydrophilic dendritic exteriors to control diazeniumdiolate NO release kinetics;

3) the successful conjugation of thiols and conversion to *S*-nitrosothiols on polyamidoamine (PAMAM) dendritic scaffolds not amenable to diazeniumdiolate chemistry;

4) the full characterization of nitrosothiol-modified dendrimer NO-release kinetics following exposure to copper, light, thermal, ascorbate, and thiol triggered mechanisms of decomposition;

5) the exploration of nitrosothiol modified dendrimers as anti-platelet agents;

6) the synthesis of multifunctional dendrimers containing mixed functionalities at the dendritic exterior relevant to drug delivery;

7) the evaluation of dendrimer cytotoxicity in cultured endothelial cells using confocal fluorescence microscopy and establishment of a clear structure activity relationship between dendrimer surface charge and vehicle toxicity.

Derivitization to contain the secondary amines necessary for N-diazeniumdiolate formation or the thiol groups necessary for conversion to *S*-nitrosothiols would potentially unlock a series of NO-releasing vehicles previously unattained by metallic, ceramic, or polymeric macromolecules. The following chapters explore the synthetic procedures necessary to create both diazeniumdiolate- and nitrosothiol-modified dendrimers and fully characterize their NO-release properties as a function of the dendritic nanoenvironment. The creation of NO-releasing dendrimers presented herein effectively supplements the field of NO-releasing macromolecules with a new tool capable of increasing the utility of medical device coatings and revolutionizing the efficacy of systemically delivered NO based therapeutics.

A
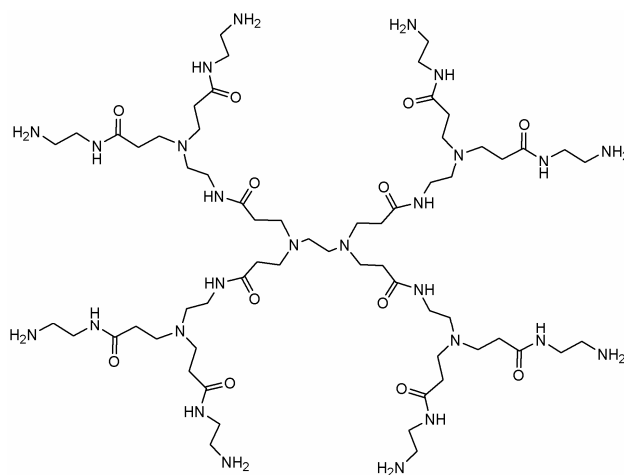
Generation 1 Polyamidoamine Dendrimer
(G1 PAMAM)

B
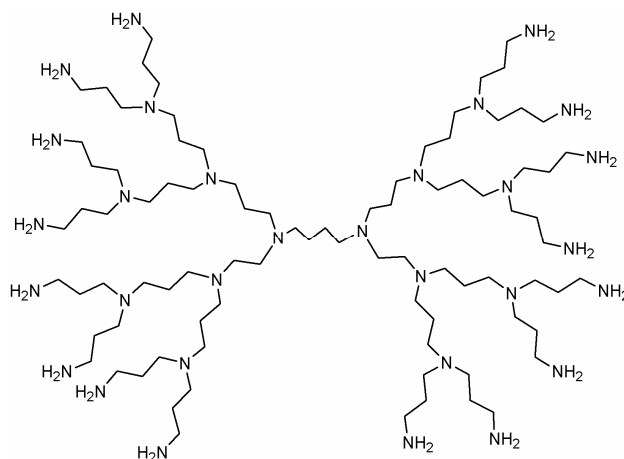
Generation 3 Polypropylenimine Dendrimer
(DAB-Am-16)

Figure 1.5   A) Generation 1 polyamidoamine dendrimer (PAMAM). B) Generation 3 polypropylenimine dendrimer with a diaminobutane core (DAB) and 16 surface amines.
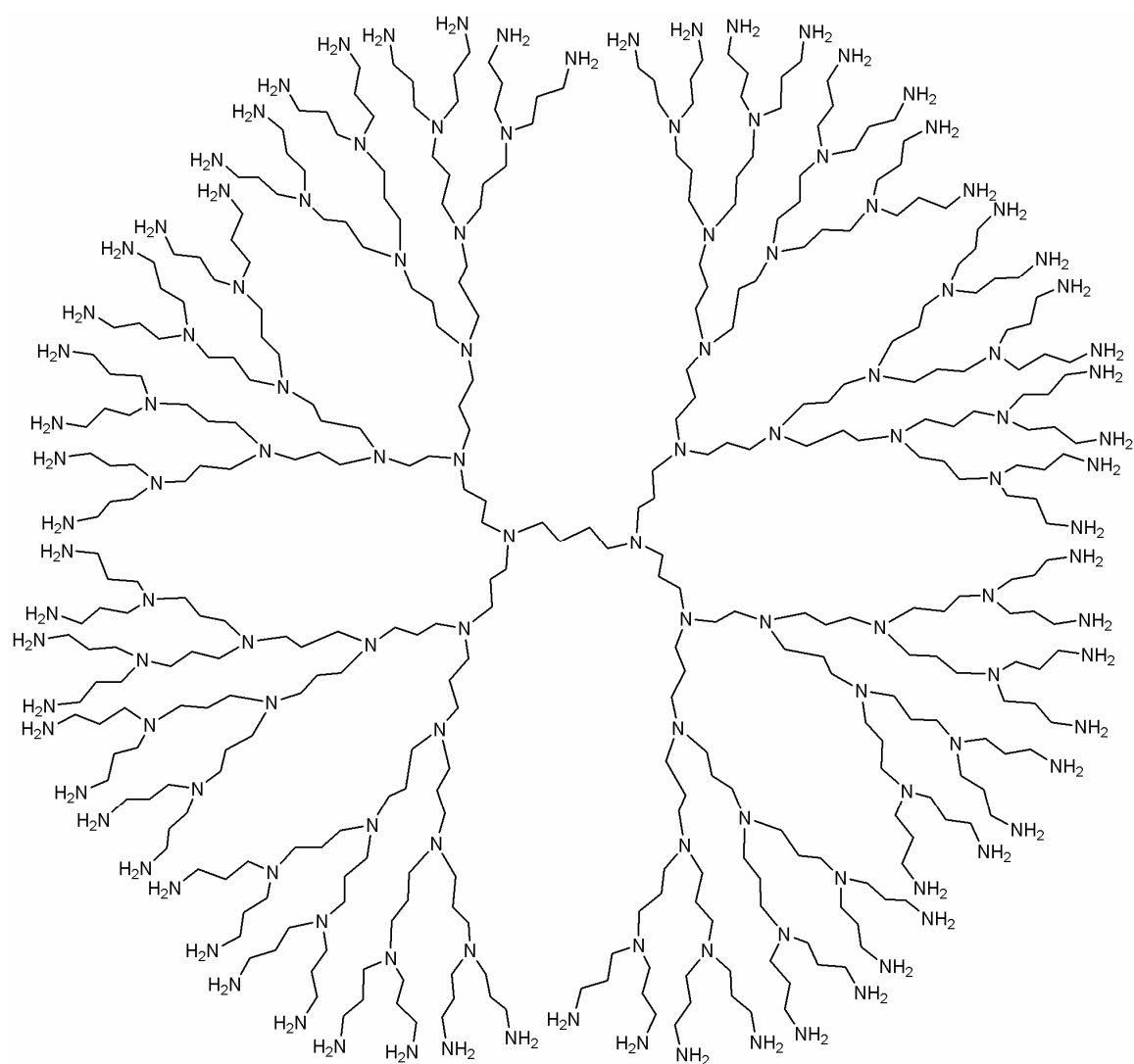
Generation 5 Polypropylenimine Dendrimer
(DAB-Am-64)

Figure 1.6   Generation 5 polypropylenimine dendrimer with a diaminobutane core (DAB) and 64 surface amines, illustrating the tremendous storage capacity for NO.

1.7 References

1. Ignarro, L. J.; Buga, G. M.; Wood, K. S.; Byrns, R. E.; Chaudhuri, G. "Endothelium-derived relaxing factor produced and released from artery and vein is nitric oxide." *Proc. Natl. Acad. Sci., U. S. A.* **1987,** *84*, 9265-9269.

2. Ignarro, L. J. "Nitric oxide: A unique endogenous signaling molecule in vascular biology." *Angew. Chem., Int. Ed.* **1999,** *38*, 1882-1892.

3. Ignarro, L. J. "Nitric oxide: A novel signal transduction mechanism for transcellular communication." *Hypertension* **1990,** *16*, 477-483.

4. Furchgott, R. F. "Endothelium-derived relaxing factor: discovery, early studies, and identification as nitric oxide." *Angew. Chem., Int. Ed.* **1999,** *38*, 1870-1880.

5. Napoli, C.; Ignarro, L. J. "Nitric oxide-releasing drugs." *Ann. Rev. Pharmacol. Toxicol.* **2003,** *43*, 97-123.

6. McMackin, C. J.; Vita, J. A. "Update on nitric oxide-dependent vasodilation in human subjects." *Methods Enzymol.* **2005,** *396*, 541-553.

7. Granger, H. J.; Ziche, M.; Hawker, J. R.; Meininger, C.; Czisny, L. E.; Zawieja, D. C. "Molecular and cellular basis of myocardial angiogenesis." *Cell. Mol. Biol. Res.* **1994,** *40*, 81-85.

8. Kondo, T.; Kobayashi, K.; Murohara, T. "Nitric oxide signaling during myocardial angiogenesis." *Mol. Cell. Biochem.* **2004,** *264*, 25-34.

9. Sanders, K. M.; Ward, S. M. "Nitric oxide as a mediator of nonadrenergic noncholinergic neurotransimission." *Am. J. Physiol.* **1992,** *262*, 379-392.

10. Shapoval, L. N. "Nitric oxide: involvement in the nervous control of cardiovascular function." *Neurophysiology* **2004,** *36*, 418-431.

11. Nathan, C.; Shiloh, M. U. "Reactive oxygen and nitrogen intermediates in the relationship between mammalian hosts and microbial pathogens." *Proc. Natl. Acad. Sci., U. S. A.* **2000,** *97*, 8841-8848.

12. Shah, V.; Lyford, G.; Gores, G.; Farrugia, G. "Nitric oxide in gastrointestinal health and disease." *Gastroenterology* **2004,** *126*, 903-913.

13. Reid, M. B. "Invited review: redox modulation of skeletal muscle contraction: what we know and what we don't." *J. App. Physiol.* **2001,** *90*, 724-731.

14. Stamler, J. S.; Meissner, G. "Physiology of nitric oxide in skeletal muscle." *Physiol. Rev.* **2001,** *81*, 209-237.

15. Marletta, M. A.; Tayeh, M. A.; Hevel, J. M. "Unraveling the biological significance of nitric oxide." *BioFactors* **1990,** *2*, 219-225.

16. Vaughn, M. W.; Kuo, L.; Liao, J. C. "Estimation of nitric oxide production and reaction rates in tissue by use of a mathematical model." *Am. J. Physiol.* **1998,** *274*, 2163-2176.

17. Marletta, M. A.; Hurshman, A. R.; Rusche, K. M. "Catalysis by nitric oxide synthase." *Curr. Opin. Chem. Biol.* **1998,** *2*, 656-663.

18. Sessa, W. C. "The nitric oxide synthase family of proteins." *J. Vasc. Res.* **1994,** *31*, 131-143.

19. Przedborski, S.; Dawson, T. M. "The role of nitric oxide in Parkinson's disease." *Methods Mol. Med.* **2001,** *62*, 113-136.

20. Naseem, K. M. "The role of nitric oxide in cardiovascular diseases." *Mol. Aspects Med.* **2005,** *26*, 33-65.

21. Williams, I. L.; Wheatcroft, S. B.; Shah, A. M.; Kearney, M. T. "Obesity, atherosclerosis and the vascular endothelium: mechanisms of reduced nitric oxide bioavailability in obese humans." *Int. J. Obesity* **2002,** *26*, 754-764.

22. Wink, D. A.; Vodovotz, Y.; Laval, J.; Laval, F.; Dewhirst, M. W.; Mitchell, J. B. "The multifaceted roles of nitric oxide in cancer." *Carcinogenesis* **1998,** *19*, 711-721.

23. Vallance, P.; Leiper, J. "Blocking NO synthesis: how, where and why?" *Nat. Rev. Drug Discovery* **2002,** *1*, 939-950.

24. Roman, L. J.; Martasek, P.; Masters, B. S. S. "Intrinsic and extrinsic modulation of nitric oxide synthase activity." *Chem. Rev.* **2002,** *102*, 1179-1189.

25. Hrabie, J. A.; Keefer, L. K. "Chemistry of the nitric oxide-releasing diazeniumdiolate functional group and its oxygen-substituted derivates." *Chem. Rev.* **2002,** *102*, 1135-1154.

26. Wang, P. G.; Xian, M.; Tang, X.; Wu, X.; Wen, Z.; Cai, T.; Janczuk, A. J. "Nitric oxide donors: chemical activities and biological applications." *Chem. Rev.* **2002,** *102*, 1091-1134.

27. Babich, H.; Zuckerbraun, H. L. "In vitro cytotoxicity of glyco-S-nitrosothiols: A novel class of nitric oxide donors." *Toxicol. in Vitro* **2001,** *15*, 181-190.

28. Hou, Y.; Wang, J.; Andreana, P. R.; Cantauria, G.; Tarasia, S.; Sharp, L.; Braunschweiger, P. G.; Wang, P. G. "Targeting nitric oxide to cancer cells: cytotoxicity studies of glyco-S-nitrosothiols." *Bioorg. Med. Chem. Lett.* **1999,** *9*, 2255-2258.

29. de Souza, G. F. P.; Yokoyama-Yasunaka, J. K. U.; Seabra, A. B.; Miguel, D. C.; de Oliveira, M. G.; Uliana, S. R. B. "Leishmanicidal activity of primary S-nitrosothiols against *Leishmania major* and *Leishmania amazonesis*: implications for the treatment of cutaneous leishmaniasis." *Nitric Oxide* **2006,** *15*, 209-216.

30. Fang, F. C. "Antimicrobial reactive oxygen and nitrogen species: concepts and controversies." *Nat. Rev. Microbiol.* **2004,** *2*, 820-832.

31. Mannick, J. B. "Immunoregulatory and antimicrobial effects of nitrogen oxides." *Proc. Am. Thorac. Soc.* **2006,** *3*, 161-165.

32. Schapiro, J. M.; Libby, S. J.; Fang, F. C. "Inhibition of bacterial DNA replication by zinc mobilization during nitrosative stress." *Proc. Natl. Acad. Sci., U. S. A.* **2003,** *100*, 8496-8501.

33. Bell, R. M.; Maddock, H. L.; Yellon, D. M. "The cardioprotective and mitochondrial depolarising properties of exogenous nitric oxide in mouse heart." *Cardiovasc. Res.* **2003,** *57*, 405-415.

34. Konorev, E. A.; Tarpey, M. M.; Joseph, J.; Baker, J. E.; Kalyanaraman, B. "S-nitrosoglutathione improves functional recovery in the isolated rat heart after cardioplegic ischemic arrest-evidence for a cardioprotective effect of nitric oxide." *J. Pharmacol. Exp. Ther.* **1995,** *274*, 200-206.

35. Schulz, R.; Kelm, M.; Heusch, G. "Nitric oxide in myocardial ischemia/reperfusion injury." *Cardiovasc. Res.* **2004,** *61*, 402-413.

36. Mellion, B. T.; Ignarro, L. J.; Myers, C. B.; Ohlstein, E. H.; Ballot, B. A.; Hyman, A. L.; Kadowitz, P. J. "Inhibition of human platelet aggregation by *S*-nitrosothiols." *Mol. Pharmacol.* **1983,** *23*, 653-664.

37. Radomski, M. W.; Rees, D. D.; Dutra, A.; Moncada, S. "*S*-nitroso-glutathione inhibits platelet activation *in vitro* and *in vivo*." *J. Pharmacol.* **1992,** *107*, 754-749.

38. de Belder, A. J.; MacAllister, R.; Radomski, M. W.; Moncada, S.; Vallance, P. J. T. "Effects of S-nitrosoglutathione in the human forearm circulation: evidence for selective inhibition of platelet activation." *Cardiovasc. Res.* **1994,** *28*, 691-694.

39. Radomski, M. W.; Moncada, S. "Regulation of platelet function by nitric oxide." *Adv. Molec. Cell Biol.* **1997,** *18*, 367-381.

40. Molloy, J.; Martin, J. F.; Baskerville, P. A.; Fraser, S. C. A.; Markus, H. S. "*S*-nitrosoglutathione reduces the rate of emolization in humans." *Circulation* **1998,** *98*, 1372-1375.

41. Salas, E.; Langford, E. J.; Marrinan, M. T.; Martin, J. F.; Moncada, S.; Debelder, A. J. "*S*-nitrosoglutathione inhibits platelet activation and deposition in coronary artery saphenous vein grats in vitro and in vivo." *Heart* **1998,** *80*, 146-150.

42. Drago, R. S.; Paulik, F. E. "The reaction of nitrogen(II) oxide with diethylamine." *J. Am. Chem. Soc.* **1960,** *82*, 96-98.

43. Drago, R. S.; Karstetter, B. R. "The reaction of nitrogen(II) oxide with various primary and secondary amines." *J. Am. Chem. Soc.* **1961,** *83*, 1819-1822.

44. Miranda, K. M.; Katori, T.; Torres de Holding, C. L.; Thomas, L.; Ridnour, L. A.; McLendon, W. J.; Cologna, S. M.; Dutton, A. S.; Champion, H. C.; Mancardi, D.; Tocchetti, C. G.; Saavedra, J. E.; Keefer, L. K.; Houk, K. N.; Fukuto, J. M.; Kass, D. A.; Paolocci, N.; Wink, D. A. "Comparison of the NO and HNO donating properties of diazeniumdiolates: primary amine adducts release HNO in Vivo." *J. Med. Chem.* **2005,** *48*, 8220-8228.

45. Davies, K. M.; Wink, D. A.; Saavedra, J. E.; Keefer, L. K. "Chemistry of the diazeniumdiolates 2. kinetics and mechanism of dissociation to nitric oxide in aqueous solution." *J. Am. Chem. Soc.* **2001,** *123*, 5473-5481.

46. Hrabie, J. A.; Klose, J. R.; Wink, D. A.; Keefer, L. K. "New nitric oxide-releasing zwitterions derived from polyamines." *J. Org. Chem.* **1993,** *58*, 1472-1476.

47. Chakrapani, H.; Showalter, B. M.; Citro, M. L.; Keefer, L. K.; Saavedra, J. E. "Nitric oxide prodrugs: diazeniumdiolate anions of hindered secondary amines." *Org. Lett.* **2007**.

48. Mowery, K. A.; Schoenfisch, M. H.; Meyerhoff, M., E.; Saavedra, J. E.; Keefer, L. K. "Polymeric diazeniumdiolates for fabricating thromboresistant electrochemical sensors via nitric oxide release." *Polym. Mater. Sci. Eng.* **1998,** *79*, 33-34.

49. Reynolds, M. M.; Frost, M. C.; Meyerhoff, M. E. "Nitric oxide-releasing hydrophobic polymers: preparation, characterization, and potential biomedical applications." *Free Radical Biol. Med.* **2004,** *37*, 926-936.

50. Frost, M. C.; Reynolds, M. M.; Meyerhoff, M. E. "Polymers incorporating nitric oxide-generating substances for improved biocompatibility of blood-contacting medical devices." *Biomaterials* **2005,** *26*, 1685-1693.

51. Smith, D. J.; Chakravarthy, D.; Pulfer, S.; Simmons, M. L.; Hrabie, J. A.; Citro, M. L.; Saavedra, J. E.; Davies, K. M.; Hutsell, T. C.; Mooradian, D.; Hanson, S. R.; Keefer, L. K. "Nitric oxide-releasing polymers containing the [N(O)NO]⁻ group." *J. Med. Chem.* **1996,** *39*, 1148-1156.

52. Pulfer, S. K.; Ott, D.; Smith, D. J. "Incorporation of nitric oxide-releasing crosslinked polyethylenimine microspheres into vascular grafts." *J. Biomed. Mater. Res.* **1997,** *37*, 182-189.

53. Verma, S.; Marsden, P. A. "Nitric oxide-eluting polyurethanes - vascular grafts of the future." *N. Engl. J. Med.* **2005,** *353*, 730-731.

54. Reynolds, M. M.; Hrabie, J. A.; Oh, B. K.; Politis, J. K.; Citro, M. L.; Keefer, L. K.; Meyerhoff, M. E. "Nitric oxide releasing polyurethanes with covalently linked diazeniumdiolated secondary amines." *Biomacromolecules* **2006,** *7*, 987-994.

55. Zhou, Z.; Meyerhoff, M. E. "Polymethacrylate-based nitric oxide donors with pendant N-diazeniumdiolated alkyldiamine moieties: synthesis, characterization, and preparation of nitric oxide releasing polymeric coatings." *Biomacromolecules* **2005,** *6*, 780-789.

56. Marxer, S. M.; Rothrock, A. R.; Nablo, B. J.; Robbins, M. E.; Schoenfisch, M. H. "Preparation of nitric oxide (NO)-releasing sol-gels for biomaterial applications." *Chem. Mater.* **2003,** *15*, 4193-4199.

57. Zhou, Z.; Annich, G. M.; Wu, Y.; Meyerhoff, M. E. "Water soluble poly(ethylenimine)-based nitric oxide donors: preparation, characterization, and potential application in hemodialysis." *Biomacromolecules* **2006,** *7*, 2565-2574.

58. Jeh, H. S.; Lu, S.; George, S. C. "Encapsulation of PROLI/NO in biodegradable microparticles." *J. Microencapsulation* **2004,** *21*, 3-13.

59. Saavedra, J. E.; Dunams, T. M.; Flippen-Anderson, J. L.; Keefer, L. K. "Secondary amine/nitric oxide complex ions, $R_2N[N(O)NO]^-$ O-functionalization chemistry." *J. Org. Chem.* **1992,** *57*, 6134-6138.

60. Saavedra, J. E.; Billiar, T. R.; Williams, D. L.; Kim, Y.-M.; Watkins, S. C.; Keefer, L. K. "Targeting nitric oxide (NO) delivery in vivo." *J. Med. Chem.* **1997,** *40*, 1947-1954.

61. Saavedra, J. E.; Shami, P. J.; Wang, L. Y.; Davies, K. M.; Booth, M. N.; Citro, M. L.; Keefer, L. K. "Esterase-sensitive nitric oxide donors of the diazeniumdiolate family: in vitro antileukemic activity." *J. Med. Chem.* **2000,** *43*, 261-269.

62. Hrabie, J. A.; Saavedra, J. E.; Roller, P. P.; Southan, G. J.; Keefer, L. K. "Conversion of proteins to diazeniumdiolate-based nitric oxide donors." *Bioconjug. Chem.* **1999,** *10*, 838-842.

63. Saavedra, J. E.; Booth, M. N.; Hrabie, J. A.; Davies, K. M.; Keefer, L. K. "Piperazine as a linker for incorporating the nitric oxide-releasing diazeniumdiolate group into other biomedically relevant functional molecules." *J. Org. Chem.* **1999,** *64*, 5124-5131.

64. Chakrapani, H.; Showalter, B. M.; Kong, L.; Keefer, L. K.; Saavedra, J. E. "V-PROLI/NO, a prodrug of the nitric oxide donor, PROLI/NO." *Org. Lett.* **2007,** *9,* 3409-3412.

65. Feldheim, D. L.; Foss, C. A., Jr., *Metal Nanoparticles: Synthesis, Characterization, and Applications*. Marcel Dekker, Inc.: New York, NY, 2002; p 338.

66. Baraton, M.-I., *Synthesis, Functionalization and Surface Treatment of Nanoparticles*. American Scientific Publishers: Stevenson Ranch, Ca., 2003.

67. Fendler, J. H., *Nanoparticles and Nanostructured Films: Preparation, Characterization and Applications*. Wiley-VCH: Weinheim, Germany, 1198; p 468.

68. Guiot, P., *Polymeric Nanoparticles and Microspheres*. CRC Press: Boca Raton, FL, 1986; p 216.

69. Rao, C. N. R.; Mueller, A.; Cheetham, A. K., *The Chemistry of Nanomaterials: Synthesis, Properties and Applications. (Volume 2 of 2)*. Wiley-VCH: Germany, 2004; p 741.

70. Mah, C.; Zolotukhin, I.; Fraites, T. J.; Dobson, J.; Batich, C.; Byrne, B. J. "Microsphere-mediated delivery of recombinant AAV vectors in vitro and in vivo." *Mol. Ther.* **2000,** *1*, S239.

71. Panatarotto, D.; Prtidos, C. D.; Hobeke, J.; Brown, F.; Kramer, E.; Briand, J. P.; Muller, S.; Prato, M.; Bianco, A. "Immunization with peptide-functionalized carbon nanotubes enhances virus-specific neutralizing antibody responses." *Chem. Biol.* **2003,** *10*, 961-966.

72. Bruchez, M.; Moronne, M.; Gin, P.; Weiss, S.; Alivisatos, A. P. "Semiconductor nanocrystals as fluorescent biological labels." *Science* **1998,** *281*, 2013-2016.

73. Chan, W. C. W.; Nie, S. M. "Quantum dot bioconjugates for ultrasensitive nonisotopic detection." *Science* **1998,** *281*, 2016-2018.

74. Edelstein, R. L.; Tamanaha, C. R.; Sheehan, P. E.; Miller, M. M.; Baselt, D. R.; Whitman, L. J.; Colton, R. J. "The BARC biosensor applied to the detection of biological warfare agents." *Biosens. Bioelectron.* **2000,** *14*, 805-813.

75. Nam, J. M.; Thaxton, C. C.; Mirkin, C. A. "Nanoparticles-based bio-bar codes for the ultrasensitive detection of proteins." *Science* **2003,** *301*, 1884-1886.

76. Mahtab, R.; Rogers, J. P.; Murphy, C. J. "Protein-sized quantum dot luminescence can distinguish between "straight", "bent", and "kinked" oligonucleotides." *J. Am. Chem. Soc.* **1995,** *117*, 9099-9100.

77. Ma, J.; Wong, H.; Kong, L. B.; Peng, K. W. "Biomimetic proecessing of nanocrystallite bioactive apatite coating on titanium." *Nanotechnology* **2003,** *14*, 619-623.

78. de la Isla, A.; Brostow, W.; Bujard, B.; Estevez, M.; Rodriquez, J. R.; Vargas, S.; Castano, V. M. "Nanohybrid scratch resistant coating for teeth and bone viscoelasticity manifested in tribology." *Mater. Resr. Innovat.* **2003,** *7*, 110-114.

79. Weissleder, R.; Elizondo, G.; Wittenburg, J.; Rabito, C. A.; Bengele, H. H.; Josephson, L. "Ultrasmall superparamagnetic iron oxide: characterization of a new class of contrast agents for MR imaging." *Radiology* **1990,** *175*, 489-493.

80. Brust, M.; Walker, M.; Bethell, D.; Schiffrin, D. J.; Whyman, R. "Synthesis of thiol-derivatised gold nanoparticles in a two-phase liquid-liquid system." *J. Chem. Soc., Chem. Comm.* **1994**, 801-802.

81. Daniel, M.-C.; Astruc, D. "Gold nanoparticles: assembly, supramolecular chemistry, quantum-size-related properties, and applications towards biology, catalysis, and nanotechnology." *Chem. Rev.* **2004,** *104*, 293-346.

82. Templeton, A. C.; Wuelfing, P. W.; Murray, R. W. "Mololayer-protected cluster molecules." *Acc. Chem. Res.* **2000,** *33*, 27-36.

83. Tkachenko, A. G.; Xie, H.; Coleman, D.; Glomm, W.; Ryan, J.; Anderson, M. F.; Franzen, S.; Feldheim, D. L. "Multifunctional gold nanoparticles." *J. Am. Chem. Soc.* **2003,** *125*.

84. Connor, E. E.; Mwamuka, J.; Gole, A.; Murphy, C. J.; Wyatt, M. D. "Gold nanoparticles are taken up by human cells but do not cause acute cytotoxicity." *Small* **2005,** *1*, 325-327.

85. Rothrock, A. R.; Donkers, R. L.; Schoenfisch, M. H. "Synthesis of nitric oxide-releasing gold nanoparticles." *J. Am. Chem. Soc.* **2005,** *127*, 9362-9363.

86. Hostetler, M. J.; Wingate, J. E.; Zhong, C.-J.; Harris, J. E.; Vachet, R. W.; Clark, M. R.; Londono, J. D.; Green, S. J.; Stokes, J. J.; Wignall, G. D.; Glish, G. L.; Porter, M. D.; Evans, N. D.; Murray, R. W. "Alkanethiolate gold cluster molecules with core diameters from 1.4 to 5.2 nanometers: core and monolayer properties as a function of core size." *Langmuir* **1998,** *14*, 17-30.

87. Hostetler, M. J.; Templeton, A. C.; Murray, R. W. "Dynamics of place-exchange reactions on monolayer-protected gold cluster molecules." *Langmuir* **1999,** *15*, 3782-3789.

88. Polizzi, M. A.; Stasko, N. A.; Schoenfisch, M. H. "Water-soluble nitric oxide-releasing gold nanoparticles." *Langmuir* **2007,** *23*, 4938-4943.

89.   Templeton, A. C.; Chen, S.; Gross, S. M.; Murray, R. W. "Water-soluble, isolable gold clusters protected by tiopronin and coenzyme A monolayers." *Langmuir* **1999,** *15*, 66-76.

90.   Schulz-Dobrick, M.; Sarathy, K. V.; Jansen, M. "Surfactant-free synthesis and functionalization of gold nanoparticles." *J. Am. Chem. Soc.* **2005,** *127*, 12816-12817.

91.   Zhang, H.; Annich, G. M.; Miskulin, J.; Stankiewicz, K.; Osterholzer, K.; Merz, S. I.; Bartlett, R. H.; Meyerhoff, M. E. "Nitric oxide-releasing fumed silica particles: synthesis, characterization, and biomedical application." *J. Am. Chem. Soc.* **2003,** *125*, 5015-5024.

92.   Shin, J. H.; Metzger, S. K.; Schoenfisch, M. H. "Synthesis of nitric oxide-releasing silica nanoparticles." *J. Am. Chem. Soc.* **2007,** *129*, 4612-4619.

93.   Stein, A.; Melde, B. J.; Schroden, R. C. "Hybrid inorganic-organic mesoporous silicates-nanoscopic reactors coming of age." *Adv. Mater.* **2000,** *12*, 1403-1419.

94.   Sayari, A.; Hamoudi, S. "Periodic mesoporous silica-based organic-inorganic nanocomposite materials." *Chem. Mater.* **2001,** *13*, 3151-3168.

95.   Jain, T. K.; Roy, I.; De, T. K.; Maitra, A. "Nanometer silica particles encapsulating active compounds: a novel ceramic drug carrier." *J. Am. Chem. Soc.* **1998,** *120*, 11092-11095.

96.   Munoz, B.; Ramila, A.; Perez-Pariente, J.; Diaz, I.; Vallet-Regi, M. "MCM-41 organic modification as drug delivery rate regulator." *Chem. Mater.* **2003,** *15*, 500-503.

97.   Lai, C.-Y.; Trewyn, B. G.; Jeftinija, D. M.; Jeftinija, K.; Xu, S.; Jeftinija, S.; Lin, V. S.-Y. "A mesoporous silica nanosphere-based carrier system with chemically removable CdS nanoparticle caps for stimuli-responsive controlled release of neurotransmitters and drug molecules." *J. Am. Chem. Soc.* **2003,** *125*, 4451-4459.

98.   Barbe, C.; Bartlett, J.; Linggen, K.; Finnie, K.; Qiang, L. H.; Larkin, M.; Calleja, S.; Bush, A.; Calleja, G. "Silica particles: a novel drug-delivery system." *Adv. Mater.* **2004,** *16*, 1959-1966.

99.   Chang, J. H.; Shim, C. H.; Kim, B. J.; Shin, Y.; Exarhos, G. J.; Kim, K. J. "Biocontinuous, thermoresponsive, L_3-phase silica nanocomposites and their smart drug-delivery applications." *Adv. Mater.* **2005,** *17*, 634-637.

100. Radin, S.; Ducheyne, P.; Kamplain, T.; Tan, B. H. "Silica sol-gel for the controlled release of antibiotics. I. synthesis, characterization, and in vitro release." *J. Biomed. Mater. Res.* **2001,** *57*, 313-320.

101.   Aughenbaugh, W.; Radin, S.; Ducheyne, P. "Silica sol-gel for the controlled release of antibiotics. II. The effect of synthesis parameters on the in vitro release kinetics of vancomycin." *J. Biomed. Mater. Res.* **2001,** *57*, 321-326.

102.   Trewyn, B. G.; Whitman, C. M.; Lin, V. S.-Y. "Morphological control of room-temperature ionic liquid templated mesoporous silica nanoparticles for controlled release of antibacterial agents." *Nano Lett.* **2004,** *4*, 2139-2143.

103.   Roy, I.; Ohulchanskyy, T. Y.; Bharali, D. J.; Pudavar, H. E.; Mistretta, R. A.; Kaur, N.; Prasad, P. N. "Optical tracking of organically modified silica nanoparticles as DNA carriers: a nonviral, nanomedicine approach for gene delivery." *Proc. Natl. Acad. Sci. U.S.A* **2005,** *102*, 279-284.

104.   Han, Y.-J.; Stucky, G. D.; Butler, A. "Mesoporous silicate sequestration and release of proteins." *J. Am. Chem. Soc.* **1999,** *121*, 9897-9898.

105.   Takahashi, H.; Li, B.; Sasaki, T.; Miyazaki, C.; Kajino, T.; Inagaki, S. "Immobilized enzymes in ordered mesoporous silica materials and improvement of their stability and catalytic activity in an organic solvent." *Microporous Mesoporous Mater.* **2001,** *44-45*, 755-762.

106.   Shin, J. H.; Schoenfisch, M. H. "Inorganic/organic hybrid silica nanoparticles as a nitric oxide delivery scaffold." *Chem. Mater.* **2007**, *in press*.

107.   Wanstall, J. C.; Homer, K. L.; Doggrell, S. A. "Evidence for, and importance of, cGMP-independent mechanisms with NO and NO donors on blood vessels and platelets." *Curr. Vasc. Pharmacol.* **2005,** *3*, 41-53.

108.   Hogg, N. "Biological chemistry and clinical potential of *S*-nitrosothiols." *Free Radical Biol. Med.* **2000,** *28*, 1478-1486.

109.   Walsh, G. M.; Leane, D.; Moran, N.; Keyes, T. E.; Forster, R. J.; Kenny, D.; O'Neill, S. "*S*-nitrosylation of platelet $\alpha_{IIb}\beta_3$ as revealed by raman spectroscopy." *Biochemistry* **2007,** *46*, 6429-6436.

110.   Root, P.; Sliskovic, I.; Mutus, B. "Platelet cell-surface protein disulphide-isomerase mediated *S*-nitrosoglutathione consumption." *Biochem. J.* **2004,** *382*, 575-580.

111.   Bell, S. E.; Shah, C. M.; Gordge, M. P. "Protein disulfide-isomerase mediates delivery of nitric oxide redox derivatives into platelets." *Biochem. J.* **2007,** *403*, 283-288.

112.   Al-Sa'doni, H. H.; Ferro, A. "*S*-nitrosothiols as nitric oxide-donors: chemistry, biology and possible future therapeutic applications." *Curr. Med. Chem.* **2004,** *11*, 2679-2690.

113. Hogg, N. "The biochemistry and physiology of *S*-nitrosothiols." *Annu. Rev. Pharmacol. Toxicol.* **2002,** *42*, 585-600.

114. Tyurin, V. A.; Tyurina, Y. Y.; Liu, S.-X.; Bayir, H.; Hubel, C. A.; Kagan, V. E. "Quantification of *S*-nitrosothiols in cells and biological fluids." *Methods in Enzymol.* **2002,** *352*, 347-360.

115. Stamler, J. S. "*S*-nitrosothiols in the blood." *Circ. Res.* **2004,** *94*, 414-417.

116. Dicks, A. P.; Swift, H. R.; Williams, D. L. H.; Butler, A. R.; Al-Sa'doni, H. H.; Cox, B. G. "Identification of Cu^+ as the effective reagent in nitric oxide formation from S-nitrosothiols." *J. Chem. Soc. Perkin Trans. 2* **1996**, 481-487.

117. Williams, D. L. H. "The chemistry of S-nitrosothiols." *Acc. Chem. Res.* **1999,** *32*, 869-876.

118. Sexton, D. J.; Muruganandam, A.; McKenney, D. J.; Mutus, B. "Visible light photochemical release of nitric oxide from *S*-nitrosoglutathione: potential photochemotherapeutic applications." *Photochem. Photobiol.* **1994,** *59*, 463-467.

119. Singh, R. J.; Hogg, N.; Joseph, J.; Kalyanaraman, B. "Mechanism of nitric oxide release from S-nitrosothiols." *J. Biol. Chem.* **1996,** *271*, 18596-18603.

120. Patel, H. M. S.; Williams, D. L. H. "Nitrosation by alkyl nitrites. Part 6. Thiolate nitrosation." *J. Chem. Soc. Perkin Trans. 2* **1990**, 37-42.

121. Ewing, J. F.; Young, D. V.; Janero, D. R.; Garvey, D. S.; Grinnell, T. A. "Nitrosylated bovine serum albumin derivatives as pharmacologically active nitrogen oxide congeners." *J. Pharmacol. Exp. Ther.* **1997,** *283*, 947-954.

122. Katsumi, H.; Nishikawa, M.; Ma, S. F.; Yamashita, F.; Hashida, M. "Physico-chemical, tissue distribution, and vasodilation characteristics of nitrosated serum albumin: delivery of nitric oxide in vivo." *J. Pharm. Sci.* **2004,** *93*, 2343-2352.

123. Katsumi, H.; Nishikawa, M.; Yamashita, F.; Hashida, M. "Development of polyethylene glycol-conjugated poly-*S*-nitrosated serum albumin, a novel *S*-nitrosothiol for prolonged delivery of nitric oxide in the blood circulation in vivo." *J. Pharmacol. Exp. Ther.* **2005,** *314*, 1117-1124.

124. Marks, D. S.; Vita, J. A.; Folts, J. D.; Keaney, J. F., Jr.; Welch, G. N.; Loscalzo, J. "Inhibition of neointimal proliferation in rabbits after vascular injury by a single treatment with a protein adduct of nitric oxide." *J. Clin. Investig.* **1995,** *96*, 2630-2638.

125. Shishido, S. M.; de Oliveira, M. G. "Polyethylene glycol matrix reduces the rates of photochemical and thermal release of nitric oxide from *S*-nitroso-*N*-acetylcysteine." *Photochem. Photobiol.* **2000,** *71*, 273-280.

126. Ishima, Y.; Sawa, T.; Kragh-Hansen, U.; Miyamoto, Y.; Matsushita, S.; Akaike, T.; Otagiri, M. "*S*-nitrosylation of human variant albumin liprizzi (R410C) confers potent antibacterial and cytoprotective properties." *J. Pharmacol. Exp. Ther.* **2007,** *320*, 969-977.

127. Hess, D. T.; Matsumoto, A.; Kim, S. O.; Marshall, H. E.; Stamler, J. S. "Protein *S*-nitrosylation: purview and parameters." *Nat. Rev. Mol. Cell Biol.* **2005,** *6*, 150-166.

128. McMahon, T. J.; Stone, A. E.; Bonaventura, J.; Singel, D. J.; Stamler, J. S. "Functional coupling of oxygen binding and vasoactivity in *S*-nitrosohemoglobin." *J. Biol. Chem.* **2000,** *275*, 16738-16745.

129. Patel, R. P.; Hogg, N.; Spencer, N. Y.; Kalyanaraman, B.; Matalon, S.; Darley-Usmar, V. M. "Biochemical characterization of human *S*-nitrosohemoglobin." *J. Biol. Chem.* **1999,** *274*, 15487-15492.

130. Ship, N. J.; Pezacki, J. P.; Kluger, R. "Rates of release of nitric oxide from HbSNO and internal electron transfer." *Bioorg. Chem.* **2003,** *31*, 3-10.

131. Singel, D. J.; Stamler, J. S. "Chemical physiology of blood flow regulation by red blood cells: the role of nitric oxide and *S*-nitrosohemoglobin." *Annu. Rev. Physiol.* **2005,** *67*, 99-145.

132. Pezacki, J. P.; Pelling, A.; Kluger, R. "*S*-nitrosylation of cross-linked hemoglobins at β-cysteine-93: stabilized hemoglobins as nitric oxide sources." *J. Am. Chem. Soc.* **2000,** *122*, 10734-10735.

133. Diesen, D.; Stamler, J. S. "S-nitrosylation and PEGylation of hemoglobin: toward a blood substitute that recapitulates blood." *J. Mol. Cell Cardiol.* **2007,** *42*, 921-923.

134. Asanuma, H.; Nakai, K.; Sanada, S.; Minamino, T.; Takashima, S.; Ogita, H.; Fujita, M.; Hirata, A.; Wakeno, M.; Takahama, H.; Kim, J.; Asakura, M.; Sakuma, I.; Kitabatake, A.; Hori, M.; Komamura, K.; Kitakaze, M. "S-nitrosylated and PEGylated hemoglobin, a newly developed artificial oxygen carrier, exerts cardioprotection against ischemic hearts." *J. Mol. Cell Cardiol.* **2007,** *42*, 924-930.

135. Shishido, S. M.; Seabra, A. B.; Loh, W.; de Oliveira, M. G. "Thermal and photochemical nitric oxide release from *S*-nitrosothiols incorporated in Pluronic F127 gel: potential uses for local and controlled nitric oxide release." *Biomaterials* **2003,** *24*, 3543-3553.

136. Seabra, A. B.; de Souza, G. F. P.; da Rocha, L. L.; Eberlin, M. N.; de Oliveira, M. G. "S-nitrosoglutathione incorporated in poly(ethylene glycol) matrix: potential use for topical nitric oxide delivery." *Nitric Oxide* **2004,** *11*, 263-272.

137.   Seabra, A. B.; da Rocha, L. L.; Eberlin, M. N.; de Oliveira, M. G. "Solid films of blended poly(vinyl alcohol)/poly(vinyl pyrrolidone) for topical S-nitrosoglutathione and nitric oxide release." *J. Pharm. Sci.* **2005,** *94*, 994-1003.

138.   Seabra, A. B.; da Silva, R.; de Oliveira, M. G. "Polynitrosated polyesters: preparation, characterization, and potential use for topical nitric oxide release." *Biomacromolecules* **2005,** *6*, 2512-2520.

139.   Seabra, A. B.; de Oliveira, M. G. "Poly(vinyl alcohol) and poly(vinyl pyrrolidone) blended films for local nitric oxide release." *Biomaterials* **2004,** *25*, 3773-3782.

140.   Duan, X.; Lewis, R. S. "Improved haemocompatibility of cysteine-modified polymers via endogenous nitric oxide." *Biomaterials* **2002,** *23*, 1197-1203.

141.   Bohl, K. S.; West, J. L. "Nitric oxide-generating polymers reduce platelet adhesion and smooth muscle cell proliferation." *Biomaterials* **2000,** *21*, 2273-2278.

142.   Bohl-Masters, K. S.; Lipke, E. A.; Rice, E. E. H.; Liel, M. S.; Myler, H. A.; Zygourakis, C.; Tulis, D. A.; West, J. L. "Nitric oxide-generating hydrogels inhibit neointima formation." *J. Biomater. Sci. Polymer Edn.* **2005,** *16*, 659-672.

143.   Frost, M. C.; Meyerhoff, M. E. "Synthesis, characterization, and controlled nitric oxide release from S-nitrosothiol-derivatized fumed silica polymer filler particles." *J. Biomed. Mater. Res., Part A* **2005,** *72*, 409-419.

144.   Frost, M. C.; Meyerhoff, M. E. "Controlled photoinitiated release of nitric oxide from polymer films containing *S*-nitroso-*N*-acetyl-DL-penicillamine derivatized fumed silica filler." *J. Am. Chem. Soc.* **2004,** *126*, 1348-1349.

145.   Rotta, J. C. G.; Lunardi, C. N.; Tedesco, A. C. "Nitric oxide release from the *S*-nitrosothiol zinc phthalocyanine complex by flash photolysis." *Braz. J. Med. Biol. Res.* **2003,** *36*, 587-594.

146.   Ohulchanskyy, T. Y.; Roy, I.; Goswami, L. N.; Chen, Y.; Bergey, E. J.; Pandey, R. K.; Oseroff, A. R.; Prasad, P. N. "Organically modified silica nanoparticles with covalently incorporated photosensitizer for photodynamic therapy of cancer." *Nano Lett.* **2007,** *7*, 2835-2842.

147.   Wheatley, P. S.; Butler, A. R.; Crane, M. S.; Fox, S.; Xiao, B.; Rossi, A. G.; Megson, I. L.; Morris, R. E. "NO-releasing zeolites and their antithrombotic properties." *J. Am. Chem. Soc.* **2006,** *128*, 502-509.

148.   Xiao, B.; Wheatley, P. S.; Zhao, X.; Fletcher, A. J.; Fox, S.; Rossi, A. G.; Megson, I. L.; Bordiga, S.; Regli, L.; Thomas, K. M.; Morris, R. E. "High-capacity hydrogen and nitric oxide adsorption and storage in a metal-organic framework." *J. Am. Chem. Soc.* **2007,** *129*, 1203-1209.

149. Caruso, E. B.; Petralia, S.; Conoci, S.; Giuffrida, S.; Sortino, S. "Photodelivery of nitric oxide from water-soluble platinum nanoparticles." *J. Am. Chem. Soc.* **2007,** *129,* 480-481.

150. Sortino, S.; Petralia, S.; Compagnini, G.; Conoci, S.; Condorelli, G. "Light-controlled nitric oxide generation from a novel self-assembled monolayer on a gold surface." *Angew. Chem., Int. Ed.* **2002,** *41*, 1914-1917.

151. Ford, P. C.; Bourassa, J.; Miranda, K.; Lee, B.; Lorkovic, I.; Boggs, S.; Kudo, S.; Laverman, L. "Photochemistry of metal nitrosyl complexes. Delivery of nitric oxide to biological targets." *Coord. Chem. Rev.* **1998,** *171*, 185-202.

152. Tfouni, E.; Krieger, M.; McGarvey, B. R.; Franco, D. W. "Structure, chemical and photochemical reactivity and biological activity of some ruthenium amine nitrosyl complexes." *Coord. Chem. Rev.* **2003,** *236*, 57-69.

153. Eroy-Reveles, A. A.; Leung, Y.; Mascharak, P. K. "Release of nitric oxide from a sol-gel hybrid material containing a photoactive manganese nitrosyl upon illumination with visible light." *J. Am. Chem. Soc.* **2006,** *128*, 7166-7167.

154. Neuman, D.; Ostrowski, A. D.; Absalonson, R. O.; Strouse, G. F.; Ford, P. C. "Photosensitized NO release from water-soluble nanoparticle assemblies." *J. Am. Chem. Soc.* **2007,** *129*, 4146-4147.

155. Hanson, S. R.; Hutsell, T. C.; Keefer, L. K.; Mooradian, D. L.; Smith, D. J. "Nitric oxide donors: a continuing opportunity in drug design." *Adv. Pharmacol.* **1995,** *34*, 383-398.

156. Stiriba, S.-E.; Frey, H.; Haag, R. "Dendritic polymers in biomedical applications: from potential to clinical use in diagnostics and therapy." *Angew. Chem. Int. Ed.* **2002,** *41*, 1329-1334.

157. Gillies, E. R.; Frechet, J. M. "Dendrimers and dendritic polymers in drug delivery." *Drug Discovery Today* **2005,** *10*, 35-43.

158. Svenson, S.; Tomalia, D. A. "Dendrimers in biomedical applications-reflections on the field." *Adv. Drug Deliv. Rev.* **2005,** *57*, 2106-2129.

159. Kukowska-Latallo, J. F.; Candido, K. A.; Cao, Z.; Nigavekar, S. S.; Majoros, I. J.; Thomas, T. P.; Balogh, L. P.; Khan, M.; Baker, J. R. "Nanoparticle targeting of anticancer drug improves therapeutic response in animal model of human epithelial cancer." *Cancer Res.* **2005,** *65*, 5317-5324.

160. Kolhe, P.; Khandare, J.; Pillai, O.; Kannan, S.; Lieh-Lai, M.; Kannan, R. M. "Preparation, cellular transport, and activity of polyamidoamine-based dendritic nanodevices with a high drug payload." *Biomaterials* **2006,** *27*, 660-669.

161.   Frechet, J. M. "Dendrimers and other dendritic macromolecules: from building blocks to functional assemblies in nanoscience and nanotechnology." *J. Polym. Sci. A: Poly. Chem.* **2003,** *41*, 3713-3725.

162.   Vogtle, F.; Stephan, H.; Johannsen, B.; Spies, H.; Klein, L. "Lipophilic urea-functionalized dendrimers as efficient carriers for oxyanions." *Chem. Comm.* **1999**, 1875-1876.

163.   Morgan, M. T.; Carnahan, M. A.; Immoos, C. E.; Ribeiro, A. A.; Finkelstein, S.; Lee, S. J.; Grinstaff, M. W. "Dendritic molecular capsules for hydrophobic compounds." *J. Am. Chem. Soc.* **2003,** *125*, 15485-15489.

164.   Patri, A. K.; Myc, A.; Bander, N. H.; Baker, J. R. J. "Synthesis and in vivo testing of J591 antibody-dendrimer conjugates for targeted prostate cancer therapy." *Bioconjug. Chem.* **2004,** *15*, 1174-1181.

Chapter 2:

Diazeniumdiolate-Modified Dendrimers as Scaffolds for Nitric Oxide Release

2.1 Introduction

Nitric oxide (NO), a diatomic free radical produced in the human body, regulates several biological functions in the cardiovascular, respiratory, and nervous systems.[1, 2] Nitric oxide is also actively involved in the immune system response and mediates macrophage destruction of foreign pathogens.[3] The complex and wide ranging roles of NO in normal physiological function thus demand methods for chemically storing and releasing NO in a controlled manner. Metal complexes, nitrosothiols, nitrosamines, and diazeniumdiolates are all examples of molecular structures that have been developed as effective NO donors.[4] Such "NO donors" facilitate the improved understanding of NO's function in biological systems and may potentially serve as therapeutic agents for a number of disease states.[5]

Diazeniumdiolate NO donors are particularly attractive because they dissociate spontaneously under physiological conditions (i.e., 37°C, pH 7.4) to yield two moles of NO per mole of NO donor.[6] *N*-bound diazeniumdiolates formed from the reaction of amines with high pressures of NO were initially reported by Drago and Paulik in the 1960's.[7, 8] The rapid discovery of NO's role in biology has resulted in the resurgence of amine based diazeniumdiolate NO donors. Keefer and coworkers have reported the synthesis and characterization of multiple small molecule diazeniumdiolates where NO release rates are governed by the chemical structure of the amine precursor.[6, 9, 10] For example,

diazeniumdiolate derivatives of the polyamine diethylenetriamine (DETA/NO) resulted in lengthy durations of NO release with a half-life ($t_{1/2}$) of 56 h. In contrast, proli/NO has a $t_{1/2}$ of only 5 s.[10]

Larger molecular frameworks have also been modified with diazeniumdiolate NO donors to produce materials capable of storing large quantities of NO. Pulfer et al. synthesized diazeniumdiolated poly(ethylene imine) microspheres which were embedded into the pores of small-diameter prosthetic grafts to prevent thrombosis via the controlled release of NO.[11] Similarly, Meyerhoff and co-workers reported the synthesis of fumed silica particles with aminoalkoxysilanes grafted on the surface as substrates for diazeniumdiolate formation. The storage of NO was mediated by the type of aminosilane grafted. The silica particles prepared via this method released up to 0.56 μmol NO/mg.[12] These NO-releasing silica particles were initially employed as fillers for preparing silicone rubber coatings for extracorporeal circuits.[12] Hrabie et al. synthesized a water soluble macromolecular NO donor with a $t_{1/2}$ of 20 d via covalent attachment of a NO donor piperazine ligand to the solvent accessible lysine residues of bovine serum albumin.[13] Nitric oxide release was initiated via the slow hydrolytic cleavage of the methoxymethyl protecting group. Proteins modified with diazeniumdiolate ligands demonstrate a strategy for increasing the stability and systemic half-life of NO donors in vivo.

Rothrock et al. reported the synthesis of NO-releasing gold monolayer protected clusters (MPCs) through diamine functionalization of bromine thiol ligands followed by subsequent amine conversion to diazeniumdiolates.[14] Although capable of releasing NO, the NO donor-modified nanoparticles were characterized by poor amine to diazeniumdiolate conversion efficiencies, lack of aqueous solubility, and limited surface functionality. Such factors warrant the development of more efficient, multifunctional nanoparticle NO donor scaffolds.

In contrast to gold and silica particles, dendrimers are hyper-branched nanostructures possessing a multivalent surface with well defined polymeric structure.[15, 16] Dendrimers are assembled by one of two general strategies: 1) the divergent method, where repeat monomers are branched outward from a central core; or, 2) the convergent method developed by Frechet et al.,[17] where the synthesis begins at the periphery and grows inward. The resulting dendrimer products are monodisperse compared to bulk polymers, and their size (2-20 nm) varies with dendrimer type and exterior functionality.[18] The structure of a generation 3 polypropylenimine dendrimer (DAB-Am-16) is shown in Figure 2.1. Produced via divergent synthesis, this dendrimer has become a widely utilized construct due to its multivalent, primary amine exterior.[16] The multifunctional surface and unique structural properties of dendrimers have resulted in their widespread utility as drug delivery agents and medical diagnostic tools in the pharmaceutical and nanotechnology industries.[18-21]

In this chapter, the development of nanoparticle NO donors that store and release large quantities of NO from dendritic scaffolds is described. The primary advantage of NO releasing dendrimers over other NO donor systems is the ability to store high concentrations of NO on a single molecular framework. The exterior of NO releasing dendrimers can also be manipulated to enable specific functionality (e.g., solubility) producing macromolecular NO donors tailored for a desired application. For example, dendrimer-based NO donors possessing lipophilic exteriors may be incorporated into hydrophobic polymers to impart thromboresistivity. Water soluble, hydrophilic dendrimers may allow for the development of therapeutic agents capable of delivering NO in vivo. The synthesis and NO storage capacity of several polypropylenimine dendrimer conjugates are presented. Furthermore, dendritic NO release kinetics are explored as a function of dendrimer size, structure of dendrimer bound amine precursor, and lipophilicity of the dendritic exterior.

2.2 Experimental Section

2.2.1 General

All reagents including generation 3 and generation 5 polypropylenimine dendrimers (DAB-Am-16 and DAB-Am-64) were purchased from the Aldrich Chemical Company (Milwaukee, WI). Methanol was distilled over magnesium prior to use. Water was purified with a Millipore Milli-Q gradient A-10 purification system (Bedford, MA). Spectra/Por® Float-A-Lyzers® were purchased from Spectrum Laboratories Inc. (Rancho Dominguez, CA). Absorption spectra were recorded on a Perkin Elmer Lambda 40 UV-Vis spectrophotometer (Norwalk, CT). Nuclear magnetic resonance (NMR) spectra were collected in $CDCl_3$, CD_3OD, or D_2O using a 400-MHz Bruker Nuclear Magnetic Resonance spectrometer. Mass spectra were acquired in positive ion mode using a Micromass Quattro II triple quadrupole mass spectrometer equipped with a nano-electrospray ionization source. Nitric oxide release was measured using a Sievers 280i Chemiluminesce Nitric Oxide Analyzer (Boulder, CO).

2.2.2 Formation of the diazeniumdiolate NO donor

Parent primary amine dendrimers and the dendrimer conjugates were dissolved in 0.5 M NaOMe/MeOH and placed in 5 mL glass vials equipped with a stir bar prior to exposure to NO gas. The vials were placed in a Parr bottle, connected to the NO-reactor, and flushed six times with Ar, followed by a series of six longer charge/discharge cycles with Ar (6 x 10 min) to remove oxygen from the stirring solutions. The Parr bottle was then filled with 5 atm of NO (purified over KOH pellets for 30 min to remove trace NO degradation products) and sealed. After 3 d the NO was expunged using the same Ar procedure described above to remove unbound NO from the dendrimer-diazeniumdiolate product solutions.

2.2.3 Characterization of NO-releasing dendrimers

Two methods were employed to characterize the formation of the *N*-bound diazeniumdiolate NO donor species. First, absorption spectroscopy was used to confirm diazeniumdiolate formation. UV-Vis spectra recorded on a Perkin-Elmer spectrophotometer in dilute MeOH solutions displayed the characteristic diazeniumdiolate absorption maximum (λ_{max}) between 250-260 nm for diazeniumdiolates in all cases.[9] Second, NO released from the polypropylenimine dendrimer conjugates was measured upon donor decomposition via chemiluminescence.[22] Aliquots (10 μL) of the NO exposed dendrimer solution were added to 0.01 M phosphate buffered saline (PBS, pH=7.4) at 37 °C to initiate NO release under physiological conditions.[23] Dendrimer concentrations ranged from 0.2 to 1.0 mM. The chemiluminescence analyzer was calibrated with NO gas (24.1 ppm). A parameter for converting the instrument response (ppb) to moles of NO was obtained via the conversion of nitrite standards to NO in a 0.1 M KOH/H_2SO_4 solution (1.19×10^{-13} moles NO/ppb). Chemiluminescence data for the NO-releasing dendrimers were represented in two graphical forms or plots: 1) chemiluminescence response in ppb NO/mg dendrimer vs. time; and, 2) the total amount of NO-release (t[NO]) vs. time. The maximum flux of NO release ($[NO]_m$) and the time required to reach that maxima (t_m) were obtained from plot 1. The half-life ($t_{1/2}$) of NO release as well as the t[NO] (μmol NO/mg) can be determined from plot 2.

2.2.4 Synthesis and characterization of dendrimer conjugates

2.2.4.1 DAB-C7-16 (**3**) (adapted from Pan and Ford[24])

(A) Heptanoyl chloride (410 mg, 2.75 mmol) was added to a stirring solution of DAB-Am-16 (200 mg, 0.12 mmol), DMF (5 mL), and triethylamine (343 mg, 3.4 mmol) at 0 °C. The ice bath was removed and the solution was stirred under nitrogen at 70 °C for 24 h. Water (3.0 mL) was added, the solution was stirred for 10 min and concentrated under reduced pressure. The orange residue was dissolved in CH_2Cl_2 (20 mL), washed with 1%

aqueous K_2CO_3 (2 x 20 mL), rinsed with brine, dried over K_2CO_3 and concentrated under reduced pressure.

(B) The residue from procedure A was immediately dissolved in THF (5 mL) and added slowly to a stirring suspension of $LiAlH_4$ (10 mmol) in THF (40 mL) under nitrogen at 0 °C. The suspension was stirred at reflux for 24 h and transferred slowly into saturated aqueous Na_2SO_4 solution (40 mL) at 5-10 °C. The THF layer was decanted, and the aqueous layer was extracted with ether (3 x 25 mL). The combined organic phase was washed with 4% aqueous K_2CO_3 (20 mL), dried over K_2CO_3, and concentrated under reduced pressure. The crude product was purified on an Al_2O_3 column (80-200 Mesh, Fischer Scientific; MeOH/$CHCl_3$, 2:98) to yield 266 mg (63%) of a viscous yellow oil. ^{1}H NMR ($CDCl_3$, δ): 0.85 (t, CH_3), 1.20-1.33 (m, CH_2), 1.39-1.72 (m, $NCH_2CH_2CH_2N$, $NCH_2CH_2CH_2$), 2.31-2.49 (m, $CH_2N(CH_2)_2$), 2.51-2.64 (m, CH_2NH). ^{13}C NMR (CDCl3, δ): 13.97 (CH_3), 22.42 (CH_2CH_3), 24.17 ($NCH_2CH_2CH_2N$), 28.69 (alkyl CH_2), 49.38 ($NCH_2CH_2CH_2NH$), 51.26 ($NHCH_2CH_2$), 51.7 ($NCH_2CH_2CH_2NH$), 51.8 ($NCH_2CH_2CH_2N$).

2.2.4.2 DAB-C7-64 (4) (adapted from Pan and Ford[24])

(A) Heptanoyl chloride (370 mg, 2.5 mmol) was added to a stirring solution of DAB-Am-64 (200 mg, 0.028 mmol), DMF (5 mL), and triethylamine (310 mg, 3.1 mmol) at 0 °C. The ice bath was removed and the solution was stirred under nitrogen at 70 °C for 24 h. Water (3.0 mL) was added, the solution was stirred for 10 min and concentrated under reduced pressure. The dark orange residue was dissolved in CH_2Cl_2 (20 mL), washed with 1% aqueous K_2CO_3 (2 x 20 mL), rinsed with brine, dried over K_2CO_3 and concentrated under reduced pressure.

(B) The residue from procedure A was immediately dissolved in THF (5 mL) and added slowly to a stirring suspension of LiAlH$_4$ (10 mmol) in THF (40 mL) under nitrogen at 0 °C. The suspension was stirred at reflux for 24 h and transferred slowly into saturated aqueous Na$_2$SO$_4$ solution (40 mL) at 5-10 °C. The THF layer was decanted, and the aqueous layer was extracted with ether (3 x 25 mL). The combined organic phase was washed with 4% aqueous K$_2$CO$_3$ (20 mL), dried over K$_2$CO$_3$, and concentrated under reduced pressure. The crude product was purified on an Al$_2$O$_3$ column (80-200 Mesh, Fischer Scientific; MeOH/CHCl$_3$, 2:98) to yield 157 mg (42%) of a dark yellow oil. ^{1}H NMR (CDCl$_3$, δ): 0.86 (t, CH_3), 1.19-1.4 (m, CH_2), 1.40-1.76 (m, NCH$_2$CH_2CH$_2$N, NCH$_2$CH_2CH$_2$), 2.30-2.49 (m, CH_2N(CH$_2$)$_2$), 2.50-2.75 (m, CH_2NH). ^{13}C NMR (CDCl3, δ): 14.21 (CH_3), 22.69 (CH_2CH$_3$), 24.12 (NCH$_2$CH_2CH$_2$N), 30.46 (alkyl CH_2), 31.81 (NHCH$_2$CH_2), 31.98 (CH_2CH$_2$CH$_3$), 50.92 (CH$_2$CH_2NHCH_2CH$_2$), 52.41 (NCH_2CH$_2$CH_2N).

2.2.4.3 DAB-C16-16 (**5**)

(Same procedure as described above for DAB-C7-16 but replacing heptanoyl chloride (C7) with palmitoyl chloride (C16) as the acylating reagent.

2.2.4.4 DAB-PO-64 (**6**) (adapted from Pantos et al.[25])

280 mg (4.8 mmol) of propylene oxide dissolved in 2 mL of water was added dropwise to 530 mg (0.074 mmol) of DAB-Am-64 dissolved in 5 mL of water. The mixture was allowed to react for 24 h at room temperature, dialyzed using a Spectra/Por® Float-A-Lyzer® (10 mL, 5000 MWCO), and lyophilized to yield 305 mg (38%) of an opaque oil. ^{1}H NMR (D$_2$O, δ): 1.13 (d, NHCH$_2$CH(OH)CH_3), 1.27 (t, NCH$_2$CH_2CH_2CH$_2$N), 1.52-1.74 (m, CH$_2$), 2.33-2.52 (m, CH_2N(CH$_2$)$_2$), 2.54 (t, CH_2NHCH$_2$), 2.68 (m, NHCH_2CH(OH)CH$_3$), 3.89 (m, NHCH$_2$CH(OH)CH$_3$). ^{13}C NMR (CDCl3, δ): 20.47 (NHCH$_2$CH(OH)CH_3), 22.13

(NCH$_2$*CH$_2$CH$_2$*CH$_2$N), 23.4 (NCH$_2$CH$_2$*CH$_2$*N), 25.17 (NCH$_2$CH$_2$*CH$_2$*NH), 47.1 (*CH$_2$*NHCH$_2$CH(OH)CH$_3$), 51.14 (N*CH$_2$*CH$_2$CH$_2$N), 51.7 (N*CH$_2$*CH$_2$CH$_2$*CH$_2$*N), 55.69 (NH*CH$_2$*CH(OH)CH$_3$), 65.97 (NHCH$_2$*CH*(OH)CH$_3$). MS (ESI) calcd: 10,885. Found: 10,537 [1054.7 (M+10H)$^{10+}$, 980.1 (M+11H)$^{11+}$].

2.2.4.5 DAB-Pro-16 and DAB-Pro-64 (**7** and **8**)

(A) 2.565 g (12 mmol) of t-boc-L-proline was dissolved in 30 mL of CH$_2$Cl$_2$ to which was added 1.37 g (12 mmol) N-hydroxy succinimide (NHS) and 2.70 g (13 mmol) dicyclohexylcarbodiimide (DCC). The solution was stirred at 0 °C for 24, filtered to removed the DCU solid impurity, concentrated under reduced pressure to yield a crude solid. The white solid was recrystallized in isopropanol and isolated to yield 3.31 g of NHS-t-boc-L-proline.

(B) 0.658g (2.1 mmol) NHS-t-boc-L-proline and 0.293 mL (2.1 mmol) added to 0.20 g (1.9 mmol) of DAB-Am-16 dissolved in 10 mL of CH$_2$Cl$_2$ and stirred for 24 h at room temperature. The solution was washed 3x with H$_2$O, 3x with saturated Na$_2$CO$_3$, dried over Na$_2$SO$_4$, and concentrated under reduced pressure to yield a white silky solid. The white solid was immediately dissolved in 4 mL of formic acid and stirred for 16 h at room temperature to remove the boc protecting groups. The formic acid was removed under vacuum and the resulting oil was dissolved in 5 mL of H$_2$O, neutralized with 6 M NaOH to pH 7, dialyzed in distilled water for 5 d, and lyophilized to yield 15.5 mg of DAB-Pro-16.

2.2.4.6 DAB-Ac-16 (**9**)

Acetic anhydride (340 mg, 3.3 mmol) and triethylamine (370 mg, 3.6 mmol) were added to a solution of DAB-Am-16 (290 mg, 0.17 mmol) dissolved in 5 mL of anhydrous MeOH. The mixture was stirred for 24 h at room temperature under nitrogen. The reaction mixture was concentrated under reduced pressure and resuspended in 10 mL of ultra pure MilliQ

water for dialysis. The product solution was dialyzed in a Spectra/Por® Float-A-Lyzer® (10 mL, 1000 MWCO) in 2 L phosphate buffer pH = 8.0 for 24 h. The buffer was discarded, the product solution dialyzed in ultrapure water for 3 d and lyophilized to yield 35 mg (8.5%) of a clear solid: ^{1}H NMR (CD$_3$OD, δ): 1.59-1.65 (br, NCH$_2$CH_2CH_2CH$_2$N), 1.65-1.80 (m, NCH$_2$CH_2CH$_2$N, NCH$_2$CH_2CH$_2$NH), 1.85 (s, CH$_3$), 2.63-2.70 (m, NCH_2CH$_2$CH_2N), 2.70-2.79 (m, NCH_2CH$_2$CH$_2$NHCO), 3.13 (t, CH_2NHCOCH$_3$). ^{13}C NMR (CD$_3$OD, δ):   22.8 (NHCOCH_3), 23.2 (NCH$_2$CH_2CH$_2$N), 26.1 (NCH$_2$CH_2CH$_2$NHCO), 38.6 (CH_2NHCOCH$_3$), 52.9 (NCH_2CH$_2$CH_2N), 53.4 (NCH_2CH$_2$CH$_2$CH_2N),   174 (C=O). MS (ESI) calcd: 2359.5. Found: 2358.9 [1180.4 (M+2H)$^{2+}$, 787.3 (M+3H)$^{3+}$, 590.8 (M+4H)$^{4+}$].

2.2.4.5 DAB-Ac-64 (**10**)

Acetic anhydride (160 mg, 1.5 mmol) and triethylamine (170 mg, 1.7 mmol) were added to a solution of DAB-Am-64 (140 mg, 0.02 mmol) dissolved in 5 mL of anhydrous MeOH. The mixture was stirred for 24 h at room temperature under nitrogen. The reaction mixture was then concentrated under reduced pressure and resuspended in 10 mL of ultra pure MilliQ water for dialysis. The product solution was dialyzed in a Spectra/Por® Float-A-Lyzer® (10 mL, 1000 MWCO) in 2 L phosphate buffer pH = 8.0 for 24 h. The buffer was discarded, the product solution dialyzed in ultrapure water for 3 d, and lyophilized to yield 26 mg (13.1%) of a clear sticky solid: ^{1}H NMR (CD$_3$OD, δ): 1.55-1.77 (m, NCH$_2$CH_2CH$_2$N, NCH$_2$CH_2CH_2CH$_2$N), 1.86 (s, CH$_3$), 2.47-2.62 (m, NCH_2CH$_2$CH_2N), 2.66-2.79 (m, NCH_2CH$_2$CH$_2$NHCO), 3.11 (t, CH_2NHCOCH$_3$). ^{13}C NMR (CD$_3$OD, δ):   22.98 (NHCOCH_3), 23.65 (NCH$_2$CH_2CH$_2$N), 38.71 (CH_2NHCOCH$_3$), 52.5 (NCH_2CH$_2$CH_2N), 173 (C=O). MS (ESI) calcd: 9858.75. Found: 9859 [1233.6 (M+8H)$^{8+}$, 1096.5 (M+9H)$^{9+}$, 987.0 (M+10H)$^{10+}$].

2.3 Results and Discussion

2.3.1 Nitric oxide releasing primary amine dendrimers

Dendrimers provide an attractive scaffold for storing NO because of their multivalent exterior. A dendrimer fully modified with diazeniumdiolates has the potential to store large quantities of NO on a single framework, thereby increasing the "payload" of NO per gram of substrate. Previously, polyamines have been shown to convert readily to diazeniumdiolates.[10] Secondary amines in the polyamine backbone react with NO to form a diazeniumdiolate NO donor that is stabilized via neighboring cationic amines. The diazeniumdiolate adduct of diethylenetriamine, a short polyamine, is depicted in Figure 2.2A. In addition to increasing the stability of the zwitterionic species, remote amines enhance the duration of NO release by providing alternate sites of protonation, thus slowing the proton driven dissociation of diazeniumdiolates to NO.[9] Polypropylenimine dendrimers are large polyamines grown in a divergent fashion, terminated by a multitude of primary amines based on the dendrimer generation. As such, the exterior of a polypropylenimine dendrimer has both a large number of nucleophilic amines to react with NO, and a multiple of neighboring amine sites for diazeniumdiolate NO donor stabilization (Figure 2.2B). Primary amines typically form unstable NO donors and decompose rapidly to NO under ambient or aqueous conditions.[8] However, the density of primary amines at the exterior and the conformational freedom of the dendritic architecture may lead to enhanced diazeniumdiolate stability over small molecule primary amine substrates.
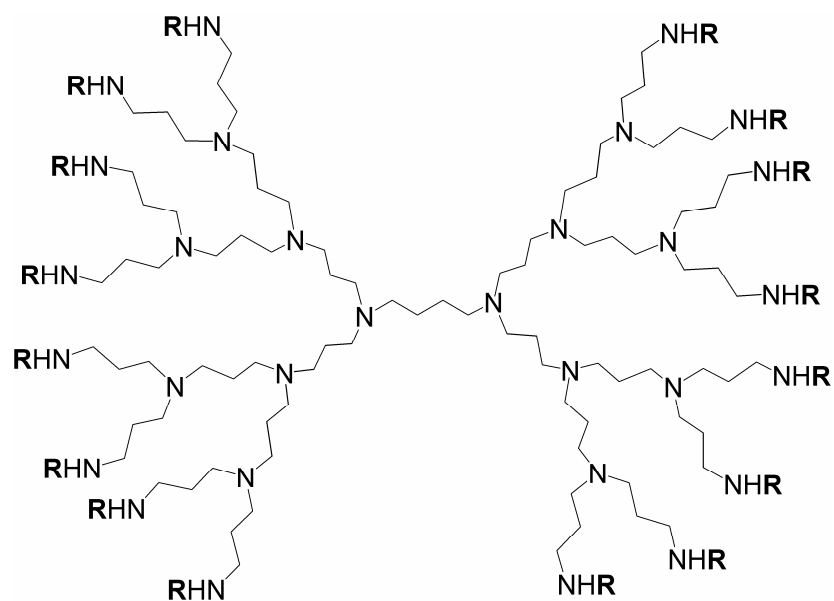
Figure 2.1   Generation 3 polypropylenimine dendrimer, DAB-Am-16, possessing a diaminobutane core and 16 primary amines where R = H.
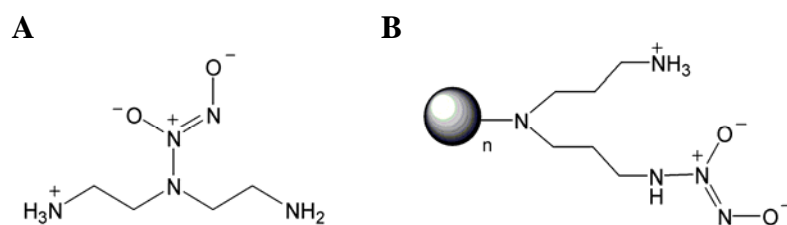
Figure 2.2   Ammonium cation stabilized diazeniumdiolates: A) diazeniumdiolate of diethylenetriamine, DETA/NO[8]; and, B) dendrimer bound diazeniumdiolate where n = 8 or 32 (DAB-Am-16 or DAB-Am-64).
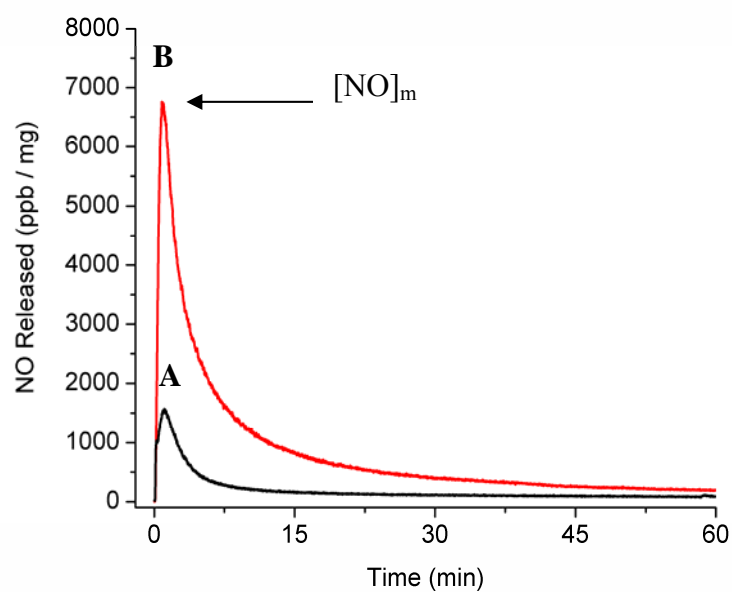
Figure 2.3   Real time NO release profiles for **1** (DAB-Am-16) charged in A) MeOH and B) NaOMe/MeOH.
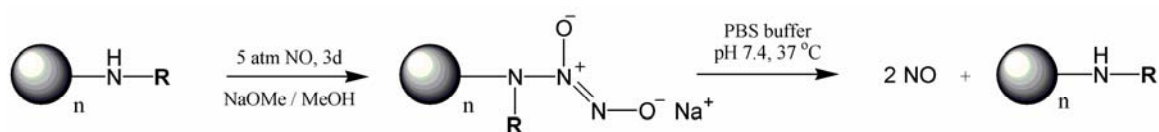
Scheme 2.1   Formation of sodium stabilized diazeniumdiolates followed by decomposition under physiological conditions to yield two moles of NO and initial dendrimer conjugate (n=16, 64).

To test the ability of primary amine terminated dendrimers to store NO via diazeniumdiolate NO donors, generation 3 polypropylenimine dendrimer (DAB-Am-16) was selected as an initial substrate for diazeniumdiolate conversion. DAB-Am-16 (**1**) was dissolved in MeOH and exposed to high pressures (5 atm) of NO for 3 d. Herein, this process will be referred to as "charging," or the introduction of the multiply charged, zwitterionic diazeniumdiolate moiety. An aliquot of the charged MeOH solution containing **1** (200 μM) was added to a reaction flask containing degassed phosphate buffered saline (PBS; 0.01 M, pH 7.4) and the corresponding NO release was monitored at physiological temperature (37 °C) by chemiluminescence.[22] Despite an initial burst of NO (Figure 2.3A), the polyamine dendrimer failed to yield the lengthy NO release durations of the polyamine diazeniumdiolate DETA/NO.

The conversion efficiency of amine precursor to diazeniumdiolate NO donor was calculated to examine the effect of the dendritic structure and amine functionality on NO storage capacity. Assuming the maximum theoretical yield of two moles of NO per one mole of amine precursor, the conversion efficiency is defined as the total moles of NO released divided by twice the number of dendrimer bound substrate amines (Equation 2.1).

Equation 2.1 $$\% \text{ Conversion} = \frac{\text{moles NO released}}{2 \text{ x moles amine}}$$

The conversion efficiency for **1** exposed to NO under these conditions was poor (<1%). Zhang et al. previously reported that the addition of methoxide base during NO exposure shifts the reaction equilibrium toward diazeniumdiolate formation by deprotonating the amine and stabilizing the diazeniumdiolate via a countercation (e.g., sodium), thereby increasing the NO addition efficiency on a macromolecular scaffold.[12] Primary amine

dendrimer **1** exposed to NO in 0.5 M NaOMe/MeOH released greater amounts of NO over preparation in MeOH alone (Figure 2.3B), with a maximum flux of NO release ($[NO]_m$) of 6760 ppb/mg. Control NaOMe/MeOH solutions did not release NO. Hereafter, all NO releasing dendrimer conjugates were prepared under basic conditions as shown in Scheme 2.1.

A similar NO release profile was observed for the sodium stabilized primary amine diazeniumdiolates of **2** (DAB-Am-64) charged under identical conditions. As shown in Table 2.1, the total NO released (t[NO]) and conversion efficiency were slightly greater for DAB-Am-64/NO, suggesting diazeniumdiolate formation in methanolic solution favors the larger, more compact globular structure. Also, the abundance of neighboring amine sites on the larger dendrimer slowed diazeniumdiolate decomposition, as evidenced by a $t_{1/2}$ of 29 min for DAB-Am-64/NO compared to 12 min for the smaller DAB-Am-16/NO. Although DAB-Am-16 and DAB-Am-64 primary amine dendrimers released NO at levels similar to previously reported macromolecular NO donors,[11-13] the conversion efficiencies of the NO donor-modified dendrimers were low, failing to harness the anticipated storage capacity offered by a dendritic scaffold.
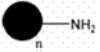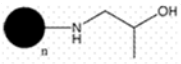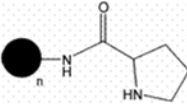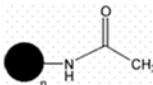
Studies were also conducted to evaluate whether the dendrimers stored nitroxyl (HNO), and the effect of HNO release (in place of NO) on the NO donor conversion efficiencies. Nitroxyl has garnered recent attention due to its importance in the pharmacological treatment of heart failure.[26] Miranda et al. reported that the primary amine diazeniumdiolate adduct of isopropylamine (IPA/NO) represents an attractive HNO donor at physiological pH.[26] Further studies by Dutton et al. have confirmed the pH dependent production of HNO and NO from primary amine diazeniumdiolate adducts using computational methods.[27] At neutral pH (7.4), primary amine adducts are predicted to release HNO, while at lower pH (3),

decomposition follows the traditional diazeniumdiolate pathway and generates two equivalents of NO.[27] Since nitroxyl primary amine adducts release NO at acidic pH, citric acid buffer (pH 3) was employed to assess whether HNO formation was responsible for the poor NO donor conversion efficiencies observed for DAB-Am-16/NO. A 67% increase in NO was detected at the lower pH, suggesting that HNO is indeed produced.   Studies are underway to further quantitate the HNO release from primary amine dendrimer diazeniumdiolates and to explore the potential of dendrimers as novel HNO donors.

2.3.2 Nitric oxide releasing secondary amine dendrimer conjugates

Secondary amines convert to diazeniumdiolates more readily than primary amines since they form more stable adducts.[8] The addition of an electron donating substituent, **R**, serves to both enhance the acidity of the amino nitrogen and provide electron density to stabilize the zwitterionic diazeniumdiolate product (Scheme 2.2).[28] Several secondary amine dendrimer conjugates were synthesized to assess the potential for increasing the NO storage on a dendritic scaffold. Modifications to yield both hydrophobic and hydrophilic NO releasing dendrimers were explored (Scheme 2.3).

Table 2.1   Summary of NO-release properties for dendrimer conjugates **1-10**.

Dendrimer	Functionality	NO Released (mmol NO / mg)	$t_{1/2}$ (min)	Conversion Efficiency
DAB-Am-16		0.44	12	2.3%
DAB-Am-64		0.69	29	3.9%
DAB-C7-16		3.5	77	38%
DAB-C7-64		3.2	86	36%
DAB-C16-16		2.2	78	35%
DAB-C16-64		--	--	--
DAB-PO-16		--	--	--
DAB-PO-64		5.6	28	47%
DAB-Pro-16		13	150	130%
DAB-Pro-64		36	117	380%
DAB-Ac-16		0.016	1.4	<0.2%
DAB-Ac-64		0.02	2.5	<0.2%
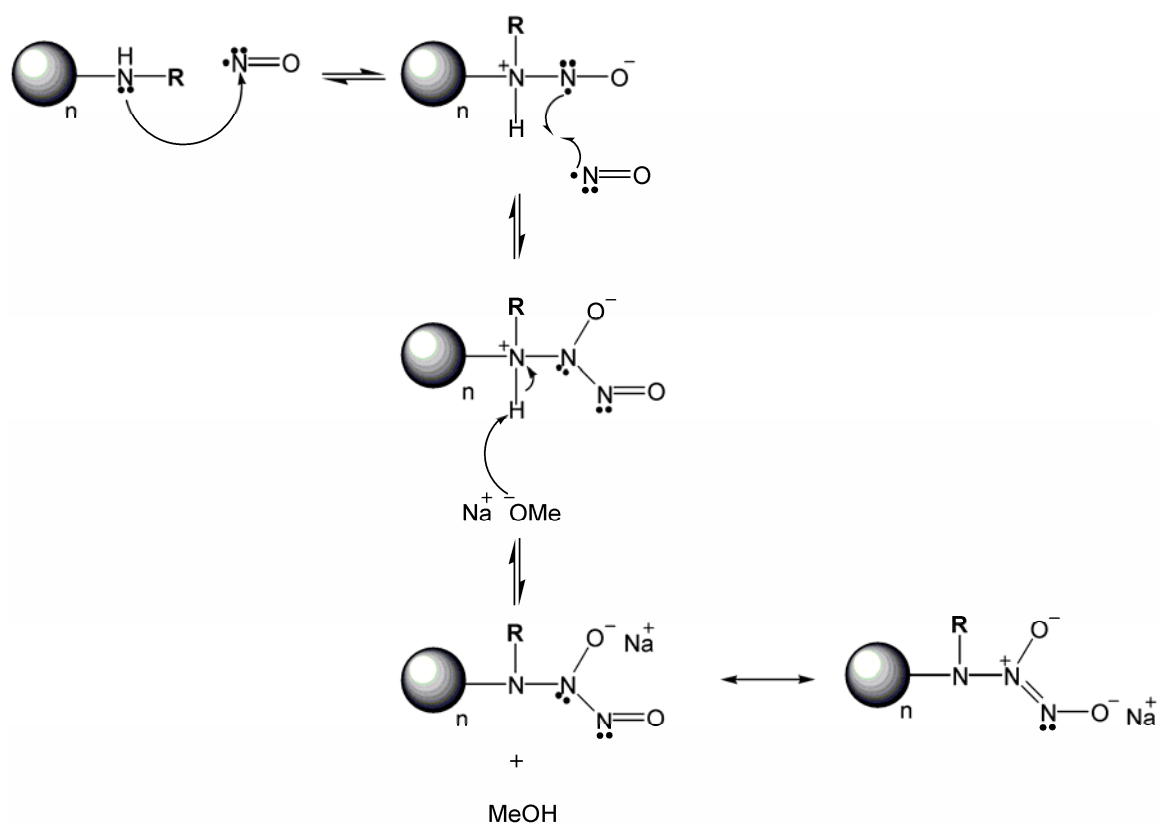
Scheme 2.2   Mechanism of diazeniumdiolate formation on dendrimer bound amine
functionalities under basic conditions.
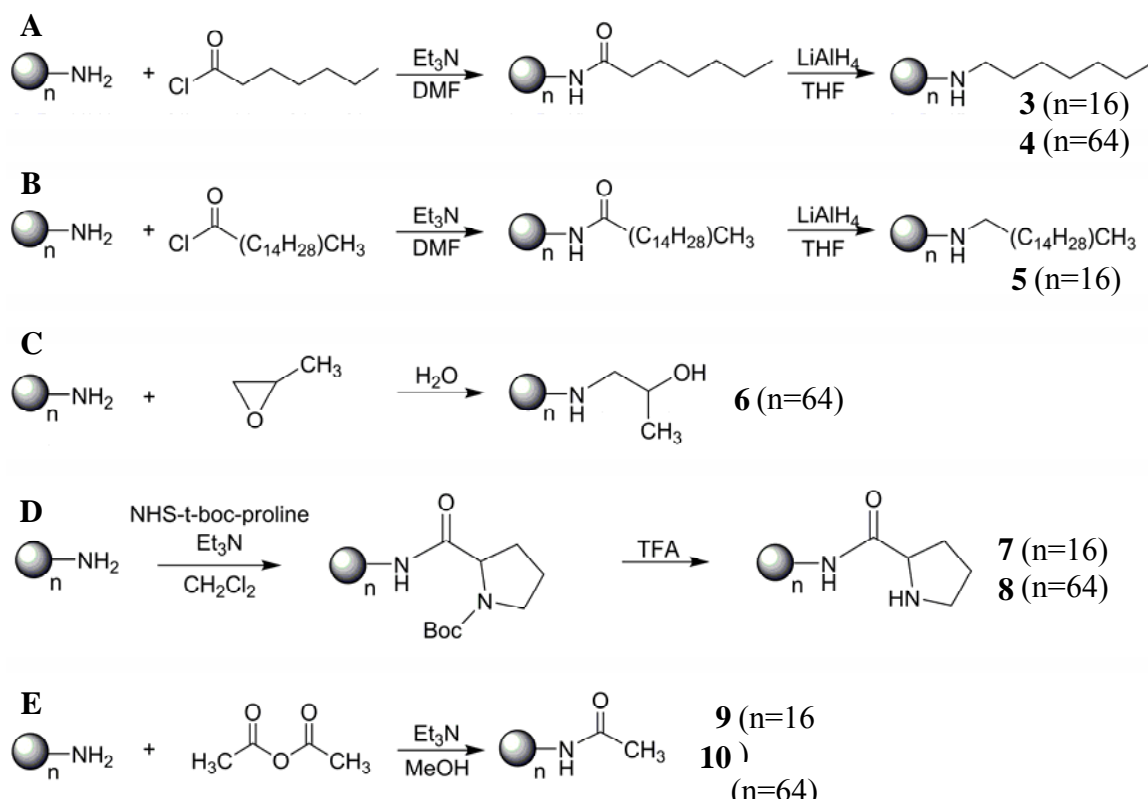
Scheme 2.3   Synthesis of polypropylenimine dendrimer conjugates. A) DAB-C7-16
             and DAB-C7-64; B) DAB-C16-16, C) DAB-PO-64; D) DAB-Pro-16
             and DAB-Pro-64; and, E) DAB-Ac-16 and DAB-Ac-64.

2.3.2.1 Reaction of DAB-Am-16 with alkyl halides

Alkylation of primary amines via the reaction with primary halides is a straightforward nucleophilic substitution reaction that results in secondary amine formation. However, the resulting amine products are also very reactive toward primary halides and will rapidly result in tertiary amine formation. Diazeniumdiolate groups will not form on tertiary amines due to the steric hinderance at the donor formation site as well the negligible tertiary amine reactivity towards NO. Initial attempts to react DAB-Am-16 with two separate alkyl bromines (1-bromopropane and 1-bromo-isopentane) resulted in a mixture of secondary and tertiary exterior amines, limiting the storage capacity of NO and the utility of this approach toward dendrimer modification.

2.3.2.2 DAB-C7-16 (**3**)

Generation 3 polypropylenimine dendrimer **1** was acylated with heptanoyl chloride and the corresponding amide was reduced with $LiAlH_4$ to produce DAB-C7-16, **3**, an alkyl terminated dendrimer (Scheme 2.3A). Following purification on an Al_2O_3 column, confirmation of the seven carbon alkyl secondary amine functionalization was obtained via ^{1}H and ^{13}C NMR. The NMR chemical shifts matched those of previously reported octyl (C8) functionalizations of other generation polypropyelenimine dendrimers.[24] The alkyl secondary amine dendrimer was exposed to NO (5 atm, NaOMe/MeOH) to form DAB-C7-16/NO. This NO donor-modified dendrimer exhibited high yields of NO release upon addition to PBS (pH 7.4, 37 °C) (Figure 2.4A). Indeed, the t[NO] from DAB-C7-16/NO corresponded to nearly 40% conversion of secondary amines to diazeniumdiolate NO donors (Table 2.1). The 3.5 μmol NO/mg released for the alkyl secondary amine dendrimer was a sizeable increase over the NO released from the primary amine substrates. Confirmation of the diazeniumdiolate functional group was obtained via UV-Vis spectroscopy. As shown in

Figure 2.5, DAB-C7-16/NO exhibits a λ_{max} of 252 nm, characteristic of the diazeniumdiolate absorption maximum.[10]

Similar to the primary amine dendrimers, the alkyl conjugate was characterized by an initial burst of NO release, reaching $[NO]_m$ in just minutes. Subsequently, significant levels of NO continued to be released for up to 14 h, albeit at a lesser rate (Figure 2.4B). Previous work by Price et al. indicated that the diazeniumdiolate decomposition rate constant (k_{obs}) and half-life for the secondary alkylamine dipropylamine diazeniumdiolate (DPA/NO) were 4.45×10^{-3} s^{-1} and 2.6 min, respectively.[29] Since the diazeniumdiolate structures for both DPA/NO and the alkyl secondary amine dendrimer NO donors (DAB-C7-16/NO) are nearly equivalent (secondary amine diazeniumdiolates bracketed by three alkyl carbons on each side), similar NO release would be expected. However, the surrounding chemical environments of the diazeniumdiolates are drastically different. The dendritic effect on the duration of NO release is evident from the lengthy NO release duration of DAB-C7-16/NO ($t_{1/2}$ = 77 min). The enhanced NO release is attributed to increased local pH upon regeneration of free secondary amines. The effective decrease in proton concentration at or near the diazeniumdiolate NO donors results in slower dissociation rates and longer overall durations of NO release.

2.3.2.3 DAB-C7-64 (**4**)

The structure of DAB-C7-16 in solution and the hydrophobic packing of the alkyl tails may affect both the extent of diazeniumdiolate formation and rates of NO release. The primary amine dendrimer with 64 exterior functionalities, **2**, exhibited slightly greater NO release properties than **1**, the smaller dendrimer. To probe the size dependence and effects of alkyl secondary amine density on NO storage, **4** (DAB-C7-64) was synthesized using generation 5 polypropylenimine dendrimer as the substrate. Changing the dendrimer size

from generation 3 to 5 showed little effect on the conversion efficiency and t[NO] for DAB-C7-16/NO and DAB-C7-64/NO (Table 2.1). The near 40% conversion achieved for both dendrimer sizes is attributed to the coulombic repulsion of multiple anionic functional groups upon diazeniumdiolate formation. Additionally, the formation of a zwitterionic species in a primarily hydrophobic environment may also contribute to the observed limit of conversion efficiency.

As shown in Figure 2.4, the NO release profiles appeared remarkably similar for both alkyl conjugates. However, DAB-C7-64/NO was characterized by a greater $[NO]_m$ and longer $t_{1/2}$. The dissimilarity of the two release profiles at early times (<30 min) indicates a slight size dependent effect on the initial rates of NO release. At longer times, DAB-C7-16/NO and DAB-C7-64/NO adopted similar rates of diazeniumdiolate decomposition.

2.3.2.4 Macromolecular NO release kinetics

The extended duration of NO release observed for DAB-C7-16/NO and DAB-C7-64/NO indicates a likely deviation from pseudo first-order kinetics reported for the dissociation of small molecule alkyl secondary amine diazeniumdiolates. Zhang et al. previously reported a method for determining an "apparent" reaction order (n) of diazeniumdiolate dissociation from silica-based NO-releasing macromolecules.[12] To determine the reaction order for dendrimer-bound diazeniumdiolate decomposition, ln υ vs. ln C_d graphs were plotted, where υ represents the dissociation rate of the *N*-diazeniumdiolate moiety ($-dC_d/dt$) and C_d is the *N*-diazeniumdiolate content (µmol/mg) of the dendritic NO donors. The reaction order (n) is given by the slope of this plot.[12] After the initial burst of NO release, both DAB-C7-16/NO and DAB-C7-64/NO shared the same order of reaction (n = 1.89) for diazeniumdiolate decomposition. The relatively high reaction order observed for the dendrimer bound alkyl secondary amine diazeniumdiolates (n = 1.89) is comparable with the value reported for the

alkyl secondary amine diazeniumdiolates on the surface of fumed silica (n = 1.75 for 1N-C1).[12] These data illustrate the complexity of macromolecular NO release kinetics, and the dependence on the pH and lipophilicity of the local chemical environment as well as contributions from nanoparticle solution structure.

2.3.2.5 Proton initiated diazeniumdiolate dissociation

The sustained duration of NO release observed from the secondary amine dendrimer conjugates at extended periods (>12 h) indicates a likely deviation from the first-order exponential decay reported for the kinetics of small molecule alkyl secondary amine diazeniumdiolates.[9] Consistent with the mechanism of decomposition for small molecule diazeniumdiolates,[9, 28] the buffer pH influenced the kinetics of NO release from the dendrimer conjugates. As expected, NO release from DAB-C7-64/NO was more rapid under acidic conditions (pH 3) and slowed drastically at pH>11 (Figure 2.6). To test the contribution of thermal degradation on NO release, decomposition was measured under an inert nitrogen atmosphere as a function of temperature. At 37°C, negligible NO was released from the NO donor-modified dendrimer conjugates. Upon increasing the temperature to 70°C, NO release was initiated albeit at an extremely low rate (~0.5 ppb/s). After 60 min, degassed PBS buffer was added to the sample, resulting in a rapid release of NO (Figure 2.7). Such behavior, combined with the pH dependent dissociation confirms that the dominate mechanism of NO release for dendrimer conjugates was proton initiated. Dendrimers stored under basic conditions at -20°C retained 96% (DAB-C7-16/NO) of the stored NO as diazeniumdiolate after 3 wks. Future studies aim to elucidate how diazeniumdiolate structure, solvent behavior, and remote amine sites alter the local dendritic environment and influence the rate of diazeniumdiolate dissociation.

A

B
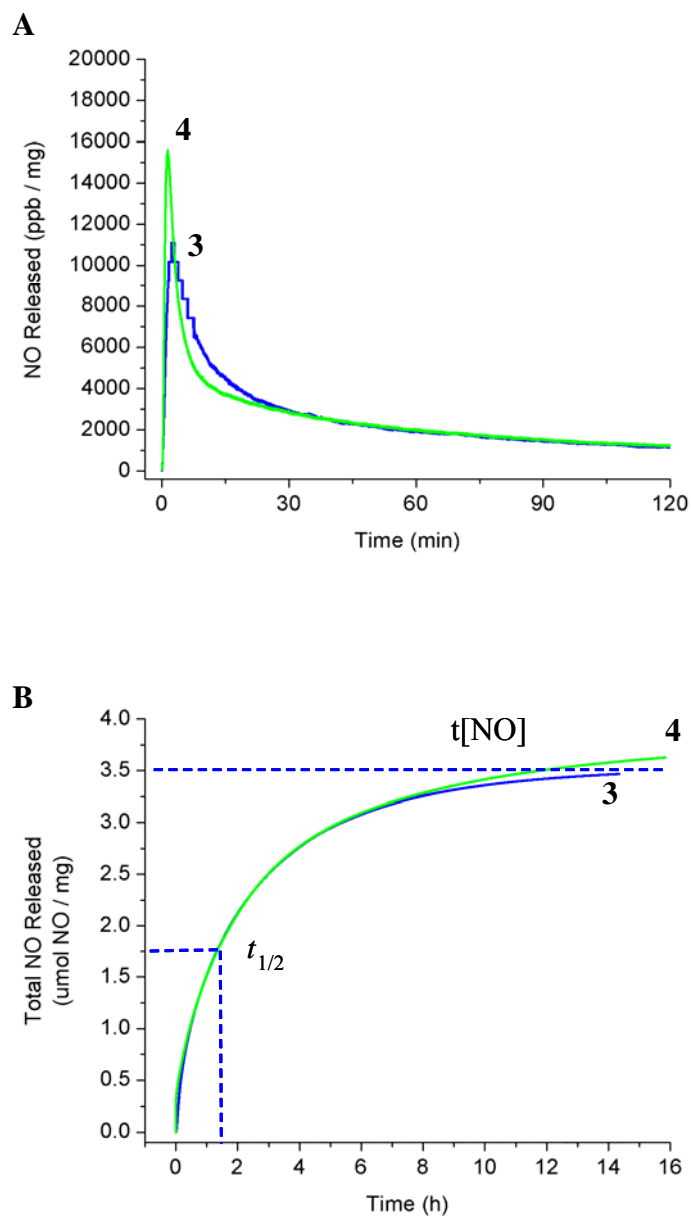
Figure 2.4   A) Real time NO release profile for NO-releasing dendrimer conjugates of **3** and **4**; and, B) plot of t[NO] vs. time for conjugates of **3** and **4** depicting values for the $t_{1/2}$ for DAB-C7-16/NO and long duration of NO release.
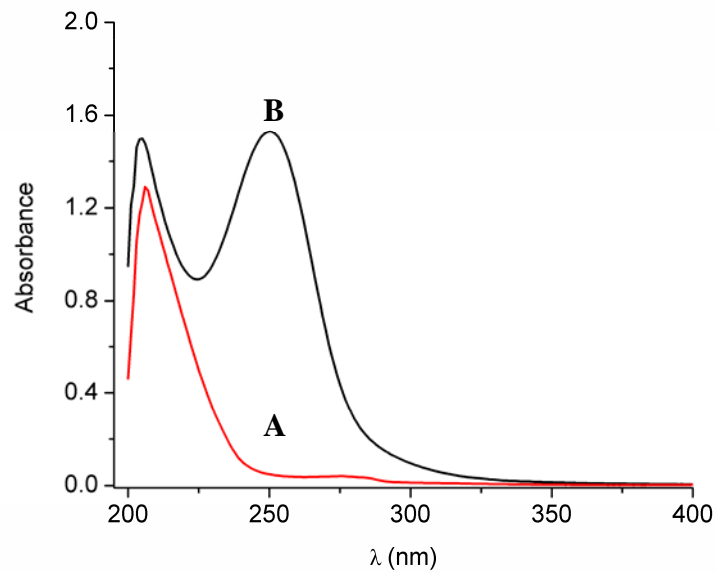
Figure 2.5   UV-Vis spectra collected in MeOH for A) DAB-C7-16 dendrimer conjugate and, B) the diazeniumdiolate functionalized dendrimer DAB-C7-16/NO.
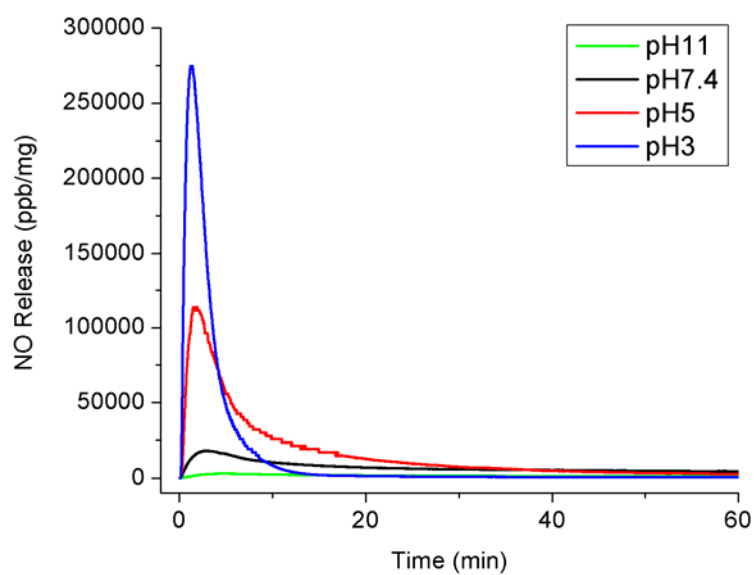
Figure 2.6   Real time NO-release curves for DAB-C7-64/NO diazeniumdiolate decomposition as a function of pH and kinetic parameters as a function of pH.
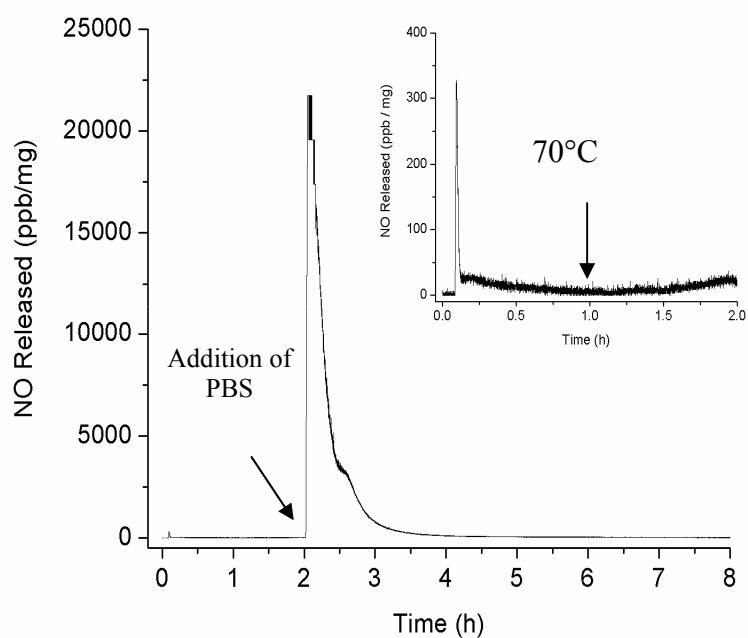
Figure 2.7   Real time NO-release curve depicting the minimal thermal degradation observed for DAB-C7-64/NO over the first several hours under a nitrogen atmosphere.   Addition of phosphate buffer resulted in rapid NO donor decomposition. (Inset: Depicts the small flux of NO upon addition of the sample, reflecting the trace amount of NO released during storage.   The temperature was increased from 37°C to 70°C as indicated.

These parameters are essential for predicting NO release kinetics from macromolecular NO donors. Efforts to develop a model for evaluating the structure-activity relationships of macromolecules and NO release rates will be of importance for designing NO releasing materials bearing therapeutic significance.

2.3.2.6 DAB-C16-16 (**5**)

Synthesis of more lipophilic diazeniumdiolate NO donors has been the goal of other studies aimed at developing NO-releasing hydrophobic polymer coatings.[30] Such coatings have been used to improve the thromboresistivity of intravascular sensors.[30] Dendrimers possessing alkyl secondary amines represent novel NO releasing macromolecules with increased lipophilicity over traditional NO donors, and may elicit similar potential as polymer dopants for preparing NO-releasing polymers. The larger payload of NO and increased duration of NO release from a dendritic scaffold may prove advantageous in formulating NO release coatings with extended NO release properties. To increase the lipophilicity of the diazeniumdiolate dendrimer conjugates, amine terminated generation 3 and 5 polypropylenimine dendrimer starting materials were reacted with palmitoyl chloride as described above for the shorter heptanoyl chlorides. The sixteen carbon tailed derivatives, DAB-C16-16 and DAB-C16-64, were extremely difficult to isolate following acylation due to their micelle like nature and partitioning into both organic and aqueous phases (Figure 2.8). Of note, only DAB-C16-16 was able to be recovered after $LiAlH_4$ reduction of the amides to secondary amines.

Following conversion to DAB-C16-16/NO, the NO-release properties for palmitoyl conjugate were very similar to the previous C7 dendrimer conjugates (Table 2.1). The half lives for DAB-C16-16/NO and DAB-C7-16/NO were 77 and 78 min, respectively. However, the more lipophilic dendrimer with the longer alkyl tails showed a much higher

76

[NO]$_m$ (36,800 ppb/mg for C16 and 11,100 ppb/mg for the C7 conjugate, Figure 2.9), likely due to a solution conformation that exposes diazeniumdiolates in polar environments (Figure 2.8B). Overall, the 3 alkyl conjugates exhibited similar $t_{1/2}$, % conversion, and total NO-released (μmol NO/ μmol amine) regardless of core size or alkyl chain length.

2.3.2.7 DAB-PO-64 (**6**)

The therapeutic implications of NO are well understood,[4, 31, 32] but failure to deliver NO to a specific cell or tissue type of interest has limited the use of NO donors as therapeutic entities. Dendrimers offer a solution to traditional drug delivery problems because of their tailored solubility, globular solution behavior, and highly functionalizable exterior. The biocompatibility of several dendritic structures, including polyester dendrimers synthesized by Frechet and co-workers possessing primary alcohols at the exterior, have been reported as acceptable for drug delivery applications.[21]

A water-soluble, hydrophilic dendrimer with terminal hydroxyl groups and secondary amines required for efficient storage of NO was synthesized to demonstrate the potential delivery vehicle for the controlled release of NO in vivo. Generation 5 polypropylenimine dendrimer **2** was reacted with propylene oxide under aqueous conditions to yield **6** (DAB-PO-64) (Scheme 2.3C).[25] Functionalization was confirmed via ^{1}H, ^{13}C NMR, and ESI/MS. Notably, the NO releasing conjugate DAB-PO-64/NO displayed the largest t[NO] of the dendrimer conjugates synthesized to date (5.6 μmol NO/mg, 46% conversion) (Figure 2.10). The enhanced storage capacity of the hydrophilic dendrimer is likely attributed to a fully extended solution structure of the dendrimer in the polar methanol solvent used during NO exposure. Indeed, the structure of polypropylenimine dendrimers are known to be responsive to solvent,[33] thereby affecting changes in globular solution behavior. Compared to the more lipophilic dendrimer of similar size (DAB-C7-64/NO), DAB-PO-64/NO was characterized

by a greater $[NO]_m$ (53,100 versus 15,600 ppb/mg). DAB-PO-64/NO also exhibited prolonged NO release for up to 16 h. As was the case with the alkyl secondary amine dendrimers, the dendrimer bound diazeniumdiolates seem to adopt a slower rate of dissociation at longer times. The reaction order for DAB-PO-64/NO decomposition was calculated to be 1.71. The slight shift toward first order kinetics is attributed to the hydrophilic nature of DAB-PO-64/NO and NO donor dissociation closer to that of small molecule diazeniumdiolates.

2.3.2.8 DAB-Pro-16 and DAB-Pro-64 (**7** and **8**).

Additional hydrophilic dendrimer conjugates were synthesized via the reaction of NHS-activated t-boc-L-proline with primary amine containing dendrimers **1** and **2**. Following amide coupling the t-boc group was removed via formic acid to yield dendrimer conjugates terminated with proline residues, each containing a single secondary amine site for diazeniumdiolate conversion (Scheme 2.3D). The small molecule diazeniumdiolate PROLI/NO has received much attention due to its short NO-release half life ($t_{1/2} < 8$ s) and its biocompatible amino acid metabolites. Upon exposing the proline dendrimer conjugates to NO, the NO-release kinetics observed were prolonged compared to the small molecule analogue (e.g., $t_{1/2} = 150$ min for DAB-Pro-16). However, the total NO release values for the proline dendrimer conjugates resulted in >300% conversion based on only 2 moles of NO possible per mol of covalently attached proline. Re-examination of the ^{1}H-NMR spectra revealed a number of un-interpretable peaks after dialysis. These conjugates warrant further experimentation due to their incredibly high storage potential and straightforward synthetic procedure. Subsequently, amide dendrimer conjugates with no secondary amines were synthesized as described below to check for possible amide reaction with NO.

A

B

Polar head group with
hydrophobic chains
packed linearly

H_2O

H_2O

CH_2Cl_2

Polar core swells,
hydrophobic chains
packed towards the interior
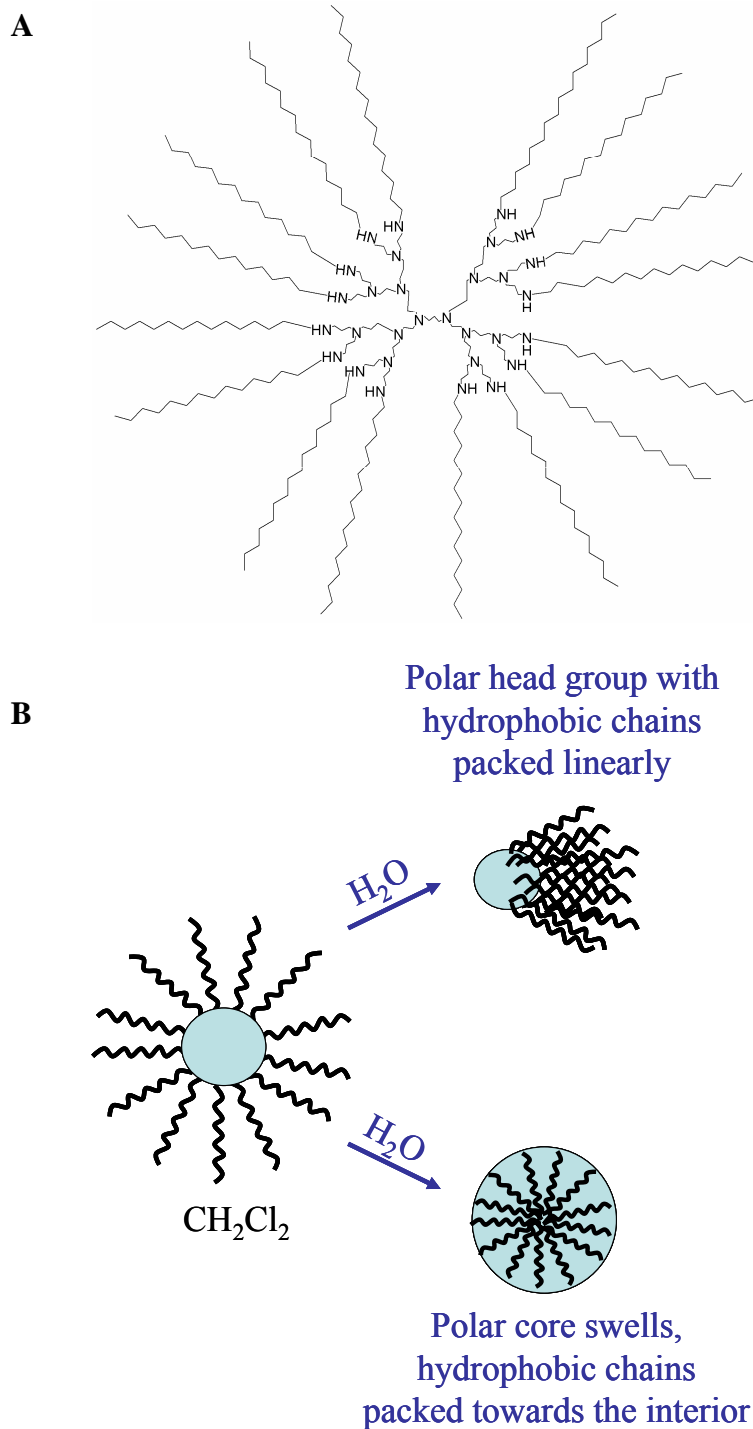
Figure 2.8   A) 2-D structure of DAB-C16-16 after $LiAlH_4$ reduction depicting the
"uni-molecular micelle" like behavior of the lipophilic dendrimer
conjugate. B) Illustration showing how DAB-C16-16 is fully extended
in organic solvents but upon exposure to water may adopt a solution
conformation exposing the polar interior and presenting easy access for
proton initiated diazeniumdiolate decomposition.
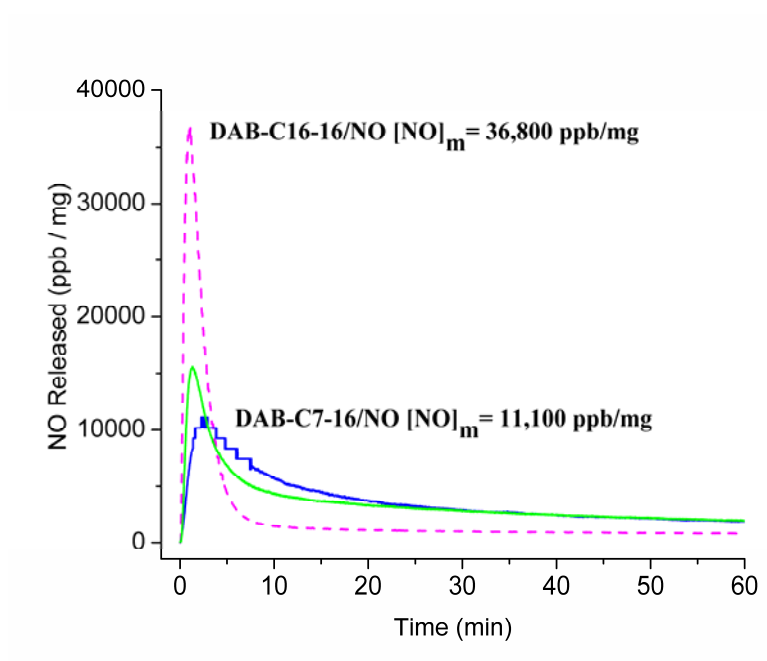
Figure 2.9   Real-time NO release curves for DAB-C16-16/NO and DAB-C7-16/NO demonstrating the difference in the $[NO]_m$ for the two dendrimer conjugates.
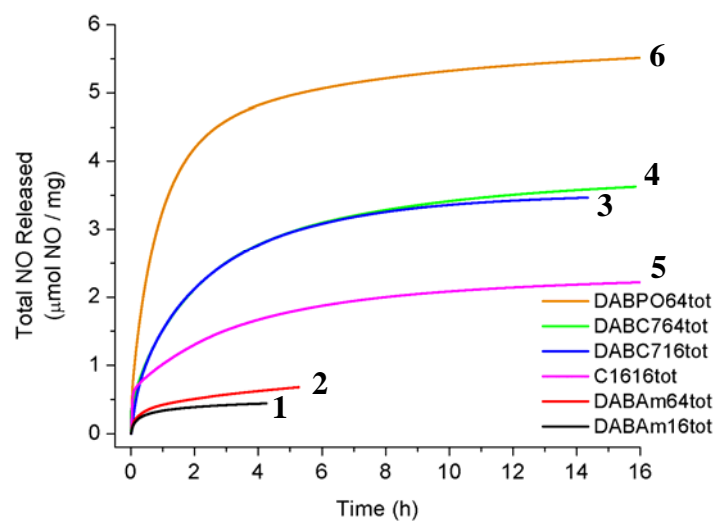
Figure 2.10   Total NO release profiles for NO-releasing dendrimer conjugates **1-6**.

*2.3.3 Amide functionalized dendrimers DAB-Ac-16 and DAB-Ac-64 (**9** and **10**)*

To demonstrate control over the NO storage potential of multivalent dendrimers, acetamide functionalities were introduced via the reaction of primary amines with acetic anhydride in the presence of triethylamine (Scheme 2.3E). The functionalization was confirmed by ^{1}H, ^{13}C NMR and ESI/MS analysis. The absence of a nucleophilic amine required for diazeniumdiolate formation makes amides an unfavorable moiety for storing NO. Following NO charging, both acetamide dendrimers (**9** and **10**) exhibited low NO release and a short half life ($t_{1/2} < 3$ min) (Table 2.1). The trace amount of NO observed (<0.2 % conversion) is attributed to NO donor formation at residual primary amine sites (from incomplete acetamide functionalization) and/or loosely associated NO within the tertiary amine backbone structure. The lack of amide reactivity towards NO suggests that the acetamide functionality may prove useful in future applications for stoichiometrically limiting the number of NO donor functional groups. Acetamide modifications have been used previously to control functionality for other dendrimer constructs.[34, 35] In addition to tuning the storage capacity of NO, the amide exterior may enable increased water solubility and eliminate the toxicity of primary amine dendrimer constructs.[34, 36]

2.4 Conclusion

A new class of NO-releasing macromolecules was prepared from primary and secondary amine functionalized dendrimers. The total NO released from secondary amine conjugates was significantly greater than from the primary amine parent dendrimers due to the enhanced stability of secondary amine diazeniumdiolates. The level of NO released (3-6 μmol NO/mg) for the secondary amine dendrimers represents the greatest "payload" of an NO-releasing macromolecule to date. Kinetic data confirmed that the mechanism of diazeniumdiolate dissociation was proton initiated. In addition to the increased storage capacity of the

dendritic architecture, the dendrimer bound NO donor half-lives greatly exceed those for small molecule equivalents, thereby illustrating a "dendritic effect" on diazeniumdiolate decomposition.

Expansion of the current work to introduce multiple functionalities on the dendritic exterior may enable the use of NO-releasing dendrimers as a vehicle for further understanding NO's role in physiological systems of interest. For example, dendrimers equipped with targeting ligands (e.g., folic acid) to deliver NO selectively to cancer cells may potentially help elucidate the mechanistic effects of NO on tumor cell biology. Fluorescent probes and/or (poly)ethyleneglycol chains may also be added to produce fully biocompatible nanoparticles capable of harnessing the therapeutic potential of NO. Such studies are currently underway.

2.5 References

1. Moncada, S.; Higgs, A. "The L-arginine-nitric oxide pathway." *N. Engl. J. Med.* **1993,** *30*, 2002-2011.

2. Marletta, M. A.; Tayeh, M. A.; Hevel, J. M. "Unraveling the biological significance of nitric oxide." *BioFactors* **1990,** *2*, 219-225.

3. Fang, F. C., "Mechanisms of nitric oxide-related antimicrobial activity." *J. Clin. Invest.* **1997,** *99*, 2818-2825.

4. Wang, P. G.; Xian, M.; Tang, X.; Wu, X.; Wen, Z.; Cai, T.; Janczuk, A. J. "Nitric oxide donors: chemical activities and biological applications." *Chem. Rev.* **2002,** *102*, 1091-1134.

5. Parker, N.; Turk, M. J.; Westrick, E.; Lewis, J. D.; Low, P. S.; Leamon, C. P., "Folate receptor expression in carcinomas and normal tissues determined by a quantitative radio-ligand binding assay." *Anal. Biochem.* **2005,** *338*, 284-293.

6. Hrabie, J. A.; Keefer, L. K. "Chemistry of the nitric oxide-releasing diazeniumdiolate functional group and its oxygen-substituted derivates." *Chem. Rev.* **2002,** *102*, 1135-1154.

7. Drago, R. S.; Paulik, F. E., "The reaction of nitrogen(II) oxide with diethylamine." *J. Am. Chem. Soc.* **1960,** *82*, 96-98.

8. Drago, R. S.; Karstetter, B. R., "The reaction of nitrogen(II) oxide with various primary and secondary amines." *J. Am. Chem. Soc.* **1961,** *83*, 1819-1822.

9. Davies, K. M.; Wink, D. A.; Saavedra, J. E.; Keefer, L. K., "Chemistry of the diazeniumdiolates 2. Kinetics and mechanism of dissociation to nitric oxide in aqueous solution." *J. Am. Chem. Soc.* **2001,** *123*, 5473-5481.

10. Hrabie, J. A.; Klose, J. R.; Wink, D. A.; Keefer, L. K. "New nitric oxide-releasing zwitterions derived from polyamines." *J. Org. Chem.* **1993,** *58*, 1472-1476.

11. Smith, D. J.; Chakravarthy, D.; Pulfer, S.; Simmons, M. L.; Hrabie, J. A.; Citro, M. L.; Saavedra, J. E.; Davies, K. M.; Hutsell, T. C.; Mooradian, D.; Hanson, S. R.; Keefer, L. K. "Nitric oxide-releasing polymers containing the [N(O)NO]⁻ group." *J. Med. Chem.* **1996,** *39*, 1148-1156.

12. Zhang, H.; Annich, G. M.; Miskulin, J.; Stankiewicz, K.; Osterholzer, K.; Merz, S. I.; Bartlett, R. H.; Meyerhoff, M. E. "Nitric oxide-releasing fumed silica particles: synthesis, characterization, and biomedical application." *J. Am. Chem. Soc.* **2003,** *125*, 5015-5024.

13. Hrabie, J. A.; Saavedra, J. E.; Roller, P. P.; Southan, G. J.; Keefer, L. K. "Conversion of proteins to diazeniumdiolate-based nitric oxide donors." *Bioconjug. Chem.* **1999,** *10*, 838-842.

14. Rothrock, A. R.; Donkers, R. L.; Schoenfisch, M. H., "Synthesis of nitric oxide-releasing gold nanoparticles." *J. Am. Chem. Soc.* **2005,** *127*, 9362-9363.

15. Svenson, S.; Tomalia, D. A. "Dendrimers in biomedical applications-reflections on the field." *Adv. Drug Deliv. Rev.* **2005,** *57*, 2106-2129.

16. Bosman, A. W.; Janssen, H. M.; Meijer, E. W., "About dendrimers: structure, physical properties, and applications." *Chem. Rev.* **1999,** *99*, 1655-1688.

17. Hawker, C. J.; Frechet, J. M., "Preparation of polymers with controlled molecular architecture. A new convergent approach to dendritic macromolecules." *J. Am. Chem. Soc.* **1990,** *112*, 7638-7647.

18. Frechet, J. M. "Dendrimers and other dendritic macromolecules: from building blocks to functional assemblies in nanoscience and nanotechnology." *J. Polym. Sci. A: Poly. Chem.* **2003,** *41*, 3713-3725.

19. Boas, U.; Heegaard, P. M. H. "Dendrimers in drug research." *Chem. Soc. Rev.* **2004,** *33*, 43-63.

20. Stiriba, S.-E.; Frey, H.; Haag, R. "Dendritic polymers in biomedical applications: from potential to clinical use in diagnostics and therapy." *Angew. Chem., Int. Ed.* **2002,** *41*, 1329-1334.

21. Gillies, E. R.; Frechet, J. M. "Dendrimers and dendritic polymers in drug delivery." *Drug Discovery Today* **2005,** *10*, 35-43.

22. Beckman, J. S.; Conger, K. A. "Direct measurement of dilute nitric oxide in solution with an ozone chemiluminescent detector." *Methods* **1995,** *7*, 35-39.

23. Marxer, S. M.; Rothrock, A. R.; Nablo, B. J.; Robbins, M. E.; Schoenfisch, M. H. "Prepartion of nitric oxide (NO)-releasing sol-gels for biomaterial applications." *Chem. Mater.* **2003,** *15*, 4193-4199.

24. Ford, W. T.; Pan, Y. "Amphiphilic dendrimers with both octyl and triethylenoxy methyl ether chain ends." *Macromolecules* **2000,** *33*, 3731-3738.

25. Pantos, A.; Tsiourvas, D.; Nounesis, G.; Paleos, C. M. "Interaction of functional dendrimers with multilamellar liposomes: design of a model system for studying drug delivery." *Langmuir* **2005,** *21*, 7483-7490.

26. Miranda, K. M.; Katori, T.; Torres de Holding, C. L.; Thomas, L.; Ridnour, L. A.; McLendon, W. J.; Cologna, S. M.; Dutton, A. S.; Champion, H. C.; Mancardi, D.;

Tocchetti, C. G.; Saavedra, J. E.; Keefer, L. K.; Houk, K. N.; Fukuto, J. M.; Kass, D. A.; Paolocci, N.; Wink, D. A. "Comparison of the NO and HNO donating properties of diazeniumdiolates: primary amine adducts release HNO in Vivo." *J. Med. Chem.* **2005,** *48*, 8220-8228.

27.   Dutton, A. S.; Suhrada, C. P.; Miranda, K. M.; Wink, D. A.; Fukuto, J. M.; Houk, K. N. "Mechanism of pH-dependent decomposition of monoalkylamine diazeniumdiolates to form HNO and NO, deduced from the model compound methylamine diazeniumdiolate, density functional theory, and CBS-QB3 calculations." *Inorg. Chem.* **2006,** *45*, 2448-2456.

28.   Houk, K. N.; Dutton, A. S.; Fukuto, J. M., "The mechanism of NO formation from the decomposition of dialkylamino diazeniumdiolates: Density functional theory and CBS-QB3 predictions." *Inorg. Chem.* **2004,** *43*, 1039-1045.

29.   Price, S. E.; Jappar, D.; Lorenzo, P.; Saavedra, J. E.; Hrabie, J. A.; Davies, K. M. "Micellar catalysis of nitric oxide dissociation from diazeniumdiolates." *Langmuir* **2003,** *19*, 2096-2102.

30.   Batchelor, M. M.; Reoma, S. L.; Fleser, P. S.; Nuthakki, V. K.; Callahan, R. E.; Shanley, C. J.; Politis, J. K.; Elmore, J.; Merz, S. I.; Meyerhoff, M. E. "More lipophilic dialkyldiamine-based diazeniumdiolates: synthesis, characterization, and application in preparing thromboresistant nitric oxide release polymeric coatings." *J. Med. Chem.* **2003,** *46*, 5153-5161.

31.   Hanson, S. R.; Hutsell, T. C.; Keefer, L. K.; Mooradian, D. L.; Smith, D. J. "Nitric oxide donors: a continuing opportunity in drug design." *Adv. Pharmacol.* **1995,** *34*, 383-398.

32.   Ignarro, L., J.; Napoli, C., "Nitric oxide-releasing drugs." *Ann. Rev. Pharmacol. Toxicol.* **2003,** *43*, 97-123.

33.   Rinaldi, P. L.; Youngs, W. J.; Yanhui, N.; Chai, M. "Structure and conformation of DAB dendrimers in solution via multidimensional NMR techniques." *J. Am. Chem. Soc.* **2001,** *123*, 4670-4678.

34.   Majoros, I. J.; Keszler, B.; Woehler, S.; Bull, T.; Baker, J. R. "Acetylation of poly(amidoamine) dendrimers." *Macromolecules* **2003,** *36*, 5526-5529.

35.   Patri, A. K.; Myc, A.; Bander, N. H.; Baker, J. R. J. "Synthesis and in vivo testing of J591 antibody-dendrimer conjugates for targeted prostate cancer therapy." *Bioconjug. Chem.* **2004,** *15*, 1174-1181.

36.   Hong, S.; Bielinska, A. U.; Mecke, A.; Keszler, B.; Beals, J. L.; Shi, X.; Balogh, L.; Orr, B. G.; Baker, J. R. "Interaction of poly(amidoamine) dendrimers with supported lipid bilayers and cells: hole formation and the relation to transport." *Bioconjug. Chem.* **2004,** *15*, 774-782.

Chapter 3

S-Nitrosothiol-Modified Dendrimers as Nitric Oxide Delivery Vehicles

3.1 Introduction

S-nitrosothiols (RSNO) are ubiquitous in human physiology and involved in a multitude of cell signaling cascades.[1] Endogenously, nitrosothiols are formed either via the reaction of free thiols with N_2O_3, the reactive nitrogen species formed following the auto-oxidation of nitric oxide (NO), or through a host of redox mechanisms involving metabolites of NO and transition metal centers.[1] Nitrosation of cysteine residues on serum albumin and the nitrosation/nitrosylation of deoxyhemoglobin account for a large portion of the 1.8 μM nitrosothiol concentration in blood.[2, 3] As the main carriers of NO in vivo, nitrosothiols regulate several biological processes including vasodilation, platelet activation, neurotransmission, and tissue inflammation.[1, 4, 5] Synthetic nitrosothiol NO donors such as *S*-nitroso-*N*-acetyl-DL-penicillamine (SNAP) have been employed to better understand the many complicated roles of NO in regulatory biology, with the most notable instance including the discovery by Ignarro and co-workers that NO is the vascular endothelial derived relaxation factor.[6]

Numerous reports have outlined the therapeutic potential of nitrosothiol adducts, including their toxicity toward cancerous cells,[7, 8] antimicrobial activity,[9-12] and cardioprotective effects during ischemia/reperfusion injury.[13-15] Perhaps the most well

documented clinical application of *S*-nitrosothiols is as anti-platelet agents, whereby RSNOs inhibit platelet aggregation without affecting vascular tone.[16-21] Despite the promising therapeutic potential of nitrosothiols, the inability to target NO to a specific site of action and the rapid systemic clearance associated with small drug molecules has seriously hindered the clinical development of nitrosothiol therapeutics. In response, several macromolecular nitrosothiol NO donors have been synthesized to store NO and expand RSNO delivery options. For example, *S*-nitrosocysteine polymer conjugates have been utilized as materials to aid in the prevention of thrombosis/restenosis[22, 23] and for the delivery of RSNOs in topical biomedical applications.[24] Meyerhoff and co-workers have employed nitrosothiol-modified fumed silica particles as polymer dopants and demonstrated tunable NO-release from hydrophobic polymers as a function of light.[25] Protein-based nitrosothiol delivery vehicles have also been explored as a strategy to extend the systemic half-lives of exogenous RSNO donors and to aid in the treatment of circulation disorders.[26-29]

The use of polymeric and protein drug conjugates have led to significant strides in NO delivery. Unfortunately, the NO storage capacity (pmol – nmol NO·mg^{-1}) and/or the number of sites for covalent attachment of additional functionalities remain limited. Previous work from our laboratory has described the synthesis of diazeniumdiolate-modified polypropylenimine dendrimer conjugates as macromolecular NO donors capable of storing up to 5.6 μmol NO·mg^{-1} with NO-release kinetics dependent on dendrimer structure.[30] Dendrimers represent attractive vehicles for NO loading because of their multivalent exterior and its ability to not only to store large amounts of NO, but its capacity for additional functionalities for increasing drug specifity .[30 31, 32] In this chapter, the synthesis and characterization of two thiol-derivatized generation 4 polyamidoamine (PAMAM) dendrimers capable of storing up to 2 μmol NO·mg^{-1} dendrimer when converted to the

corresponding nitrosothiol NO donors (Figure 3.1) are reported. S-nitrosothiols have received considerable attention as the primary NO carriers in blood and their decomposition mechanisms represent alternative strategies for controlled NO-release, albeit under conditions distinct from diazeniumdiolates.[31] The effect of SNAP-modified G4 dendrimer on platelet aggregation is explored and compared to SNAP, the analogous small molecule nitrosothiol, to confirm the retention of biological activity of dendrimer bound RSNOs.

3.2 Experimental Section

3.2.1 General

Generation 4 polyamidoamine dendrimer (G4-PAMAM), *N*-acetyl-L-cysteine, trityl chloride, triphenylmethanol, boron trifluoride diethyl etherate (BF$_3$-etherate), isopentylnitrite, L-glutathione, ethylenediamine tetraacetate (EDTA), *N*-hydroxy succinimide, dicyclohexylcarbodiimide, 5,5'-dithio-bis(2-nitrobenzoic acid) (DTNB), and triethylamine were purchased from the Aldrich Chemical Company (Milwaukee, WI). *N*-acetyl-D,L-penicillamine and anhydrous sodium bisulfate were purchased from Fluka. Sodium nitrite and anhydrous pyridine were purchase from Acros Organic. All other common laboratory salts and solvents were purchased from Fisher Scientific. Water was purified using a Millipore Milli-Q gradient A-10 purification system (Bedford, MA). Spectra/Por® Float-A-Lyzers® were purchased from Spectrum Laboratories Inc. (Rancho Dominguez, CA). Absorption spectra were recorded on a Perkin Elmer Lambda 40 UV-Vis spectrophotometer (Norwalk, CT). Nuclear magnetic resonance (NMR) spectra were collected in CDCl$_3$ and D$_2$O (Sigma-Aldrich) using a 400-MHz Bruker Nuclear Magnetic Resonance spectrometer. Mass spectra were acquired on a Kratos MALDI AXIMA CFR plus instrument in linear mode (2 GHz), power 160. Dendrimer samples for mass analysis were prepared at a concentration of 2 mg/mL in a sinapinic acid matrix, 1:1

CH$_3$CN/TFA (0.05%). Size exclusion chromatography was performed on a Wyatt DAWN EOS light scattering instrument interfaced with an Amersham Biosciences Akta FPLC system equipped with a Wyatt Optilab refractometer and Wyatt dynamic light scattering module. Nitric oxide release was measured using a Sievers 280i Chemiluminesce Nitric Oxide Analyzer (Boulder, CO) as described previously.[33]

3.2.2 Synthesis and characterization of dendrimer conjugates

3.2.2.1 3-Acetamido-4,4-dimethylthietan-2-one (**1**)

To an ice-cooled solution of *N*-acetyl-DL-penicillamine (4.0 g, 21 mmol) dissolved in 10 mL of anhydrous pyridine under N$_2$, acetic anhydride (5.9 mL, 63 mmol) was added dropwise over the course of 30 min. The solution was warmed to room temperature and stirred for 18 h. The stirring mixture was diluted with 150 mL of CHCl$_3$, washed with 0.1 M HCl (3 x 50 mL), and the organic layer dried over MgSO$_4$. The CHCl$_3$ was concentrated under reduced pressure and the crude thiolactone product was precipitated and triturated in 100 mL of petrolatum ether, filtered, rinse with ether, and dried to yield 1.05 g (29%) of white crystalline solid. ^{1}H NMR (CDCl$_3$, δ): 1.60 (s, CH_3), 1.82 (s, CH_3), 2.02 (s, NHCOCH_3), 5.64 (d, CH), 6.52 (br, NHCOCH$_3$). ^{13}C NMR (CDCl$_3$, δ): 22.46 (NHCOCH$_3$), 26.13 (C(CH$_3$)$_2$), 30.13 (CH$_3$), 51.04 (CH), 169.34 (NHCOCH$_3$), 191.79 (SCO).

3.2.2.2 G4-NAP (**2**)

Thiolactone (**7**) (80 mg, 0.46 mmol) was added in slight excess (1.2:1) to the number of amines of G4-PAMAM dendrimer (81 mg, 5.7 μmol) dissolved in a stirring solution of CH$_2$Cl$_2$. The mixture was stirred for 5 h under N$_2$ at room temperature, concentrated under reduced pressure, resuspended in 10 mL of ultrapure water, and dialyzed for 3 d against ultrapure water (3 x 3 L, 5,000 MW co). The thiol modified dendrimer was lyophilized to yield 129 mg (89%) of white powder. NMR (D$_2$O, δ): 1.30 (d, R(CH_3)$_2$SH), 1.97 (s,

NHCOCH_3), 2.25-2.40 (br, R$_2$NCH$_2$CH_2CO), 2.48-2.59 (br, NHCH$_2$CH_2NR$_2$), 2.67-2.83 (br,

R$_2$NCH_2CH$_2$CO), 3.12-3.30 (br, NHCH_2CH$_2$NR$_2$, NHCH_2CH_2NHCO), 4.30 (s,

NHCOCHC(CH$_3$)$_2$SH). ^{13}C NMR (D$_2$O, δ): 21.86 (NHCOCH$_3$), 32.46 (C(CH$_3$)$_2$), 36.54

(CH$_3$), 51.30 (CH), 169.34 (NHCOCH$_3$), 191.79 (SCO)23.25 (CH$_3$), 25.97 (COCH$_2$CH$_2$CO),

33.66 (CH$_2$), 49.96 (CH), 67.97 (SC(Ph)$_3$), 127.4 (C$_4$), 128.5 (C$_3$), 129.92 (C$_2$), 144.48 (C$_1$),

166.9 (OCOCH), 168.8 (COCH$_2$CH$_2$$C$O), 171.04 (NH$COCH_3$). MW$_{theoretical}$: 25,300 g/mol,

MW$_{MALDI}$: 23,000 g/mol, MW$_{SEC}$: 23,700 g/mol.

3.2.2.3 G4-SNAP (**3**)

G4-NAP dendrimer (23 mg, 1 μmol) was added to 2 mL of stirring MeOH on ice,

followed by the addition of 1 mL of 1M HCl and the dropwise addition of a 2.2 molar excess

of NaNO$_2$ (9.6 mg, 0.14 mmol) to free thiols dissolved in 1 mL of H$_2$O. The solution was

stirred at 0 °C in the dark for 30 min and concentrated under reduced pressure (water bath <5

°C) to yield a crystalline green glassy solid on the walls of the vessel. The green product was

reconstituted in 2 mL of cold EtOH, the salt byproducts were removed via a 0.2 μm syringe

filter, and filtrate was placed under vacuum to remove the EtOH to yield 22.8 mg (92%) of

10 (G4-SNAP).

3.2.2.4 S-Trityl-N-acetyl-L-cysteine (**4**)

N-acetyl-L-cysteine (7.0 g, 43.7 mmol) was dissolved in 30 mL of concentrated acetic

acid followed by the addition of triphenylmethanol (11.4 g, 44 mmol) and BF$_3$-etherate (8.2

mL, 65 mmol) and the solution was stirred for 3 h at 25 °C. The solution was treated with

150 mL of water and 80 mL of a saturated sodium acetate solution, chilled on ice, and

filtered to yield a white slurry. The slurry was extracted with diethyl ether, concentrated

under reduced pressure, and dried overnight to yield 15.02 g (85%) of a white solid. ^{1}H NMR

(CDCl$_3$, δ): 1.88 (s, NHCOCH_3), 2.67 (m, CH_2S-Trt), 4.35 (q, CH), 6.2 (d, NHCOCH$_3$), 7.18

(t, aromatic, H_4), 7.26 (t, aromatic, H_3), 7.38 (d, aromatic, H_2) . ^{13}C NMR (CDCl$_3$, δ): 23.26 (*CH$_3$*), 33.59 (*CH$_2$*), 55.29 (*CH*), 67.49 (S*C*(Ph)$_3$), 127.36 (C$_4$), 128.49 (C$_3$), 129.92 (C$_2$) ,144.7 (C$_1$) , 171.77 (NH*C*OCH$_3$), 174.33 (*C*OOH).

3.2.2.5 N-Succinimidyl-S-trityl-N-acetyl-L-cysteine ester (**5**)

2 (4.0 g, 10 mmol) and *N*-hydroxy succinimide (1.15 g, 10 mmol) were dissolved in 50 mL CH$_2$Cl$_2$ under N$_2$, cooled to 0 °C, and stirred for 5 min.   Dicyclohexylcarbodiimide (DCC) (2.26 g, 11 mmol) was added and the stirring solution was allowed to warm to 25 °C and stirred for 18 h.   The white solid DCU byproduct was removed via filtration and the CH$_2$Cl$_2$ filtrate was concentrated under reduced pressure to yield 4.13 g (84%) of the white solid activated ester. ^{1}H NMR (CDCl$_3$, δ): 1.94 (s, NHCOC*H$_3$*), 2.79 (m, C*H$_2$*S-Trt), 2.82 (s, COC*H$_2$*C*H$_2$*CO), 4.71 (q, C*H*), 5.81 (d, N*H*COCH$_3$), 7.22 (t, aromatic, H$_4$), 7.30 (t, aromatic, H$_3$), 7.49 (d, aromatic, H$_2$) . ^{13}C NMR (CDCl$_3$, δ): 23.25 (*CH$_3$*), 25.97 (CO*C*H$_2$*C*H$_2$CO), 33.66 (*CH$_2$*), 49.96 (*CH*), 67.97 (S*C*(Ph)$_3$), 127.4 (C$_4$), 128.5 (C$_3$), 129.92 (C$_2$) ,144.48 (C$_1$) , 166.9 (O*C*OCH), 168.8 (*C*OCH$_2$CH$_2$*C*O), 170.0 (NH*C*OCH$_3$).

3.2.2.6 G4-Cys (**6**)

1.23 mL of a 10% G4-PAMAM/MeOH solution (100 mg, 7 µmol dendrimer) was added to 10 mL of stirring CH$_2$Cl$_2$ under N$_2$.   Triethylamine (Et$_3$N) (75 mg, 740 µmol) and activated ester **3** (328 mg, 675 µmol) were then added and the solution was stirred overnight at 25 °C. The CH$_2$Cl$_2$ product solution was washed twice with a saturated sodium carbonate solution (2 x 30 mL) and once with saturated sodium bisulfate (pH ~ 0.2), dried over MgSO$_4$, filtered, and concentrated under reduced pressure to yield a clear glassy solid.   The trityl protecting group was immediately removed via the addition of 10 mL of a TFA solution (95% TFA, 2.5% TIPS, 2.5% H$_2$O) on ice. The TFA/product solution was stirred for 1 h at 0 °C, treated with 25 mL of H$_2$O, and washed with diethyl ether (3 x 50 mL). The aqueous

layer was frozen and lyophilized to yield 110 mg of a white flaky solid (67%). ^{1}H NMR

(D_2O, δ): 1.95 (s, NHCOCH_3), 2.64-2.71 (br, R_2NCH$_2$CH_2CO), 2.79 (m, CH_2SH), 3.12-3.33

(br, NHCH_2CH$_2$NR$_2$, NHCH_2CH_2NHCO), 3.35-3.5 (br, R_2NCH_2CH$_2$CO), 3.51-3.63 (br,

R_2NCH$_2$CH_2CO), 4.30 (s, NHCOCHCH$_2$SH). ^{13}C NMR (D_2O, δ): 23.25 (CH_3), 25.97

(COCH_2CH_2CO), 33.66 (CH_2), 49.96 (CH), 67.97 (SC(Ph)$_3$), 127.4 (C$_4$), 128.5 (C$_3$), 129.92

(C$_2$) ,144.48 (C$_1$) , 166.9 (OCOCH), 168.8 (COCH_2CH_2CO), 170.0 (NHCOCH$_3$).

MW$_{theoretical}$: 23,500 g/mol, MW$_{MALDI}$: 21,200 g/mol, MW$_{SEC}$: 20,630 g/mol.

3.2.2.7 G4-CysNO (**7**)

G4-Cys dendrimer (110 mg, 5.2 µmol) was dissolved in 10 mL of a MeOH/H_2O mixture

(9:1) and added to 90 mL of rapidly stirring toluene. The inhomogeneous mixture was then

treated with excess isopentyl nitrite (10 mL, 69 mmol) to convert the free thiols to *S*-

nitrosothiol NO donors. After the solution was stirred under Ar for 2 h at room temperature

and in the dark, the pink precipitate on the walls of the reaction flask was removed and dried

under vacuum at 0 °C for 24 h to yield 88 mg (75%) of **7** (G4-CysNO).

3.2.3 Ellman's assay for quantification of free thiols

39.6 mg (0.1 mmol) of 5,5'-dithio-bis(2-nitrobenzoic acid) (DTNB) was dissolved in 50

mL of a 50 mM sodium acetate solution and refrigerated until use. Dendrimer samples were

dissolved in water (0.4 mg/mL) and diluted into 3 different dilutions (1:5, 1:10, 1:20) for

reaction with the DTNB. For the assay, 1 mL quartz cuvets were filled with 840 µL of

ultrapure H_2O, 50 µL of the DTNB sodium acetate solution, 100 µL of Tris buffer (1M, pH =

8.0), and 10 µL of the thiol terminated dendrimer sample. The cuvets were incubated at 37

°C for 5 min and the optical density was measured at 412 nm. The absorbance values for

each dendrimer dilution were divided by the extinction coefficient of the DTNB mixed

disulfide complex (13,600 M^{-1}cm^{-1}) resulting in a concentration of thiols in solution. Thiol

concentration was divided by moles of dendrimer in solution to obtain moles of thiol/mol dendrimer. (n=3 dilutions, values are represented as standard deviation of the mean)

3.2.4 NO-release testing of nitrosothiol containing dendrimers

Chemiluminescence[34] was employed to quantify the NO released from the *S*-nitrosothiol dendrimer conjugates upon exposure to various triggers previously identified to initiate nitrosothiol decomposition in the literature (e.g., copper, light, ascorbate and temperature). Total NO release (t[NO], μmol NO/mg) was used to quantify storage efficiency of the thiol-modified dendrimers. The percent yield values in Table 1 were calculated based on 64 theoretical amines on the dendrimer starting material, the successful conversion of these amines to 64 surface thiols, and their modification to 64 *S*-nitrosothiol moieties. Aliquots (10 μL) of the dendrimer products in 5 mM EDTA in water for G4-CysNO or EtOH for G4-SNAP were added to a reaction flask containing 10 mM phosphate buffered saline (PBS, pH=7.4) with 5 mM EDTA to chelate trace copper in the media. A large excess of EDTA was required to completely remove initial bursts of NO-release attributed to Cu^{2+} ion impurities in solution. A chelator was not employed during Cu^{2+}-mediated NO-release testing. All NO-release testing was conducted at physiological temperature (37 °C) except when testing the rates of thermal decomposition. Dendrimer concentrations in the 30 mL reaction flask ranged from 300-700 nM. The chemiluminescence analyzer was calibrated with NO gas (24.1 ppm). The value for converting instrument response (ppb) to moles of NO was obtained via the conversion of known concentrations of nitrite standards to NO in a 0.1 M KOH/H_2SO_4 solution (1.34×10^{-13} moles NO/ppb). During photo-initiated NO release experiments 60, 100, or 200 W bulbs were employed (Crystal Clear, General Electric). The light source was positioned ~5 inches from the sample. Copper solutions were prepared by dissolving $CuBr_2$ in the running buffer (200 -1000 μM) prior to degassing the sample.

Chemiluminescence data for the NO-releasing dendrimers were represented in two graphical forms or plots: 1) chemiluminescence response in ppb NO/mg dendrimer versus time; and, 2) the total amount of NO-release (t[NO], μmol NO/mg) versus time. Kinetic parameters including the maximum flux of NO release ($[NO]_m$) and the time required to reach that maxima (t_m) were obtained from plot 1 while the half-life ($t_{1/2}$) of NO release was determined from plot 2.

3.2.5 Platelet rich plasma isolation

Fresh platelets were prepared from venous blood drawn from healthy volunteers in accordance with institutional guidelines. Whole blood (42.5 ml blood to 7.5 ml anticoagulant) was drawn into a syringe containing citrate (3.2% by weight, pH = 7.4). Platelet rich plasma (PRP) was obtained by centrifugation (200 x g, 20 min) at 25 °C. The platelet rich plasma was centrifuged at 1000 x g for 10 min at room temperature to obtain a platelet pellet. The platelet pellet was suspended in the original volume of Tyrode's buffer (without divalent cations, 137 mM NaCl, 3 mM KCl, 3 mM sodium phosphate, 2 mM sodium bicarbonate, 5 mM glucose, 10 mM Hepes) and centrifuged as in the last step. The final pellet was suspended in Tyrode's buffer at 200,000 platelets/μL, as measured with a Heska hematological analyzer.

3.2.6 Aggregation studies

Aliquots of platelets in Tyrode's buffer at 200,000 platelets/μl were placed in the optical cuvettes in the aggregometer (Chrono-Log Whole Blood Aggregometer) and equilibrated to 37 °C while stirring. DMSO stocks of NO donor compounds (or neat DMSO as a carrier control) were diluted 1/100 into the stirred platelet suspensions and allowed to incubate for 15 min. Aggregation reactions were initiated by adding 100 x stocks of $CaCl_2$ for a final calcium concentration of 10 mM and 100 NIH unit/ml stocks of human α-thrombin for a

final concentration of 1 NIH unit/ml. The degree to which test agents inhibited thrombin-mediated platelet aggregation was estimated from the final extent of aggregation (turbidity change) at 25 min. The turbidity changes of each sample were normalized to the turbidity observed for the DMSO carrier. Dose response curves represent the average of two independent sets of measurements on different days with different blood donors tested n=3 times each. The error bars represent standard error of the mean between the two sets of measurements.

3.3 Results and Discussion

3.3.1 Synthesis of thiol modified dendrimers

3.3.1.1 G4-NAP (**2**)

Previously, Wang and co-workers developed a strategy toward increasing the cellular uptake of *S*-nitrosothiols in human prostate cancer cells by first reacting amino sugars with the cyclized thiol, 3-acetamido-4,4-dimethylthietan-2-one.[8, 35] Utilizing a similar approach to modify the exterior amines of a generation 4 PAMAM dendrimer, *N*-acetyl-D,L-penicillamine was cyclized in low yields (29%) to **1** (3-acetamido-4,4-dimethylthietan-2-one) with acetic anhydride and pyridine.[36] The G4-PAMAM dendrimer was then modified with thiol in one step via the reaction of the surface primary amines with thiolactone (**1**) (Scheme 3.1). Following dialysis and lyophilization, the extent of G4-NAP (**2**) modification was assessed via ^{1}H NMR and the Ellman's assay[37, 38] to quantify the number of free thiols attached to the dendrimer scaffold.   The integrated intensity of the protons on the geminal methyl substituents adjacent to the terminal thiols (C(CH_3)SH) was compared to the interior methylene protons inside the dendrimer to confirm attachment of the *N*-acetyl-D,L-penicillamine groups (Figure 3.2 and 3.3). The number of immobilized thiol groups was

calculated to be 63 (Equation 3.1), correlating well with number of free thiols assayed on the dendrimer surface 62.1 ± 2.2 (Ellman's assay).

Equation 3.1 $\dfrac{Intensity_{(COCH_3)}}{3x} = \dfrac{H_a's}{Intensity_{(A)}}$ Where x = number of NAP groups

$$\dfrac{0.491}{3x} = \dfrac{0.978}{124 + 4x} \qquad 60.88 = 0.97x \qquad x = 62.76$$

Size exclusion chromatography (SEC) was employed to assess both the molecular weight and purity of the dendrimer conjugate. SEC revealed negligible low molecular weight impurities following the synthesis and isolation of product. However, a significant population of high molecular weight species was observed (Figure 3.4A). Although the *N*-acetyl-D,L-penicillamine-modified dendrimer contained 20% multimer by weight, the majority of the sample was the fully reduced 23,700 MW G4-NAP. Multimer formation was attributed to the presence of intra- and/or inter-dendrimer disulfide crosslinks but dendrimer conjugates were not stored/prepared under reducing conditions as such chemistry proved incompatible with subsequent *S*-nitrosothiol formation. High resolution MALDI-TOF mass spectrometry of **2** prepared in a sinapinic acid matrix indicated that the molecular weight of G4-NAP was 23,000 g/mol, further validating the SEC data. A summary of dendrimer characterization data is provided in Table 3.1.

Figure 3.1   Generation 4 polyamidoamine (PAMAM) dendrimer containing a completely modified exterior (64 thiols) of *S*-nitroso-*N*-acetyl-D,L-penicillamine (G4-SNAP) or *S*-nitroso-*N*-acetylcysteine (G4-CysNO).

Scheme 3.1   Synthesis of *S*-nitrosothiol modified generation 4 PAMAM dendrimer, G4-SNAP (**3**).

For Fully Thiol Modified (x = # of thiols)
H_a = 124 internal protons + 4(x)
H_f = 124 internal protons + 2(x)
H_c = 124 internal protons + 2(x)
H_e = 124 internal protons

For Unmodified Branches
H_a = 124 internal protons
H_b = 128 external protons
H_c = 124 internal +128 external protons
H_d = 128 external protons
H_e = 124 internal protons
H_f = 124 internal +128 external protons

Figure 3.2   Proton assignments for G4-PAMAM dendrimer illustrating the difference between unmodified dendrimer branches (primary amines) and modified branches where R = CH_3 (G4-NAP), H (G4-Cys).

Figure 3.3 ^{1}H NMR spectrum of G4-NAP (**2**) dendrimer in D$_2$O with proton assignments referenced in Figure 3.2.

G4-Cys SEC Chromatography

G4-Cys (20,630 g/mol)

G4-NAP SEC Chromatography

G4-NAP (23,700 g/mol)

Figure 3.4   Size exclusion chromatographs of A) G4-Cys and B) G4-NAP thiol modified dendrimers illustrating the distribution between the higher molecular weight multimers (1) and the dominant single molecular weight dendrimer (2).

Table 3.1   Characterization data for generation 4 PAMAM thiol conjugates G4-NAP and G4-Cys and NO storage efficiency once converted to the corresponding *S*-nitrosothiol NO donors.

| | # thiols / mol | | Molecular Weight | | | | NO Storage Efficiency | |
	Ellman's	^{1}H NMR	MALDI	SEC	% multimer	M_w/M_n	μmol NO·mg^{-1}	% yield
G4-NAP	62 ± 2	63	23,000	23,700	20%	1.03 ± 0.15	1.7 ± 0.2	79%
G4-Cys	49 ± 4	58	21,200	20,630	16%	1.04 ± 0.11	2.1 ± 0.2	87%

3.3.1.2 G4-Cys (**6**)

Although the synthetic procedure described above yields G4-NAP thiol-modified dendrimer in two steps, this straightforward approach may not be useful when other functionalities need to be appended to the dendrimer scaffold. The opening of the thiolactone ring results in the formation of highly reactive thiols which may interfere/compete with remaining dendrimer amines during conjugation of additional moieties. Thus, protected *S*-trityl-*N*-acetyl-L-cysteine was employed as a precursor to nitrosothiol formation allowing for future orthogonal coupling to the dendritic exterior. A similar approach was described previously to synthesize cysteine-modified poly(propyleneimine) dendrimers to allow native chemical ligation of both oligopeptides and recombinant proteins.[39] *N*-acetyl-L-cysteine was trityl-protected using a mixture of triphenyl methanol and BF$_3$-etherate in concentrated acetic acid (Scheme 3.2).[25]   Upon neutralization with saturated sodium acetate and extraction in ether, the white solid **4** was isolated (85% yield). Following activation to the succinimidyl ester **5,** the *S*-trityl-*N*-acetyl-L-cysteine-protected thiol was coupled to G4 PAMAM by reaction with the dendrimer's exterior amines. The trityl protected dendrimer conjugate was then treated with trifluoroacetic acid to remove the trityl protecting groups. The dendrimer product was dissolved in water, washed with ether, and lyophilized to yield **6** (G4-Cys) as a white flaky solid (67%). The number of free thiols attached to the dendrimer exterior for the Cys conjugate was calculated to be 58 (Equation 3.2) as confirmed by ^{1}H NMR spectroscopy (Figure 3.5).

Equation 3.2 $\dfrac{Intensity_{(COCH_3)}}{3x} = \dfrac{H_c's}{Intensity_{(C)}}$ Where x = number of Cys groups

$$\frac{1.0}{3x} = \frac{1.38}{124 + 2x} \qquad\qquad 124 = 2.14x \qquad x = 57.86$$

Size exclusion chromatography (SEC) of G4-Cys resulted in similar chromatograms as described above for G4-NAP, whereby 16% high molecular weight species was detected arising from dendrimers crosslinked via disulfide bridges (Figure 3.4B). The molecular weight of the higher molecular weight impurity calculated from light scattering data was 44,550 g/mol, approximately double the mass of the dominate G4-Cys single dendrimer (20,630 g/mol), suggesting dimer formation. MALDI-TOF mass spectrometry confirmed that the molecular weight of the prominent G4-Cys species was 21,200 g/mol consistent with the molecular weight observed in SEC. The protection/deprotection strategy employed herein may be useful in the future synthesis of multifunctional NO-releasing dendrimers since it allows for orthogonal coupling of multiple agents to the dendrimer scaffold without interfering with the thiol structure.

3.3.2 Conversion to S-nitrosothiol dendrimers

To convert the thiols to *S*-nitrosothiols, acidified nitrite solutions were employed. When compared to their alkyl nitrite counterparts, such solutions are faster and more efficient at nitrosothiol formation.[40] The tertiary thiol (G4-NAP) and primary thiol (G4-Cys) dendrimers provide macromolecules with different thiol stabilities and chemical properties when converted to the corresponding NO donors. Dendrimer **2** (G4-NAP) was dissolved in a 50:50 mixture of MeOH / 1M HCl and treated with $NaNO_2$ on ice. The acidified nitrite solution rapidly turned green indicating *S*-nitroso-*N*-acetyl-D,L-penicillamine (SNAP) formation. Following removal of the solvent under reduced pressure at 0 °C, the nitrosothiol-modified dendrimer was reconstituted in cold ethanol and removed from the salt byproducts via filtration. The ethanol was again removed at 0 °C to yield **3** as a green polymer film in 92% yield. Low temperatures and shielding from light were maintained throughout the isolation procedure to prevent NO release and the formation of insoluble aggregates.

Primary nitrosothiol adducts (e.g., *S*-nitroso-cysteine) have been historically difficult to isolate following nitrosothiol formation due to poor RSNO stability.[41] Similarly, the acidified nitrite approach described above proved troublesome when working with the G4-Cys dendrimer. Removal of the solvent led to an insoluble polymerized network of thiol dendrimers. As an alternative strategy to convert free thiols of **6** to *S*-nitrosothiol NO donors, the dendrimer was dissolved in a methanol/water solution, added to 200 mL of stirring toluene, and treated with isopentyl nitrite.[25] After reaction with the organic nitrite source for 2 h, a pink precipitate was observed on the walls of the flask. The precipitate was removed via filtration and dried under vacuum to yield **7** (G4-CysNO, 75%). As *S*-nitrosothiol dendrimer conjugates proved susceptible to thermal decomposition, low temperatures were employed during all isolation steps to minimize NO donor degradation and prevent dendrimer disulfide cross linking.

G4-SNAP and G4-CysNO nitrosothiol dendrimer conjugates possessed characteristic absorption maxima governed by the tertiary or primary thiol structures (Figure 3.6). The G4-SNAP dendrimer had an intense broad band at 341 nm ($\pi \rightarrow \pi^*$) and a weaker absorption maxima at 596 nm ($n \rightarrow \pi^*$) giving the anti conformer of the tertiary thiol its greenish color.[42, 43] The G4-CysNO conjugate had a similar $\pi \rightarrow \pi^*$ transition at 320 nm and a blue shifted $n \rightarrow \pi^*$ transition at 545 nm.

Scheme 3.2   Synthesis of G4-CysNO, S-nitrosothiol modified generation 4 PAMAM
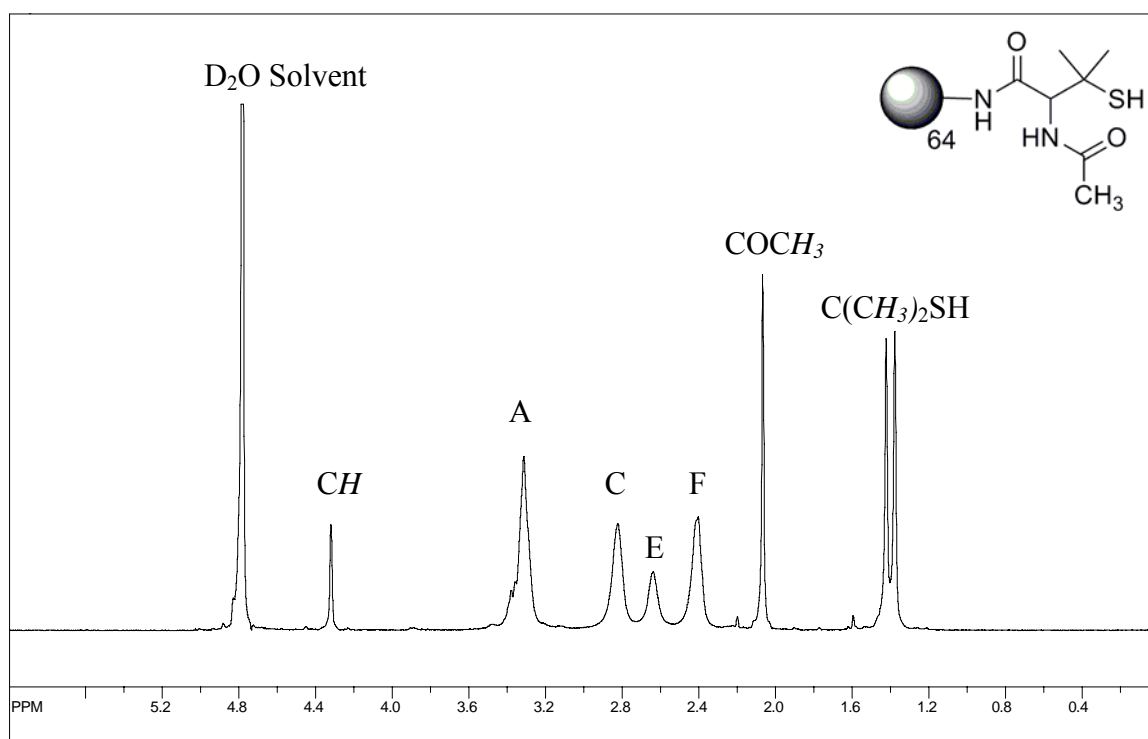   dendrimer.
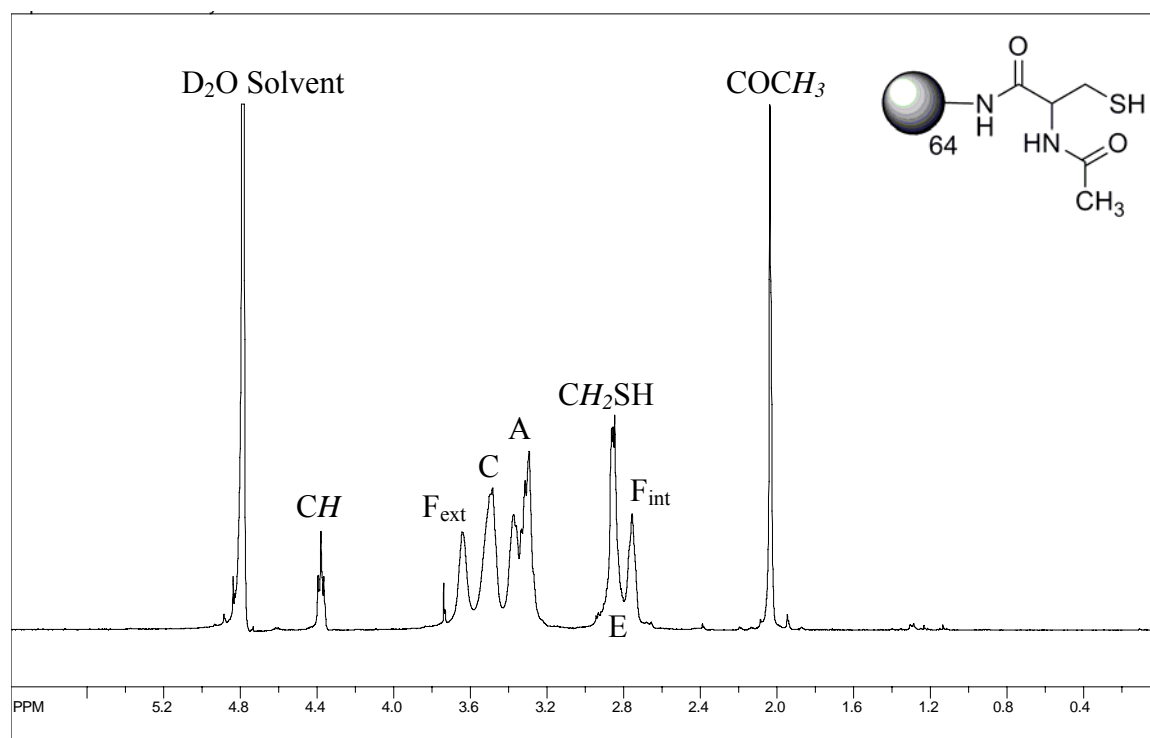
Figure 3.5 ^{1}H NMR spectrum of G4-Cys (**6**) dendrimer in D$_2$O with proton assignments referenced in Figure 3.2.
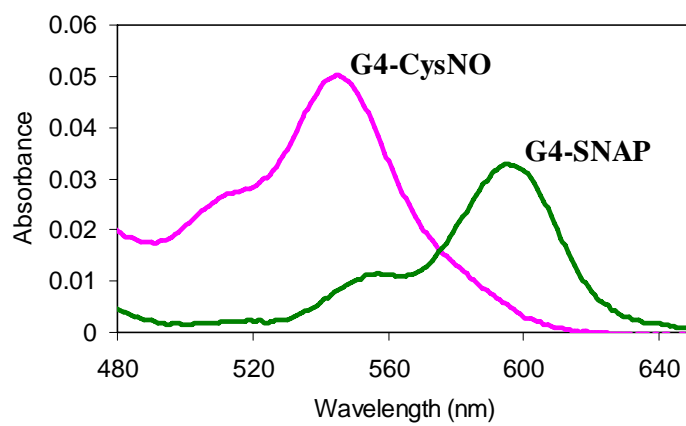
Figure 3.6   UV-Vis absorption spectra of G4-SNAP and G4-CysNO dendrimer
conjugates (2 mg/mL in EtOH solutions).

A. Copper Mediated Decomposition

B. Photo-initiated Decomposition

C. Transnitrosation
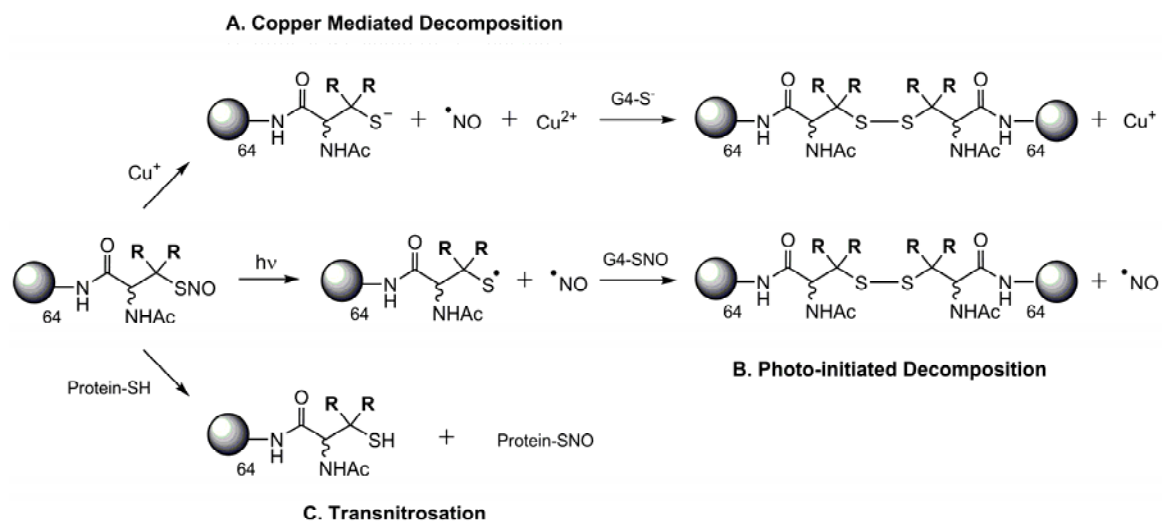
Scheme 3.3   Mechanisms of nitrosothiol decomposition and NO release from G4-RSNO dendrimer conjugates.

110

3.3.3 Characterization of NO storage through RSNO decomposition

3.3.3.1 Copper mediated NO-release

A major mechanism of *S*-nitrosothiol decomposition is mediated via the Cu^+/Cu^{2+} redox couple and copper containing enzymatic metal centers.[5, 43, 44] Previous work has confirmed that the breakdown reaction proceeds via the reduction of Cu^{2+} by trace thiolate anion in solution to yield Cu^+ that subsequently reduces RSNO compounds to initiate NO release (Scheme 3.3A).[44] An aqueous solution containing copper bromide ($CuBr_2$) was utilized to decompose the *S*-nitrosothiol dendrimer conjugates to NO and corresponding dendritic disulfides. All copper mediated NO-release testing was performed in phosphate buffered saline (PBS, pH = 7.4) at physiological temperature (37 °C) and in the dark.

The real-time NO-release profiles for copper initiated NO release from G4-SNAP (**3**) and G4-CysNO (**7**) are shown in Figure 3.7 (A and B). The tertiary *S*-nitrosothiols of G4-SNAP exhibited a more rapid release of NO as evidenced by the maximum intensity of NO release, $[NO]_m$. For example at 1 mM Cu^{2+}, the $[NO]_m$ for G4-SNAP was 92,100 ppb/mg whereas the $[NO]_m$ for G4-CysNO was only 26,200 ppb/mg. The kinetics of G4-SNAP dendrimer decomposition exhibited small changes as a function of Cu^{2+} concentration with 0.2 and 0.6 mM Cu^{2+} possessing nearly identical NO-release profiles. However, $[NO]_m$ of the primary *S*-nitrosothiol terminated dendrimer G4-CysNO scaled with copper concentration (Figure 3.7B, Table 3.2) but never reached the same intensity as the G4-SNAP NO-release. The full set of kinetic parameters including the time required to reach the maximum flux (t_m) and half life of NO-release ($t_{1/2}$) are given in Table 3.2.

The difference in copper-initiated NO release is attributed to the *S*-nitrosothiol structure. According to previous reports, primary small molecule nitrosothiols such as *S*-nitrosoglutathione (GSNO) are oxidized to the GSSG disulfide in the presence of Cu^{2+} which

effectively chelates remaining Cu^{2+} in solution and thus slows nitrosothiol decomposition.[45] However, S-nitroso-N-acetyl-$_{D,L}$-penicillamine (SNAP) does not chelate copper via the resulting disulfide and decomposes rapidly to yield NO even at substoichiometric quantities.[45]   In the presence of copper, the macromolecular RSNO donors presented herein exhibited the same characteristic NO release behavior as the small molecule analogues reported in the literature. This phenomenon is best indicated by the total NO-release curves shown in Figure 3.7C. At 0.2 mM Cu^{2+}, only 12 min were required for the G4-SNAP dendrimer (**3**) to achieve complete NO release, whereas the G4-CysNO dendrimer (**7**) slowly decomposed to NO over a period of 15 h. Despite the variable NO-release kinetics, the same level of total NO released (t[NO], Table 3.1) was achieved regardless of the copper concentration corresponding to 79% NO-storage efficiency for the synthesis of the G4-SNAP dendrimer and 87% for G4-CysNO.

In the development of S-nitrosothiol therapeutics, copper-mediated NO-release holds minimal promise due the lack of free-circulating Cu^{2+}. Ascorbate has often been mistaken as another trigger to initiate S-nitrosothiol decomposition as its concentration in the blood is appreciable (81 μM).[46] However, ascorbate mediates NO release only through the reduction of trace metal ions in solution which then promote NO release.[47] In the presence of EDTA, the dendritic nitrosothiols exhibited no increase in the rate of NO release upon exposure to concentrations of ascorbate up to 2 mM, suggesting that ascorbate is not a viable initiator of S-nitrosothiol dendrimer decomposition (data not shown). Of note, this does not rule out the possibility of other agents capable of facilitating the one-electron reduction to release NO for future therapeutic applications.[5]
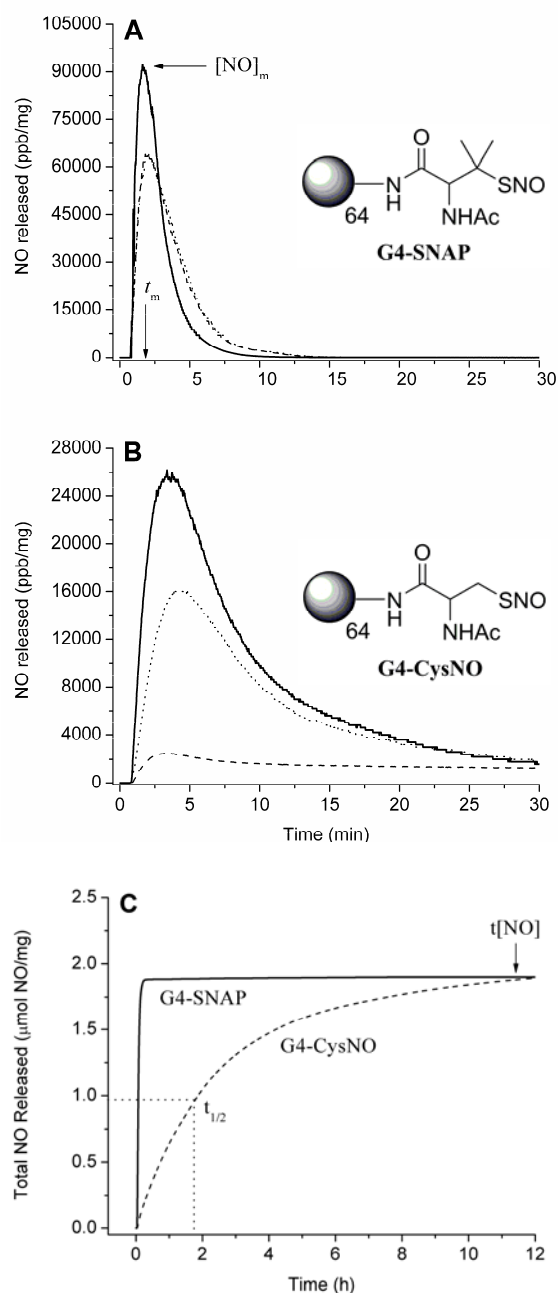
Figure 3.7   A) NO-released from **3** (G4-SNAP) exposed to 200 μM (---), 600 μM
(······), and 1 mM (—) Cu^{2+} in PBS buffer at 37 °C. B) NO-released from
7 (G4-CysNO) exposed to 200 μM (---), 600 μM (······), and 1 mM (—)
Cu^{2+} in PBS buffer at 37 °C. C) Total NO-release curves of G4-SNAP
and G4-CysNO illustrating the kinetic difference between tertiary and
primary nitrosothiol decomposition at 200   M Cu^{2+}. (Data is truncated
at 12 h, despite the increase of G4-CysNO-release for up to 15 h.)

Table 3.2   Kinetic parameters for NO-release from generation 4 PAMAM nitrosothiol conjugates G4-SNAP and G4-CysNO as a function of decomposition trigger and concentration.

| G4 Dendrimer | Trigger | | $t_{1/2}$ (min) | $[NO]_m$ (ppb/mg) | t_m (min) |
	type	[conc]			
G4-SNAP	Cu^{2+}	0.2 mM	2.3	63000	1.1
		0.6 mM	2.2	58700	1.3
		1 mM	1.5	92100	0.9
	light	60 W	200	1990	7.5
		100 W	97	2360	9.5
		200 W	34	5800	2.0
	37 °C	--	ND	158	6.4
G4-CysNO	Cu^{2+}	0.2 mM	106	2510	2.6
		0.6 mM	16	15900	3.1
		1 mM	7	26200	2.7
	light	60 W	97	1480	10.1
		100 W	90	1790	24.4
		200 W	49	2210	27.4
	37 °C	--	ND	116	8.8

114
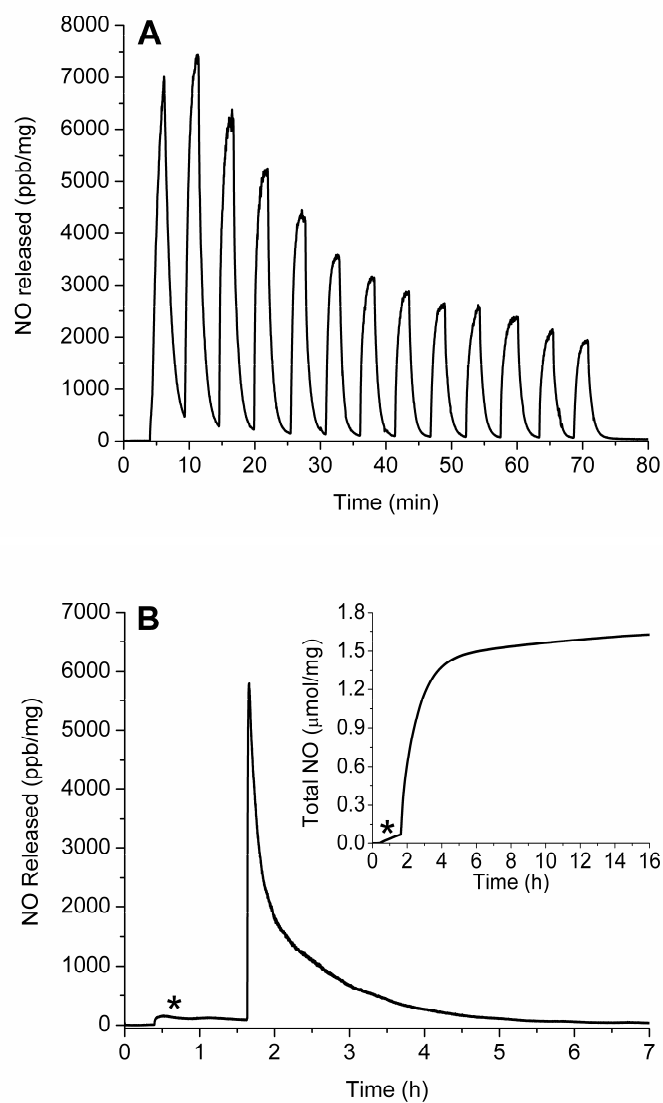
Figure 3.8   A) Phototriggered on/off behavior of G4-SNAP dendrimer conjugate (**3**) at 200 W. Sample was irradiated at 2 min intervals followed by 3 min of darkness B) Permanent irradiation of G4-SNAP at 200 W illustrating the long first order decay over several hours. The * signifies thermal NO-release at 37 °C prior to exposing the dendrimer to the light source. (Inset: Total NO release curve for G4-SNAP.)

115

3.3.3.2 Photoinitiated NO-release

Photoinitiated NO-release is another well-characterized mechanism of RSNO decomposition.[48] Irradiation at either RSNO absorption maximum has been shown to result in homolytic cleavage of the S-N bond to yield NO and a thiyl radical in a process that is approximately first-order.[48] Electron paramagnetic resonance spectra of spin-trapped thiyl radicals have been reported as concrete evidence for the phototriggered homolysis of the S-N bond.[49] Photolysis of dendrimer nitrosothiol conjugates with a broad spectrum white light source also yielded a dendritic thiyl radical and NO (Scheme 3.3B). The reaction is further propagated when the resulting thiyl radical reacts with a neighboring RSNO branch to produce a disulfide and additional NO (Scheme 3.3B). Consistent with previously reported observations for nitrosothiol decomposition,[25] the NO-release from G4-SNAP and G4-CysNO dendrimers was dependent on light intensity and followed first order decay (Table 3.2). The nitrosothiol-modified dendrimers were also extremely responsive to the light source and exhibited a clear on/off behavior when the light was removed. The behavior of G4-SNAP exposed to repeat cycles of 2 min light irradiation followed by 3 min of darkness is shown in Figure 3.8A. When the 200 W light source was removed, the signal rapidly returned to baseline. The intensities of $[NO]_m$ slowly declined during subsequent irradiations, as expected with the depletion of RSNO. Homolytic cleavage of the S-N bond may also result via thermal decomposition of RSNO donors, albeit at a much slower rate. The difference between the slow thermal decomposition of G4-SNAP dendimer (9.31 pmol NO·mg^{-1}·s^{-1}, indicated by the asterisk) and the rate of NO-release upon exposed to 200 W light is shown in Figure 3.8B.

Overall, G4-SNAP dendrimer was more susceptible to changes in light intensity than G4-CysNO. Both dendrimers resulted in similar half-lives and $[NO]_m$ at 200W (Table 3.2) but

the most significant kinetic variation between the two conjugates was observed at early periods (<30 min). The initial rates of phototriggered decomposition for the G4-CysNO dendrimer were also slower than the G4-SNAP conjugate as indicated by the time required to reach the maximum flux (t_m) (Table 3.2). This initial delay and lower intensity of G4-CysNO release is explained by a "cage effect" imposed by the G4-CysNO dendrimer conjugate whereby a more compact solution structure results in the increased frequency of geminate radical pair recombination and slows the initial rates of NO release.[50,51] Indeed, Shishido et al. have demonstrated that photogeneration of NO from *S*-nitroso-*N*-acetylcysteine in a PEG matrix resulted in a 22-fold decrease in the intial rate of RSNO decomposition when compared to normal aqueous media.[51] Additionally, the PEG microenvironment reduced the rates of thermal decomposition at room temperature. The increased stability of the macromolecular G4-CysNO structure in this work suggests a "dendritic effect" on phototriggered NO release. This "cage effect" may be manipulated in future biomedical applications by increasing dendrimer size (G5-G8) or through the attachment of poly(ethylene glycol) functionalities to the dendrimer exterior leading to increased storage and handling of *S*-nitrosothiols.

3.3.4 S-nitrosothiol inhibition of platelet aggregation

Free nitric oxide inhibits platelet aggregation via a guanylyl-cyclase dependent mechanism.[16] However, the signaling actions of RSNOs are not completely dependent on the release of free NO and the mechanism by which they deliver NO to platelets is much debated.[52] Transnitrosation[5] between RSNO and membrane bound protein thiols provides a mechanism for direct cellular communication and transfer of NO. Transnitrosation can be defined as the transfer of the nitroso functional group from a nitrosothiol donor to a free thiol

as shown in Scheme 3.3C. Indeed, transnitrosation reactions between exogenous NO donors and proteins on the platelet surface are well characterized.[53-55]

The efficacy of the G4-SNAP dendrimer conjugate at inhibiting thrombin-catalyzed platelet aggregation was examined to compare the biological activity of the RSNO-modified dendrimers to free small molecule SNAP. Platelet aggregation as monitored by the loss of turbidity in solution using an aggregometer is shown in Figure 3.9 for the small molecule SNAP and G4-SNAP dendrimer. A dose-dependent inhibition of platelet aggregation was observed for the SNAP NO donor with 75% inhibition observed at 100 μM SNAP (Figure 3.9A). Solutions prepared with equimolar RSNO functionalites on G4-SNAP dendrimer (estimated at 64 RSNO per mol dendrimer) exhibited a pronounced inhibition of thrombin-mediated aggregation regardless of dendrimer concentration (Figure 3.9B). At 25 μM SNAP functionality on the G4-SNAP conjugate (390 nM dendrimer), a 62% reduction in aggregation was observed compared to only a 17% inhibition for 25 μM small molecule SNAP. The abundance of RSNO donors localized on the dendritic structure was far more effective at inhibiting platelet aggregation compared to small molecule SNAP in solution. Control G4-NAP (**2**) and *N*-acetyl-D,L-penicillamine without NO were also evaluated at concentrations up to 100 μM and showed minimal effects on platelet aggregation. The inactivity of the thiol controls and the absence of SNAP decomposition triggers in these experiments (e.g., light, copper, etc.) indicate that the observed inhibition of platelet aggregation was mediated via transnitrosation and any resulting nitrogen species derived from transnitrosation. [53-55]
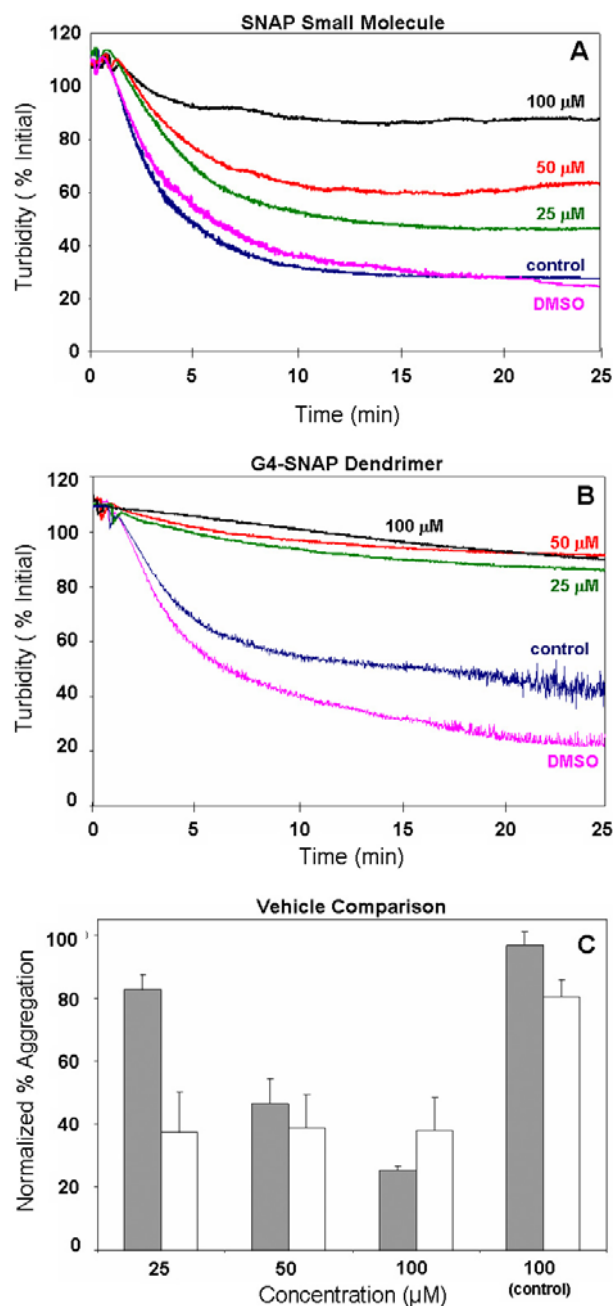
Figure 3.9   Human thrombin-initiated platelet aggregation in the presence of A) SNAP small molecule or B) G4-SNAP dendrimer conjugate. Turbity changes of the 0-100 uM RSNO donors were normalized to the DMSO signal (100%). C) Normalized percent aggregation for SNAP (gray) and G4-SNAP dendrimer (white). Control represents aggregation in 100 μM thiol control (*N*-acetyl-D,L-penicillamine or G4-NAP.   Error is represented as standard error of the mean for two independent blood samples tested n=3 times each.

3.3.5 Glutathione initiated NO-release

The absence of plasma or blood components in in vitro studies that influence NO delivery and transnitrosation is one of the confounding factors that clout the effects of RSNO in clinical studies.[15] Glutathione (GSH) is present in blood at concentrations near 500 μM and plays a key role as an antioxidant and as a reducing agent for thiol containing proteins. Moreover, GSH and other thiols have been shown to decompose nitrosothiol donors through direct transnitrosation and result in disulfide bond formation (e.g., GSSG) and the liberation of multiple NOx species.[49] Previously, Singh et al. studied the transnitrosation process between the GSH/SNAP small molecule pair, revealing that the rate of SNAP decomposition increased with increasing concentrations of GSH up to 500 μM.[49] These experiments, performed under aerobic conditions, led to large amounts of nitrite formation (NO_2^-) and the exact quantities of NO released were not determined. To date, no studies have been conducted to directly measure the quantities of NO released from nitrosothiols in the presence of physiological concentrations of GSH.

The NO evolved from G4-SNAP upon exposure to physiologically relevant GSH concentrations was measured under anaerobic conditions and the NO generated from G4-SNAP decomposition was removed from the sample and carried to the detector by a stream of $N_{2(g)}$. The total NO-release versus time for G4-SNAP (13 μM) exposed to GSH (0.5-10 mM) is shown in Figure 3.10. The rate of NO-release was the greatest at 500 μM GSH, the physiological concentration of GSH in blood, reaching a maximum flux ($[NO]_m$) of 1429 ppb NO·mg^{-1}·s^{-1} (191 pmol NO·mg^{-1}·s^{-1}) after 45 min. Direct comparison of the NO-release curves at 500 μM and zero added GSH, conditions under which the dendrimer only releases NO via thermal decomposition at 37 °C, is shown in Figure 3.11. In the absence of light, copper, or free thiol, G4-SNAP failed to generate large quantities of NO. Increasing the

GSH concentration resulted in a dose-dependent decrease in the total NO (t[NO]) observed, presumably from GSH scavenging NO at high GSH concentrations.[56] All of the glutathione experiments resulted in lower t[NO] when compared to the rapid production of NO when G4-SNAP was exposed to 200 mM Cu^{2+}, yielding 100% percent release of the covalently bound NO (Figure 3.10). A summary of the NO-release properties of G4-SNAP in the presence of GSH is provided in Table 3.3.

As illustrated by the chemiluminescence experiments described above, spontaneous generation of NO in 500 μM GSH results in NO donor behavior similar to diazeniumdiolates, whereby large concentrations of NO are rapidly released into solution. These findings suggest that the effect of GSH and other blood components is critical for understanding the translation of nitrosothiol data generated in vitro toward in vivo animal or clinical studies. Indeed, direct transnitrosation reactions between other nitrosothiols and GSH have been monitored spectroscopically and favor the production of the more stable GSNO adduct.[49] Due to the vast excess of GSH over every other thiol in blood, it is likely that the transfer of NO will be effectively unidirectional from any *S*-nitrosothiol to glutathione.[49] Glutathione represents a sink for the transnitrosation process and the fate of GSNO decomposition is of significant importance. Current studies are underway to understand the decomposition of GSNO in the presence of GSH in order to further explore thiol-initiated mechanisms of NO-release.
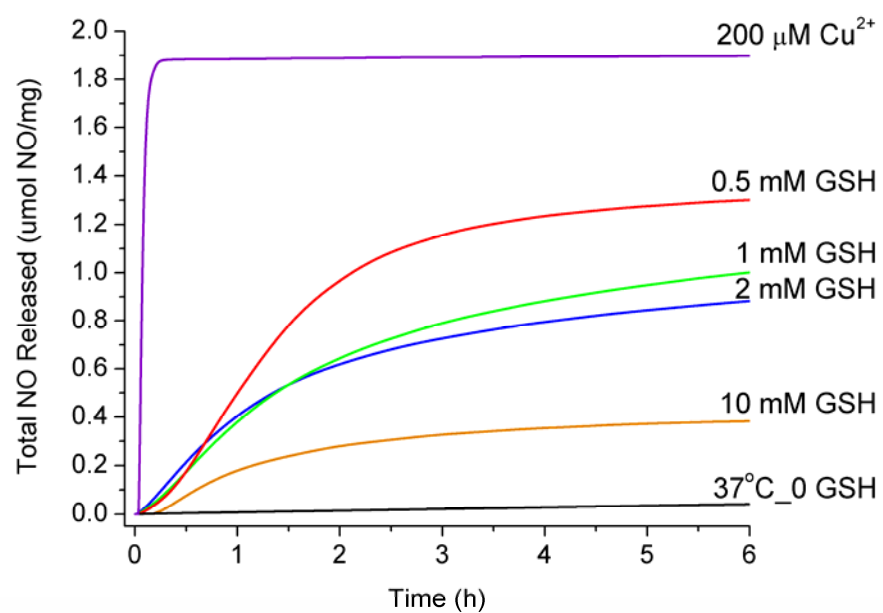
Figure 3.10   Total NO-release curves of G4-SNAP exposed to variable triggers of
                RSNO donor decomposition.
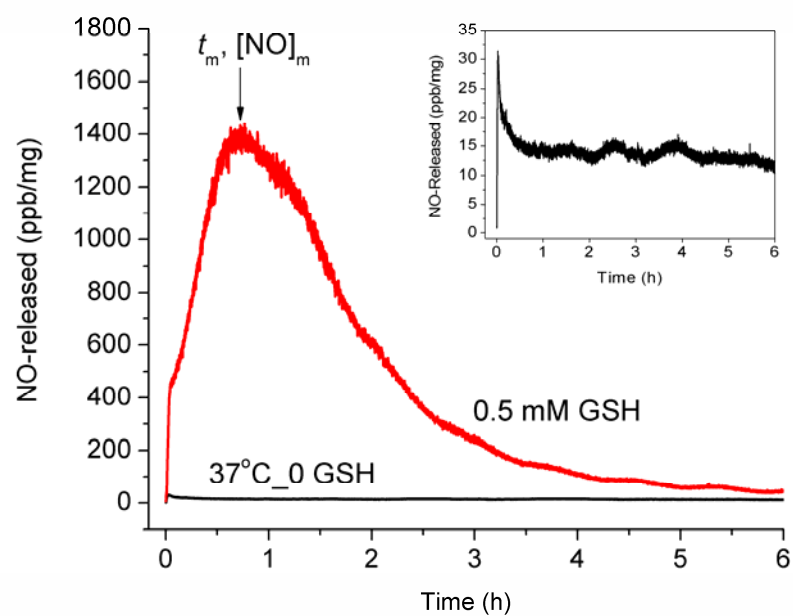
Figure 3.11   Real-time detection of NO-released from DMR-SNAP in the presence of 500 μM GSH compared to the slow decomposition of the RSNO donor at 37 °C. (Inset: Close-up of the thermally initiated NO-release data at 37 °C.)

Table 3.3   NO-release properties for G4 DMR-SNAP exposed to various triggers
for RSNO decomposition.

Trigger		t[NO] (μmol NO·mg^{-1})		$[NO]_m$ (ppb·mg^{-1})	t_m (min)
		6 h	16 h		
Cu^{2+}	200 μM	1.89	1.90	63000	1.1
Glutathione	0.5 mM	1.30	1.39	1430	43
	1 mM	1.01	1.21	990	31
	2 mM	0.88	1.05	1020	18
	10 mM	0.38	0.40	570	17
Thermal	37 °C	0.04	NA	30	1.4

3.4 Conclusion

The synthesis of thiol-modified G4-PAMAM dendrimers and their conversion to *S*-nitrosothiol NO donors represents a new class of NO-releasing dendrimer constructs. The dendrimer scaffold enables the enhanced storage of RSNO donors compared to previously reported nitrosothiol delivery vehicles. For example, G4-PAMAM (MW 14,215 g/mol) has 64 surface sites for NO loading (Figure 3.1) compared to only 14 for a fully reduced serum albumin conjugate (MW ~66,000g/mol).[26] The G4-SNAP and G4-CysNO dendrimers effectively stored and released 1.7 ± 0.2 and 2.1 ± 0.2 μmol NO·mg^{-1}, respectively, when using known triggers of nitrosothiol decomposition such as Cu^{2+} and light. The anti-platelet activity of G4-SNAP dendrimer was 45% more effective at preventing platelet aggregation at 25 μM than the corresponding small molecule NO donor SNAP. The on/off triggering of NO-release and the ability to undergo transnitrosation reactions with biological substrates (e.g., platelets) allows for careful control of NO-release previously unattainable with diazeniumdiolate-modified dendrimers.[30]

Since NO donors are highly reactive, targeting NO to specific tissues or cell types is challenging. An advantage of the dendritic scaffold over other potential RSNO drug delivery vehicles is the ease in which multiple surface functionalities may be appended to the dendrimer exterior. For example, Baker and co-workers have synthesized dendrimers containing the methotrexate (an anti-cancer drug), fluorescent probes for imaging, and folic acid residues for targeting the delivery vehicle to cancerous tissue in vivo.[57] Work is underway in our laboratory to synthesize multi-functional dendrimer conjugates that integrate the recent advancements in nanoparticle drug delivery with the current mechanistic understanding of nitrosothiols in physiology to create highly specialized NO-releasing therapeutics.

3.5 References

1.   Hogg, N. "The biochemistry and physiology of S-nitrosothiols." *Annu. Rev. Pharmacol. Toxicol.* **2002,** *42*, 585-600.

2.   Tyurin, V. A.; Tyurina, Y. Y.; Liu, S.-X.; Bayir, H.; Hubel, C. A.; Kagan, V. E. "Quantification of *S*-nitrosothiols in cells and biological fluids." *Methods in Enzymology* **2002,** *352*, 347-360.

3.   Stamler, J. S. "S-nitrosothiols in the blood." *Circ. Res.* **2004,** *94*, 414-417.

4.   Al-Sa'doni, H. H.; Ferro, A. "S-nitrosothiols as nitric oxide-donors: chemistry, biology and possible future therapeutic applications." *Curr. Med. Chem.* **2004,** *11*, 2679-2690.

5.   Hogg, N. "Biological chemistry and clinical potential of *S*-nitrosothiols." *Free Radical Biol. Med.* **2000,** *28*, 1478-1486.

6.   Ignarro, L. J. "Nitric oxide: A unique endogenous signaling molecule in vascular biology." *Angew. Chem. Int. Ed.* **1999,** *38*, 1882-1892.

7.   Babich, H.; Zuckerbraun, H. L. "In vitro cytotoxicity of glyco-S-nitrosothiols: A novel class of nitric oxide donors." *Toxicol. in Vitro* **2001,** *15*, 181-190.

8.   Hou, Y.; Wang, J.; Andreana, P. R.; Cantauria, G.; Tarasia, S.; Sharp, L.; Braunschweiger, P. G.; Wang, P. G. "Targeting nitric oxide to cancer cells: cytotoxicity studies of glyco-S-nitrosothiols." *Bioorg. Med. Chem. Lett.* **1999,** *9*, 2255-2258.

9.   de Souza, G. F. P.; Yokoyama-Yasunaka, J. K. U.; Seabra, A. B.; Miguel, D. C.; de Oliveira, M. G.; Uliana, S. R. B. "Leishmanicidal activity of primary *S*-nitrosothiols against *Leishmania major* and *Leishmania amazonesis*: implications for the treatment of cutaneous leishmaniasis." *Nitric Oxide* **2006,** *15*, 209-216.

10.   Fang, F. C. "Antimicrobial reactive oxygen and nitrogen species: concepts and controversies." *Nat. Rev. Microbiol.* **2004,** *2*, 820-832.

11.   Mannick, J. B. "Immunoregulatory and antimicrobial effects of nitrogen oxides." *Proc. Am. Thorac. Soc.* **2006,** *3*, 161-165.

12.   Schapiro, J. M.; Libby, S. J.; Fang, F. C. "Inhibition of bacterial DNA replication by zinc mobilization during nitrosative stress." *Proc. Natl. Acad. Sci. U. S. A.* **2003,** *100*, 8496-8501.

13. Bell, R. M.; Maddock, H. L.; Yellon, D. M. "The cardioprotective and mitochondrial depolarising properties of exogenous nitric oxide in mouse heart." *Cardiovasc. Res.* **2003,** *57*, 405-415.

14. Konorev, E. A.; Tarpey, M. M.; Joseph, J.; Baker, J. E.; Kalyanaraman, B. "S-nitrosoglutathione improves functional recovery in the isolated rat heart after cardioplegic ischemic arrest-evidence for a cardioprotective effect of nitric oxide." *J. Pharmacol. Exp. Ther.* **1995,** *274*, 200-206.

15. Schulz, R.; Kelm, M.; Heusch, G. "Nitric oxide in myocardial ischemia/reperfusion injury." *Cardiovasc. Res.* **2004,** *61*, 402-413.

16. Mellion, B. T.; Ignarro, L. J.; Myers, C. B.; Ohlstein, E. H.; Ballot, B. A.; Hyman, A. L.; Kadowitz, P. J. "Inhibition of human platelet aggregation by *S*-nitrosothiols." *Mol. Pharmacol.* **1983,** *23*, 653-664.

17. Radomski, M. W.; Rees, D. D.; Dutra, A.; Moncada, S. *Br. J. Pharmacol.* **1992,** *107*, 745-749.

18. de Belder, A. J.; MacAllister, R.; Radomski, M. W.; Moncada, S.; Vallance, P. J. T. "Effects of *S*-nitrosoglutathione in the human forearm circulation: evidence for selective inhibition of platelet activation." *Cardiovasc. Res.* **1994,** *28*, 691-694.

19. Radomski, M. W.; Moncada, S. "Regulation of platelet function by nitric oxide." *Adv. Molec. Cell Biol.* **1997,** *18*, 367-381.

20. Molloy, J.; Martin, J. F.; Baskerville, P. A.; Fraser, S. C. A.; Markus, H. S. "*S*-nitrosoglutathione reduces teh rate of emolization in humans." *Circulation* **1998,** *98*, 1372-1375.

21. Salas, E.; Langford, E. J.; Marrinan, M. T.; Martin, J. F.; Moncada, S.; Debelder, A. J. "*S*-nitrosoglutathione inhibits platelet activation and deposition in coronary artery saphenous vein grats in vitro and in vivo." *Heart* **1998,** *80*, 146-150.

22. Bohl, K. S.; West, J. L. "Nitric oxide-generation polymers reduce platelet adhesion and smooth muscle cell proliferation." *Biomaterials* **2000,** *21*, 2273-2278.

23. Bohl-Masters, K. S.; Lipke, E. A.; Rice, E. E. H.; Liel, M. S.; Myler, H. A.; Zygourakis, C.; Tulis, D. A.; West, J. L. "Nitric oxide-generating hydrogels inhibit neointima formation." *J. Biomater. Sci. Polymer Edn.* **2005,** *16*, 659-672.

24. Seabra, A. B.; da Silva, R.; de Oliveira, M. G. "Polynitrosated polyesters: preparation, characterization, and potential use for topical nitric oxide release." *Biomacromolecules* **2005,** *6*, 2512-2520.

25.   Frost, M. C.; Meyerhoff, M. E. "Synthesis, characterization, and controlled nitric oxide release from S-nitrosothiol-derivatized fumed silica polymer filler particles." *J. Biomed. Mater. Res., Part A* **2005,** *72*, 409-419.

26.   Ewing, J. F.; Young, D. V.; Janero, D. R.; Garvey, D. S.; Grinnell, T. A. "Nitrosylated bovine serum albumin derivatives as pharmacologically active nitrogen oxide congeners." *J. Pharmacol. Exp. Ther.* **1997,** *283*, 947-954.

27.   Katsumi, H.; Nishikawa, M.; Ma, S. F.; Yamashita, F.; Hashida, M. "Physico-chemical, tissue distribution, and vasodilation characteristics of nitrosated serum albumin: delivery of nitric oxide in vivo." *J. Pharm. Sci.* **2004,** *93*, 2343-2352.

28.   Katsumi, H.; Nishikawa, M.; Yamashita, F.; Hashida, M. "Development of polyethylene glycol-conjugated poly-S-nitrosated serum albumin, a novel S-nitrosothiol for prolonged delivery of nitric oxide in the blood circulation in vivo." *J. Pharmacol. Exp. Ther.* **2005,** *314*, 1117-1124.

29.   Marks, D. S.; Vita, J. A.; Folts, J. D.; Keaney, J. F., Jr.; Welch, G. N.; Loscalzo, J. "Inhibition of neointimal proliferation in rabbits after vascular injury by a single treatment with a protein adduct of nitric oxide." *J. Clin. Investig.* **1995,** *96*, 2630-2638.

30.   Stasko, N. A.; Schoenfisch, M. H. "Dendrimers as a scaffold for nitric oxide release." *J. Am. Chem. Soc.* **2006,** *128*, 8265-8271.

31.   Boas, U.; Heegaard, P. M. H. "Dendrimers in drug research." *Chem. Soc. Rev.* **2004,** *33*, 43-63.

32.   Frechet, J. M. J. "Dendrimers and other dendritic macromolecules: From building blocks to functional assemblies in nanoscience and nanotechnology." *J. Polym. Sci. Part A: Polym. Chem.* **2003,** *41*, 3713-3725.

33.   Marxer, S. M.; Rothrock, A. R.; Nablo, B. J.; Robbins, M. E.; Schoenfisch, M. H. "Prepartion of nitric oxide (NO)-releasing sol-gels for biomaterial applications." *Chem. Mater.* **2003,** *15*, 4193-4199.

34.   Beckman, J. S.; Conger, K. A. "Direct measurement of dilute nitric oxide in solution with an ozone chemiluminescentdetector." *Methods* **1995,** *7*, 35-39.

35.   Hou, Y.; Wang, J.-Q.; Ramirez, J.; Wang, P. G. "Glyco-S-nitrosothiols: sugar-SNAP, a new type of nitric oxide donor." *Methods in Enzymology* **1999,** *301*, 242-249.

36.   Moynihan, H. A.; Roberts, S. M. "Preparation of some novel S-nitroso compounds as potential slow-release agents in nitric oxide in vivo." *J. Chem. Soc. Perkin Trans. 1* **1994**, 797-805.

37.   Ellman, G. L. *Arch. Biochem. Biophys.* **1959,** *82*, 70-77.

38.   Van Horn, J. D.; Bulaj, G.; Goldenberg, D. P.; Burrows, C. J. *J. Biol. Inorg. Chem.* **2003,** *8*, 601-610.

39.   van Baal, I.; Malda, H.; Synowsky, S. A.; van Dongen, J. L. J.; Hackeng, T. M.; Merkx, M.; Meijer, E. W. "Multivalent peptide and protein dendrimers using native chemical ligation." *Angew. Chem. Int. Ed.* **2005,** *44*, 5052-5057.

40.   Patel, H. M. S.; Williams, D. L. H. "Nitrosation by alkyl nitrites. Part 6. Thiolate nitrosation." *J. Chem. Soc. Perkin Trans. 2* **1990**, 37-42.

41.   Askew, S. C.; Barnett, D. J.; McAninly, J.; Williams, D. L. H. *J. Chem. Soc., Perkin Trans 2* **1995**, 741-745.

42.   Bartberger, M. D.; Houk, K. N.; Powell, S. C.; Mannion, J. D.; Lo, K. Y.; Stamler, J. S.; Toone, E. J. "Theory, spectroscopy, and crystallographic analysis of *S*-nitrosothiols: Conformational distribution dictates spectroscopic behavior." *J. Am. Chem. Soc.* **2000,** *122*, 5889-5890.

43.   Williams, D. L. H. "The chemistry of *S*-nitrosothiols." *Acc. Chem. Res.* **1999,** *32*, 869-876.

44.   Dicks, A. P.; Swift, H. R.; Williams, D. L. H.; Butler, A. R.; Al-Sa'doni, H. H.; Cox, B. G. "Identification of Cu^+ as the effective reagent in nitric oxide formation from *S*-nitrosothiols." *J. Chem. Soc. Perkin Trans. 2* **1996**, 481-487.

45.   Singh, R. J.; Hogg, N.; Goss, S. P. A.; Antholine, W. E.; Kalyanaraman, B. "Mechanism of superoxide dismutase/H_2O_2-mediated nitric oxide release from *S*-nitrosogluathione--role of glutamate." *Arch. Biochem. Biophys.* **1999,** *372*, 8-15.

46.   Frei, B.; England, L.; Ames, B. N. "Ascorbate is an outstanding antioxidant in human blood plasma." *Proc. Natl. Acad. Sci. U. S. A*. **1989,** *86*, 6377-6381.

47.   Scorza, G.; Pietraforte, D.; Minetti, M. "Role of ascorbate and protein thiols in the release of nitric oxide from S-nitrosoalbumin and *S*-nitroso-glutathione in human plasma." *Free Radic. Biol. Med.* **1997,** *22*, 633-642.

48.   Sexton, D. J.; Muruganandam, A.; McKenney, D. J.; Mutus, B. "Visible light photochemical release of nitric oxide from *S*-nitrosoglutathione: potential photochemotherapeutic applications." *Photochem. Photobiol.* **1994,** *59*, 463-467.

49.   Singh, R. J.; Hogg, N.; Joseph, J.; Kalyanaraman, B. "Mechanism of nitric oxide release from *S*-nitrosothiols." *J. Biol. Chem.* **1996,** *271*, 18596-18603.

50.   Lu, J.-M.; Wittbrodt, J. M.; Wang, K.; Wen, Z.; Schlegel, H. B.; Wang, P. G.; Cheng, J.-P. "NO affinities of *S*-nitrosothiols: a direct experimental and computational

investigation of RS-NO bond dissociation energies." *J. Am. Chem. Soc.* **2001,** *123,* 2903-2904.

51. Shishido, S. M.; de Oliveira, M. G. "Polyethylene glycol matrix reduces the rates of photochemical and thermal release of nitric oxide from *S*-nitroso-N-acetylcysteine." *Photochem. Photobiol.* **2000,** *71*, 273-280.

52. Wanstall, J. C.; Homer, K. L.; Doggrell, S. A. "Evidence for, and importance of, cGMP-independent mechanisms with NO and NO donors on blood vessels and platelets." *Curr. Vasc. Pharmacol.* **2005,** *3*, 41-53.

53. Walsh, G. M.; Leane, D.; Moran, N.; Keyes, T. E.; Forster, R. J.; Kenny, D.; O'Neill, S. "*S*-nitrosylation of platelet $\alpha_{IIb}\beta_3$ as revealed by raman spectroscopy." *Biochemistry* **2007,** *46*, 6429-6436.

54. Root, P.; Sliskovic, I.; Mutus, B. "Platelet cell-surface protein disulphide-isomerase mediated *S*-nitrosoglutathione consumption." *Biochem. J.* **2004,** *382*, 575-580.

55. Bell, S. E.; Shah, C. M.; Gordge, M. P. "Protein disulfide-isomerase mediates delivery of nitric oxide redox derivatives into platelets." *Biochem. J.* **2007,** *403*, 283-288.

56. Hogg, N.; Singh, R. J.; Kalyanaraman, B. "The role of glutathione in the transport and catabolism of nitric oxide." *FEBS Lett.* **1996,** *382*, 223-228.

57. Kukowska-Latallo, J. F.; Candido, K. A.; Cao, Z.; Nigavekar, S. S.; Majoros, I. J.; Thomas, T. P.; Balogh, L. P.; Khan, M. K.; Baker, J. E. J. "Nanoparticle targeting of anticancer drug improves therapeutic response in animal model of human epithelial cancer." *Cancer Res.* **2005,** *65*, 5317-5324.

Chapter 4:

Cytotoxicity of Polypropylenimine Dendrimer Conjugates on Cultured Endothelial Cells

4.1 Introduction

As described in Chapter 1, dendrimers represent polymeric drug delivery vehicles that possess a well-defined, three-dimensional structure and a multivalent exterior which can be modified to contain a multitude of unique surface groups.[1, 2] These hyperbranched molecules are synthesized either by a divergent method whereby repeat monomers are branched outward from a central core, or a convergent method from which the synthesis begins at the periphery and is grown inward.[3] The dendritic architecture offers a solution to traditional drug delivery problems by allowing for the tailored solubility and tissue specific targeting of drugs through ligand or antibody immobilization to the multivalent surface.[4, 5] Recently, dendrimers have been employed as a substrate for delivering a wide range of therapeutic agents including water insoluble drugs,[6, 7] anti-cancer chemotherapeutics,[8-10] and oligonucleotides for enhanced gene transfection.[11]

Some of the most promising non-viral gene delivery systems are dendritic structures with cationic amine exteriors, namely the polyamidoamine (PAMAM) and polypropylenimine (PPI) dendrimers.[12] These synthetic vector systems form nucleic acid/dendrimer complexes through the interaction of cationic dendrimer exteriors with the negatively charged phosphates on the DNA backbone. Since Haensler et al. first reported the use of PAMAM

dendrimers to mediate efficient gene transfection in vitro,[13] numerous reports have explored the use of dendrimers as gene delivery vehicles, carefully detailing transfection efficiency as a function of carrier size, surface charge, and exterior functionality.[11, 14-17]   Although cationic amine-terminated dendrimers are suitable carriers to enhance gene transfection, the toxicity of these novel delivery vehicles and their unfavorable interactions with cellular membranes has slowed their widespread clinical application.[11] Indeed, Duncan et al. recently reviewed the toxicity of amine containing dendrimers and concluded that amine-terminated dendrimers (e.g., PPI, PAMAM) exhibited size dependent cytotoxic effects based on the number of free amines at the surface.[18] To further elucidate the mechanism of primary amine dendrimer toxicity, Hong et al. demonstrated that positively charged amine-terminated dendrimers induced the formation of nanoscale holes upon interaction with artificial lipid bilayers.[19] Possible mechanisms of hole formation include dendrimer-mediated removal of lipids from the membrane[20] or direct insertion of the amine-terminated dendrimers into the membrane.[21] Several other studies have been conducted illustrating that both negatively charged and neutral dendrimers were non-toxic, clearly demonstrating the structure/toxicity relationship that is governed primarily by the functional groups on the dendrimer surface.[18, 22-26]

In this chapter, the cytotoxic effects of model dendritic systems against human umbilical vein endothelial cells (HUVEC) are evaluated and provide further mechanistic insight into the structure/toxicity relationship of multi-functional polypropylenimine dendrimers. Time-dependent changes in the plasma membrane permeability of HUVEC toward propidium iodide (PI) and the concomitant release of cytosolic LDH were used to quantify cytotoxicity. Laser scanning confocal microscopy was employed to monitor both the interaction of fluorescently-labeled dendrimers with the plasma membrane of HUVEC and the effect of

dendrimer adhesion on the membrane potential of intracellular mitochondria. Chemical modification of the surface amines on the parent dendrimer and conversion to neutral acetamide or poly(ethylene glycol) functionalities reduced both the visible adhesion of dendrimers to the plasma membrane of cultured HUVEC and their cytotoxicity, illustrating that removal of the cationic charges from the dendrimer's surface is a necessary step in the synthesis of fully biocompatible drug delivery vehicles.

4.2 Experimental Section

4.2.1 General

Tetramethylrhodamine methylester (TMRM) was purchased from Molecular Probes (Eugene, OR). Polypropylenimine dendrimer (DAB-Am-64) starting material, propidium iodide (PI), poly(ethylene glycol) monomethyl ether (M-PEG$_{2000}$), Kaiser test kit, and all other reagents were purchased from the Aldrich Chemical Company (Milwaukee, WI). Methanol was distilled over magnesium prior to use. Water was purified with a Millipore Milli-Q gradient A-10 purification system (Bedford, MA). Spectra/Por® Float-A-Lyzers® were purchased from Spectrum Laboratories Inc. (Rancho Dominguez, CA). Nuclear magnetic resonance (NMR) spectra were collected in deuterated water (D$_2$O) using a 400-MHz Bruker Nuclear Magnetic Resonance spectrometer (Brucker, Germany). Mass spectra were acquired using a Micromass Quattro II triple quadrupole mass spectrometer equipped with a nano-electrospray ionization source in positive-ion mode. Absorption spectra were recorded on a Perkin Elmer Lambda 40 UV-vis spectrophotometer (Norwalk, CT). Fluorescence measurements were performed using a FluoStar Galaxy plate reader (BMG LabTechnologies, Inc., Durham, NC). Confocal fluorescence microscopy experiments were performed using an LSM 510 laser scanning confocal microscope (Carl Zeiss, Thornwood, NY).

4.2.2 Synthesis and characterization of dendrimer conjugates

4.2.2.1 DAB-Ac$_{40}$-FITC$_2$ **(1)**

DAB-Am-64 (300 mg, 0.042 mmol) was dissolved in 30 mL of anhydrous methanol under an inert argon atmosphere and to the stirring solution was added acetic anhydride (126 µL, 1.34 mmol) and pyridine (119 µL, 1.47 mmol) to stoichiometrically convert half of the primary amines on the dendrimer to acetamide functionalities. The solution was stirred for 24 h and then 10 mL of anhydrous methanol containing fluorescein isothiocyanate (FITC) (49 mg, 0.126 mmol) was added to stoichiometrically attach 3 fluorescent residues per dendrimer. The solution was stirred for an additional 24 h in the dark and then separated into several aliquots for purification or further functionalization. 5 mL of the product solution was concentrated under reduced pressure, dissolved in water, and added to a Spectra/Por$^{®}$ Float-A-Lyzer$^{®}$ (5 mL, 1000 MWCO) for dialysis in 2 L of 0.5 M NaCl for 24 h, followed by dialysis in ultrapure Milli-Q water for 3 d (3 x 2L). The aqueous sample was frozen and lyophilized to yield 21 mg of an orange solid: ^{1}H NMR (D$_2$O, δ): 1.2-1.70 (m, NCH$_2$C*H*$_2$CH$_2$N, NCH$_2$C*H*$_2$C*H*$_2$CH$_2$N), 1.80 (s, COCH$_3$), 1.86 (s, COCH$_3$), 2.07-2.54 (m, NC*H*$_2$CH$_2$C*H*$_2$N, NC*H*$_2$CH$_2$CH$_2$NH), 2.72 (m, NCH$_2$CH$_2$C*H*$_2$NH$_2$), 2.91 (m, NCH$_2$CH$_2$C*H*$_2$NHCOCH$_3$), 3.04 (m, NCH$_2$CH$_2$C*H*$_2$NHCOCH$_3$). ESI-MS calculated MW: 9121.4 g/mol, experimental MW$_{avg}$: 9624.9 g/mol [1190.9 (M+8H)$^{8+}$, 1386.1 (M+7H)$^{7+}$, 1615.4 (M+6H)$^{6+}$]. UV/Vis (MeOH): λ$_{mac}$= 504 nm.

4.2.2.2 DAB-Ac$_{59}$-FITC$_2$ **(2)**

Acetic anhydride (32 µL, 0.34 mmol) and pyridine (27 µL, 0.34 mmol) were added to 5 mL of product solution containing dendrimer **1** to fully acetylate the remaining primary amines on the fluorescently labeled dendrimer**.** The solution was stirred for 24 h in the dark, concentrated under reduced pressure, resuspended in water, and dialyzed against 2 L of 0.5

M NaCl for 24 h, followed by dialysis in ultrapure Milli-Q water for 3 d (3 x 2L). The aqueous sample was frozen and lyophilized to yield 26 mg of an orange solid: ^{1}H NMR (D$_2$O, δ): 1.4-1.70 (m, NCH$_2$CH$_2$CH$_2$N, NCH$_2$CH$_2$CH$_2$CH$_2$N), 1.84 (s, COCH$_3$), 2.2-2.62 (m, NCH$_2$CH$_2$CH$_2$N, NCH$_2$CH$_2$CH$_2$NH), 3.03 (m, NCH$_2$CH$_2$CH$_2$NHCOCH$_3$). ESI-MS calculated MW: 10,425 g/mol, experimental MW$_{avg}$: 10,206 g/mol [1702.0 (M+6H)$^{6+}$, 2041.9 (M+5H)$^{5+}$, 2552.7 (M+4H)$^{4+}$]. UV/Vis (MeOH): $λ_{mac}$= 504 nm.

4.2.2.3 Synthesis of 4-nitro-phenyl-MPEG (adapted from Kojima et al.)[27]

Poly(ethylene glycol) monomethyl ether (M-PEG$_{2000}$) (10 g, 5 mmol) was dissolved in a stirring solution of THF (400 mL) to which 4-nitrophenyl chloroformate (2.01 g, 10 mmol) and triethylamine (1.39 mL, 10 mmol) were added. The solution was stirred for 2 d, the THF was removed under reduced pressure, and the crude product was resuspended in toluene (100 mL). The salt impurities were removed via filtration and the final product was precipitated from toluene with copious amounts of ether. The white precipitate was dried to yield 4.68 g (2.1 mmol, 43%) of activated M-PEG$_{2000}$ and proton assignments matched those previously reported in the literature. ^{1}H NMR (CDCl$_3$, δ): 3.36 (s, OCH$_3$), 3.44 (m, CH$_2$OCH$_3$), 3.52 (m, COOCH$_2$CH$_2$O), 3.55-3.75 (br, OCH$_2$CH$_2$O), 3.79 (m, OCH$_2$CH$_2$OCH$_3$), 4.41 (dd, COOCH$_2$CH$_2$O), 7.48 (d, aromatic), 8.25 (d, aromatic).

4.2.2.4 DAB-Ac$_{40}$-PEG$_4$-FITC$_2$ (**3**)

Activated M-PEG$_{2000}$ (443 mg, 0.2 mmol) was added to 5 mL of product solution containing dendrimer **1** to covalently attach long poly(ethylene glycol) chains to the remaining primary amines on the fluorescently labeled dendrimer. The solution was stirred for 24 h in the dark, concentrated under reduced pressure, resuspended in water, and dialyzed in a Spectra/Por® Float-A-Lyzer® (10 mL, 5000 MWCO) against 2 L of 0.5 M NaCl for 24 h, followed by dialysis in ultrapure Milli-Q water for 3 d (3 x 2L). The aqueous sample was

frozen and lyophilized to yield 143 mg of an orange solid: ^{1}H NMR (D$_2$O, δ): 1.39-1.78 (m, NCH$_2$CH$_2$CH$_2$N, NCH$_2$CH$_2$CH$_2$CH$_2$N), 1.87 (s, COCH$_3$), 2.2-2.65 (m, NCH$_2$CH$_2$CH$_2$N, NCH$_2$CH$_2$CH$_2$NH), 2.84 (m, NCH$_2$CH$_2$CH$_2$NH$_2$), 3.07 (m, NCH$_2$CH$_2$CH$_2$NHCO-PEG), 3.28 (s, OCH$_3$), 3.41 (m, CH$_2$OCH$_3$), 3.50-3.70 (br, OCH$_2$CH$_2$O), 3.78 (m, OCH$_2$CH$_2$OCH$_3$), 4.09 (m, NHCOOCH$_2$CH$_2$O), 4.23 (m, NHCOOCH$_2$CH$_2$O). ESI-MS: (unable to resolve a high molecular weight species with identical sampling procedure)

4.2.3 Ninhydrin assay for the detection of free amines

The following procedure was adapted from Sarin et al. and uses the reagents in a standard commercially available Kaiser Test kit.[28] Dendrimer samples were diluted to 3 µM in absolute EtOH (n=4 dilutions) and 700 uL was added to a quartz cuvet, followed by 50 µL of phenol (80% in ethanol), 50 µL KCN in H$_2$O/pyridine, and 25 µL of ninhydrin (6% in EtOH). The solutions were capped, heated at 100 °C for 10 min, and the spectroscopic absorption maxima of the Ruhemanns blue chromophore was measured at 570 nm via absorption spectroscopy. Absorbance values for dendrimers **1-3** were averaged (n=4), normalized to the absorption maxima of the FITC chromophore (λ_{max}=504 nm) as an internal standard, and compared to the ninhydrin response of 3 µM G4-PAMAM possessing 64 exterior amines at the surface. Values represent the number of remaining amines per mol dendrimer conjugate and are given as the standard deviation of the mean. **1** (DAB-Ac$_{40}$-FITC$_2$) = 24.9 ± 4.9, **2** (DAB-Ac$_{59}$-FITC$_2$) = 3.7 ± 1.5, **3** (DAB-Ac$_{40}$-PEG$_4$-FITC$_2$) = 21.2 ± 5.5.

4.2.4 Cell culture

Human umbilical vein endothelial cells (HUVEC) were purchased from Genlantis (Cat. #PH200050N, Genlantis Inc., CA) and propagated in Genlantis's serum containing endothelial growth medium (Cat. # PM 211500) according to the manufacturer's protocol.

4.2.5 Propidium iodide (PI) viability assay

HUVEC were plated on 24-well tissue culture treated dishes (BD Bioscience #353047) at a density of 3.0×10^5 cells/ml (150×10^3 cells/well) and incubated overnight at 37^oC, in 5% CO_2/95% air for 18-20 h. For the PI assay, the incubation buffer was aspirated from each of the wells and replaced with 500 µL of Krebs-Ringer-HEPES (KRH) buffer containing (mM): 115 NaCl, 5 KCl, 1 $CaCl_2$, 1 KH_2PO_4, 1.2 $MgSO_4$, 25 HEPES, pH 7.4, supplemented with 30 µM of PI [16]. The fluorescence of the cells in the absence and/or presence of 3 µM dendrimer conjugates (**1**, **2** or **3**) was monitored using a FluoStar Galaxy plate reader (BMG Labtech, Durham, NC) with excitation and emission filters set at 544 and 640 nm, respectively. Fluorescence was acquired at 15 min intervals for a total of 150 min. An additional 20 min incubation of cells with 40 µM digitonin was required to completely permeabilize not only plasma membrane of HUVEC but also other internal membranes (including nuclear envelope) these conditions guarantee full access of PI to intracellular nucleic acids for achieving a maximum PI fluorescence. Cell viability was presented as increase in PI_fluorescence from each well expressed as percentage of maximal obtained in cells treated with digitonin (100% cell death).

4.2.6 Lactate dehydrogenase (LDH) assay

20 µL aliquots of incubation buffer were removed from the plate used for the PI assay and stored at -20^oC in black 96-well plates (Greiner, Monroe, NC) for subsequent LDH assays. Briefly, 96-well plates containing aliquots of incubation buffer were warmed to 37^oC

and LDH activity was measured from the rate of NADH production after adding 180 μl of the buffer containing (mM): 0.22 NAD$^+$, 11.1 sodium lactate and 11.1 hydrazine, pH 8.0 into each well.[29] The kinetics of NADH fluorescence was monitored using a FluoStar Galaxy plate reader using 340 nm excitation and 460 nm emission filters. The LDH activity was expressed as the rate of relative fluorescence units (RFU) per min per well. Results were normalized to maximal LDH activity in each well obtained from samples treated with 40 μM of digitonin for 20 min.

4.2.7 Imaging with laser scanning confocal microscopy

For confocal microscopy study HUVEC (3.0 x 10^5 cells/ml) were plated on round glass slides (Fisher Scientific, Pittsburgh, PA) and incubated overnight in 1 mL of Genlantis' growth medium at 37°C, 5%CO$_2$ in a humidified environment. The cells on the coverslip were preloaded with TMRM, a mitochondria specific fluorescent dye (100 nM, for 30 min at 37°C) and placed into an environmental chamber (37°C, 5 %CO$_2$, 100% humidity) of the stage of fluorescent confocal microscope Zeiss LSM 510 (Carl Zeiss, Thornwood, NY). Incubation medium was replaced with 1 mL of KRH buffer containing 30 μM PI and 3 μM FITC-dendrimer and confocal images of HUVEC were acquired every 5min for 30 min total using a 63x N.A. 1.4 planapochromat oil immersion lens with pinholes set to 1.0 Airy units in both the red (TMRM) and green (FITC) channels. Fluorophores were excited with the 543-nm line of a HeNe laser (TMRM) and the 488-nm line of an Ar laser (FITC), with laser intensities attenuated to 0.05%. Green and red fluorescence were separated by a dichroic filter (NFT 545) and recorded in channels 2 and 3 of the LSM 510 using band-pass (BP 500-530) and long-pass (LP 560) filters, respectively. (Fluorophore absorption/emission spectra provided by manufacturer and dendrimer absorption spectra are shown in Figure 4.1)

4.2.8 Statistics

Differences between the effects of dendrimers on cultured cells were analyzed using one-way ANOVA with Fisher's multiple comparisons post hoc test, $p < 0.05$ as the criterion of significance. All experiments were repeated at least three times and results were expressed as means ± SEM. When error bars are not shown, they fall within the diameters of the symbols.
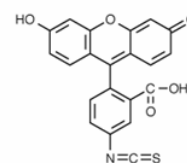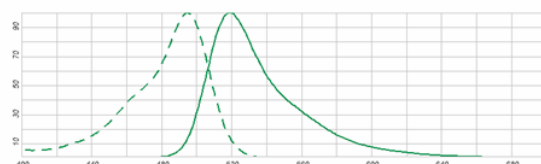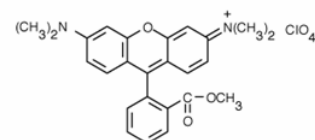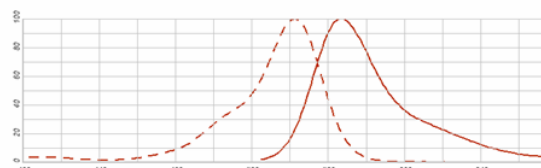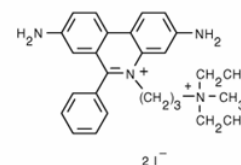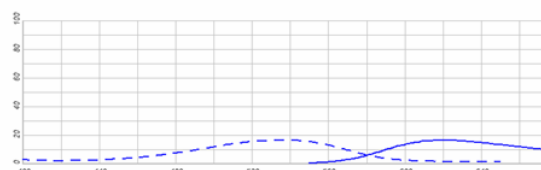
Figure 4.1   Absorption (dotted) and emission (solid) spectra of all fluorescent dyes used in the current work as provided by the manufacturer (Invitrogen).
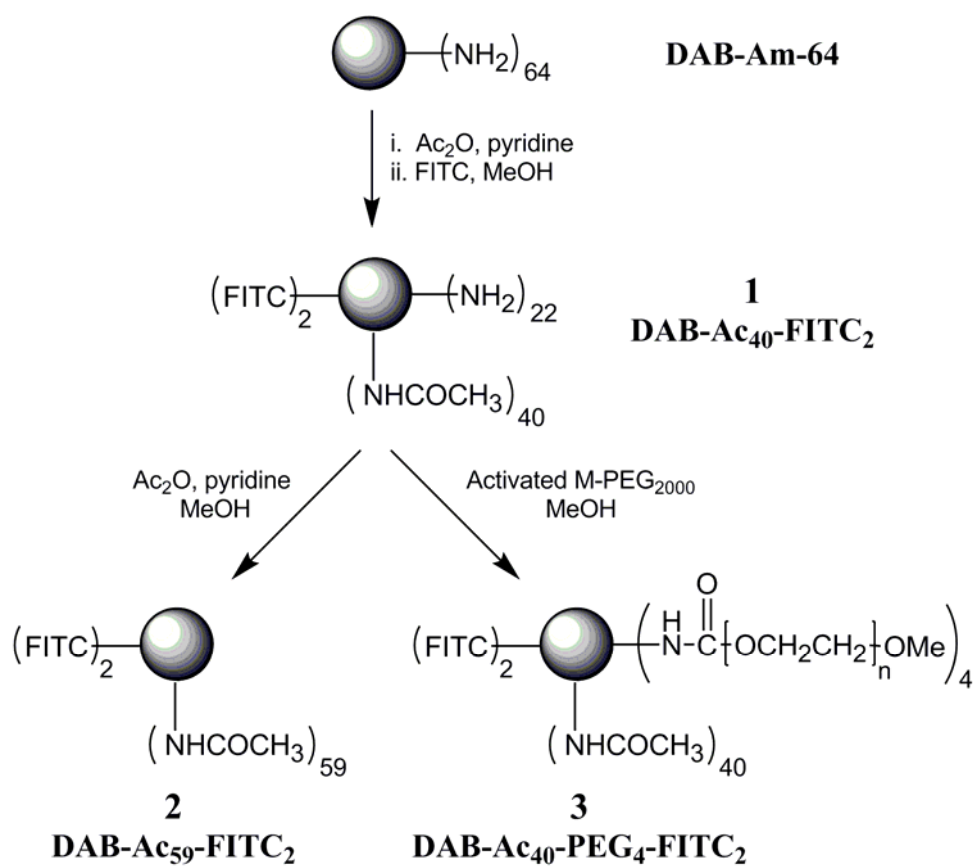
Scheme 4.1 Synthesis of multifunctional dendrimer conjugates. (DAB-Am-64: parental unmodified generation 5 polypropylenimine dendrimer; FITC: fluorescein isothiocyanate)

4.3 Results and Discussion

4.3.1 Synthesis and characterization of dendrimer conjugates

Generation 5 polypropylenimine dendrimer (DAB-Am-64) was chosen as the starting material due to its previously reported toxicity in drug delivery applications and its capacity for a large number of additional functionalities.[4, 18] The cytotoxicity of DAB-Am-64 and other amine-containing dendrimers is mediated by non-specific interactions of the positively charged primary amines with lipid membranes.[22] Therefore, we stoichiometrically targeted half of the surface positive charges on the parental dendrimer (DAB-Am-64) for conversion into acetamides via reaction with acetic anhydride (Scheme 4.1). Previously, amide dendritic exteriors have been used to increase water solubility and eliminate the toxicity of primary amine dendrimer constructs.[19, 30] The partially acetylated product was then fluorescently labeled with FITC to produce a fully traceable dendrimer conjugate **1** (Scheme 4.1, DAB-Ac$_{40}$-FITC$_2$) for studying the interaction of mixed amine/amide dendrimers with cultured cells. Fluorescent labeling of dendrimer drug delivery scaffolds enables the direct monitoring of cellular interactions in vitro and also imparts a molecular probe to study future bio-distribution in vivo.[10, 31] The modified dendrimer was dialyzed for 96 h, lyophilized, and analyzed via nuclear magnetic resonance spectroscopy (^{1}H-NMR) and electrospray ionization mass spectrometry (ESI/MS). The calculation and assignment of all of the protons on DAB-Am-64 is shown in Figure 4.2. The extent of amide functionalization (40 of 64 amines) was calculated from the integration ratio of the protons on the newly formed amide (COCH_3) to the aliphatic methylene protons of the DAB-Am-64 dendritic interior (Figure 4.3) according to Equations 4.1 and 4.2:

Equation 4.1

$$\frac{3x}{Intensity_{(COCH_3)}} = \frac{D+E\ H's}{Intensity_{(D+E)}} \qquad \text{Where } x = \text{number of acetamide groups}$$

$$\frac{3x}{1.48} = \frac{252}{2.10} \qquad 6.3x = 372.96 \qquad x = 59.2 \text{ acetamide groups}$$

Equation 4.2

$$\frac{3x}{Intensity_{(COCH_3)}} = \frac{B+C\ H's}{Intensity_{(B+C)}} \qquad \text{Where } x = \text{number of acetamide groups}$$

$$\frac{3x}{1.48} = \frac{372}{3.14} \qquad 9.42x = 550.56 \qquad x = 58.4 \text{ acetamide groups}$$

To determine the number of fluorophores attached to the dendrimer scaffold the fluorescein dye structure and proton assignments are shown in Figure 4.4. The integrated ratio of the aromatic protons on the fluorophore to the protons alpha to the exterior amine (CH_2NH_2) indicated approximately 2 FITC residues per dendrimer according to Equations 4.3 and 4.4:

Equation 4.3

$$\frac{6x}{Intensity_{(d+e)}} = \frac{D+E\ H's}{Intensity_{(D+E)}} \qquad \text{Where } x = \text{number of fluorophores}$$

$$\frac{6x}{.094} = \frac{252}{2.10} \qquad 12.6x = 23.68 \qquad x = 1.88 \text{ FITC /dendrimer}$$

Equation 4.4

$$\frac{6x}{Intensity_{(d+e)}} = \frac{B+C\ H's}{Intensity_{(B+C)}} \qquad \text{Where } x = \text{number of fluorophores}$$

$$\frac{6x}{.094} = \frac{372}{3.14} \qquad 18.84x = 34.97 \qquad x = 1.85 \text{ FITC /dendrimer}$$

DAB-Am-64

Unique Carbons	# C's	# H's
1	2	4
2	2	4
3	4	8
4	28	56
5	52	104
6	32	64
7	32	64
8	32	64
9	64	128
10	64	128
11	64	128

A = protons on 11	= 128 H's
B = protons on 9	= 128 H's
C = protons on 2,3,5,6,8	= 244 H's
D = protons on 4,7,10	= 248 H's
E = protons on 1	= 4 H's
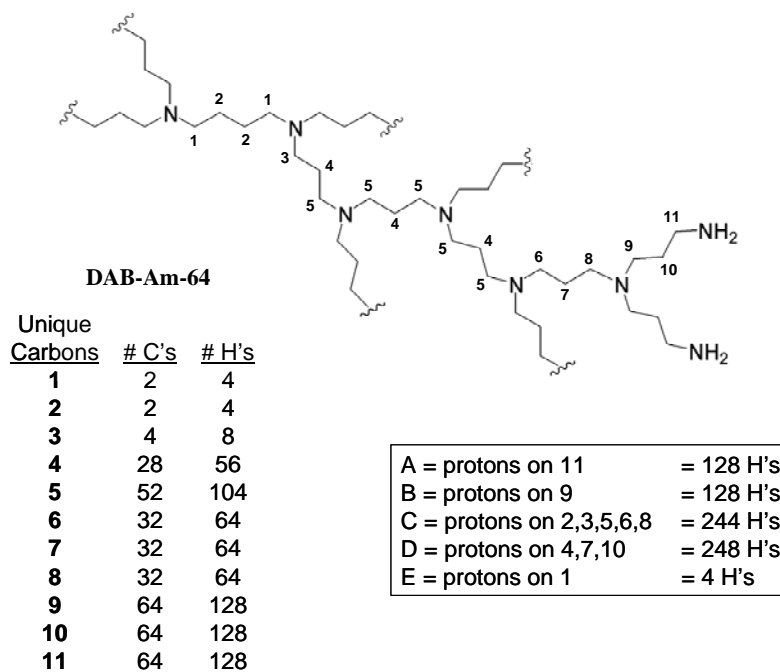
Figure 4.2   Proton assignments for the complete hyper-branched structure of DAB-Am-64 separated in to classes **A-E** with the corresponding number of protons detailed for each class.
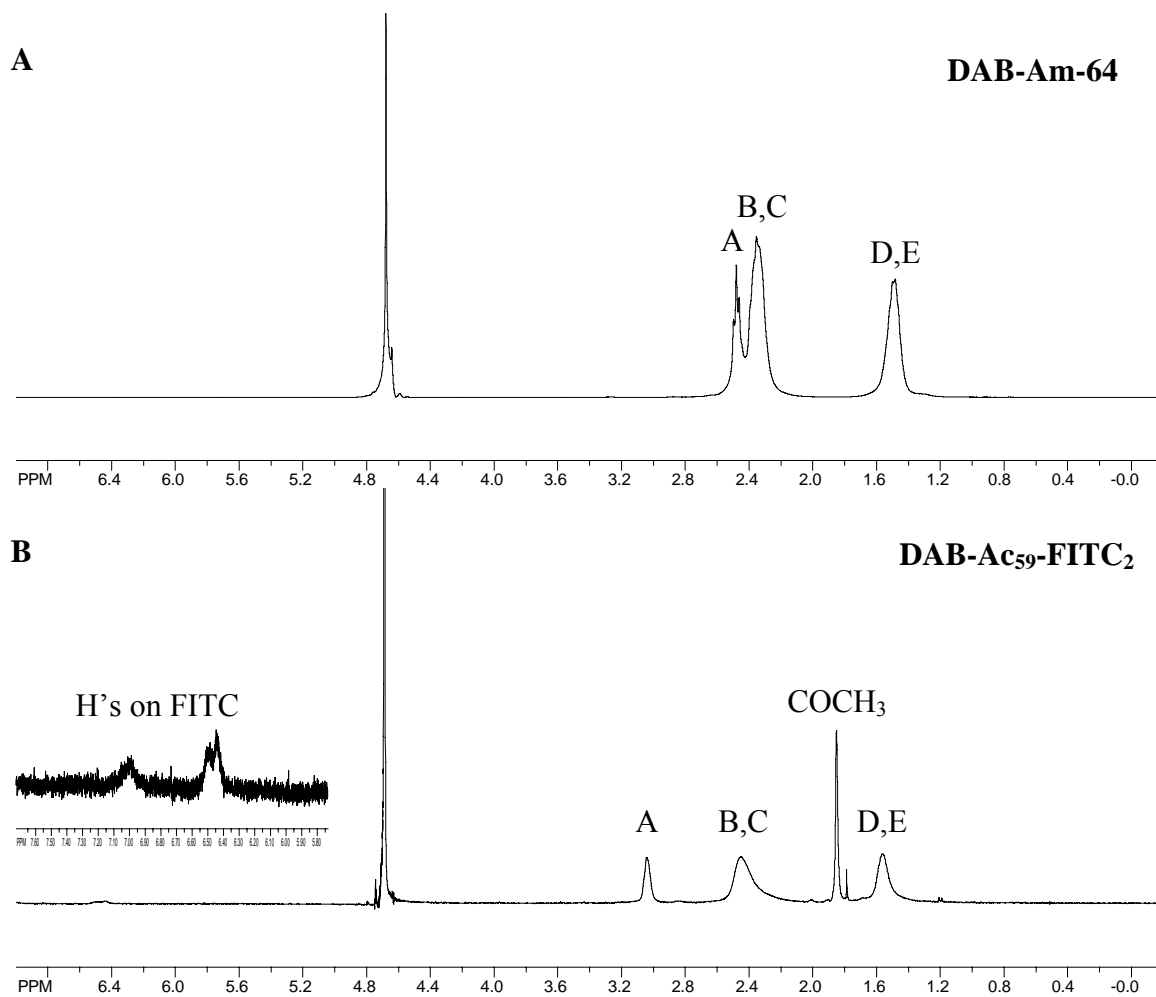
Figure 4.3   Representative NMR spectra interpretation for A) DAB-Am-64 and B) DAB-Ac$_{59}$-FITC$_2$.
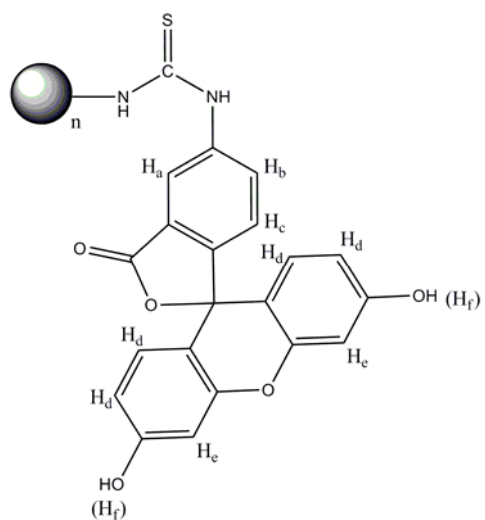
Figure 4.4   Structure of fluorescein isothiocyanate conjugated to an amine terminated dendrimer with proton classifications for NMR spectra interpretation.

The remaining exterior amines of the partially acetylated and FITC-labeled dendrimer **1** (DAB-Ac$_{40}$-FITC$_2$) were further modified as shown in Scheme 4.1. Dendrimer **1** was reacted with either excess acetic anhydride to fully acetylate the dendrimer surface yielding dendrimer **2** (DAB-AC$_{59}$-FITC$_2$) or with 4-nitrophenyl poly(ethylene glycol) monomethylether (activated M-PEG$_{2000}$) following a previously reported procedure[27] to yield PEG-ylated dendrimer **3** (DAB-Ac$_{40}$-PEG$_4$-FITC$_2$). Dendrimer conjugates **1-3** thereby provide a unique set of fluorescently labeled macromolecules, comprising defined percentages of amine, amide, or PEG modification, from which to study dendrimer induced cytotoxicity *in vitro*. A quantitative ninhydrin assay was then conducted on the dendrimers to determine the number of free amines per molecule of dendrimer.[28] Dendrimer **1** retained 24.9 $\pm$ 4.9 primary amines after partial acetylation, dendrimer **2** contained 3.7 $\pm$ 1.5 remaining amines after full acetylation, and PEG modified dendrimer **3** possessed 21.2 $\pm$ 5.5 solvent accessible amines after coupling of the activated PEG moieties, indicating attachment of ~4 hydrophilic PEG chains. The quantification of amines *per* dendrimer molecule correlated with the number of amines predicted from NMR and ESI-MS data analysis (**1** = 22 NH$_2$; **2** = 3 NH$_2$; **3** = 18 NH$_2$); in all cases the predicted number of remaining amines was within the error of the number of amines determined via the colorimetric assay.

4.3.2 Cytotoxicity of dendrimer conjugates

The toxicity of amine containing dendrimer constructs has been studied against a range of target tissue cell lines from hamster ovarian cells[14] to human embryonic kidney cells.[32] However, upon systemic administration of a delivery system, the therapeutic first comes into contact with the endothelium which ultimately mediates the delivery of the drug to other tissues.[33, 34] The present study evaluates the cytotoxicity of the dendrimer conjugates toward cultured human umbilical vein endothelial cells (HUVEC) as a model of the intravascular

lining that first interacts with dendrimer delivery vehicles upon intravenous injection. Additionally, endothelial cells are a primary target for gene therapies used to treat many cardiovascular conditions including restenosis and myocardial ischemia.[26]

To assess the cytotoxicity of the various dendrimer conjugates, HUVEC were plated to 85% confluency in 24-well plates and treated with dendrimer conjugates (3 μM) in KRH buffer containing 30 μM propidium iodide (PI). In cultures possessing healthy cells with intact membranes, PI is non-fluorescent and does not enter the cell. When the plasma membrane is compromised, PI diffuses into the cell and binds to nuclear chromatin, producing an increase in red fluorescence.[35, 36] The viability of HUVEC was calculated from the observed PI fluorescence intensity normalized to the maximum values achieved after complete permeabilization of the plasma membranes of the entire HUVEC population with digitonin (40 μM), a recognized non-ionic detergent that solubilizes membrane-bound cholesterol leaving non-selective pores in biological membranes.[37]

HUVEC treated with 3 μM dendrimer **1** (DAB-Ac$_{40}$-FITC$_2$) exhibited rapid changes in plasma membrane permeability as evidenced by the sharp increase in PI fluorescence after only 30 min (Figure 4.5A). The rise is indicative of substantial acute toxicity of this agent. After 150 min, the fluorescence signal began to plateau and >90% of the cells in culture were dead. The temporal dynamics of plasma membrane disruption by dendrimer **1** was further confirmed by measuring the release of LDH, a cytosolic enzyme, from the same cells. As shown in Figure 4.5B, the LDH activity from aliquots of the incubation buffer also increased over time after exposure to dendrimer **1** but at a slight delay compared to the passage of the smaller PI. Notably, the PI assay demonstrated more than 50% cell death after 60 min of dendrimer exposure, while the LDH release reached only 20% of the maximum. Therefore, the release of LDH initiated by amine-containing dendrimers occurred at longer incubation

148

times than the increase in PI fluorescence from the same cells, indicating that the size of the holes in the plasma membrane increased progressively with time; cells first became permeable to the 698 Da PI molecules and later to the 140 kDa LDH enzyme. Both assays clearly indicate that amine-containing dendrimer **1** caused permeabilization and disruption of the plasma membrane integrity in a time-dependent fashion, thus confirming that dendrimers with cationic amines at their surfaces are cytotoxic and that partial acetylation is insufficient at eliminating the deleterious effects of amine-presenting delivery vehicles. These data provide experimental validation to the molecular dynamics simulations reported by Larson and co-workers that suggested pore formation could be induced by 50% acetylated PAMAM dendrimers on simulated DPPC bilayers.[21]

The viability of HUVEC exposed to 3 μM dendrimers **2** and **3** is also shown in Figure 4.5. No observable cytotoxicity was detected for either dendrimer using the PI (Fig. 4.5A) or LDH (Fig. 4.5B) assays and there was no statistical differences between the effect of dendrimers **2** and **3** (p=NS). After 150 min of incubation of HUVEC, the level of PI labeling and LDH release remained unchanged from initial levels, indicating that the fully amidated and PEG-modified exteriors did not disrupt the plasma membrane integrity. These data are in accord with the previously observed enhancement of dendrimer's biocompatibility through modification of surface functionalities.[14, 22, 32, 38]
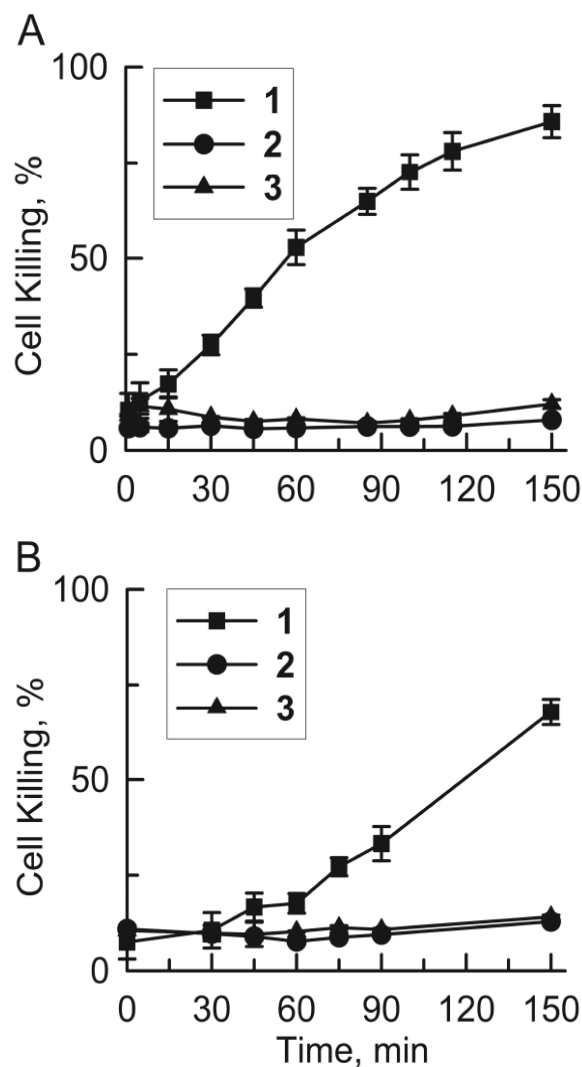
Figure 4.5   Cytotoxicity of dendrimer conjugates in cultured HUVEC. A) Time dependent cell killing as evaluated using PI assay: (-■-) dendrimer **1** (DAB-Ac$_{40}$-FITC$_2$), (-●-) dendrimer **2** (DAB-Ac$_{59}$-FITC$_2$), (-▲-) dendrimer **3** (DAB-Ac$_{40}$-PEG$_4$-FITC$_2$). B) Time dependence of dendrimer-mediated release of LDH from cultured HUVEC: (-■-) dendrimer **1** (DAB-Ac$_{40}$-FITC$_2$), (-●-) dendrimer **2** (DAB-Ac$_{59}$-FITC$_2$), (-▲-) dendrimer **3** (DAB-Ac$_{40}$-PEG$_4$-FITC$_2$). The data are means ± SEM of three independent experiments.

4.3.3 Confocal laser scanning microscopy of dendrimer interactions with HUVEC

4.3.3.1 Disruption of the plasma membrane integrity by amine containing dendrimers

The exact mechanism of gene transfection for cationic dendrimers is unknown, but the ability to disrupt the plasma membrane and induce hole formation as previously described resembles the physical process by which other non-viral transfection agents induce pores to deliver DNA cargo (e.g. lipofectamine).[39, 40] Interaction of the cationic delivery vehicle with the membrane is essential, but large disruptions may cause an influx of extracellular fluid and initiate a cascade of apoptotic events including the depolarization of intracellular mitochondria.

To visually monitor the time-dependent changes in membrane permeability, HUVEC were cultured onto glass slides in KRH buffer containing 30 μM propidium iodide (PI), treated with dendrimer conjugates (3 μM), and imaged via confocal fluorescence microscopy. Fluorescent labeling of the dendrimer conjugates enabled direct visualization of the interaction between the dendrimer and the plasma membrane of cultured cells. Figure 4.6 depicts HUVEC exposed to the partially modified, amine containing dendrimer **1.** After 30 min, fluorescently-labeled dendrimer **1** appeared to completely permeate the plasma membrane and progressively accumulate within the intracellular compartment, either via diffusion through newly formed holes or an endocytotic mechanism proposed previously for other dendrimer conjugates.[41] A rapid increase in the number of red fluorescent nuclei was also observed, visually confirming the kinetics of PI uptake as shown in Figure 4.5. The sequence of images (Fig. 4.6) clearly illustrates that increases in red fluorescence (PI uptake) coincide with the increase of the green fluorescence (dendrimer uptake) throughout the entire cell population. In the absence of dendrimers, cells retained their viability for up to 90 min and confocal images demonstrated no significant increase in red fluorescence of PI over the

time course of the experiment (data not shown). In similar experimental setup, exposure of HUVEC cells to dendrimer conjugate **2** or **3** resulted in no appreciable increase in PI fluorescence, consistent with the PI and LDH cytotoxicity assays (Fig. 4.5A and 4.5B).

4.3.3.2 Cellular adhesion of dendrimers **1-3** and mitochondrial depolarization

The series of confocal microscopy images shown in Figure 4.7 illustrate the time dependent changes in HUVEC viability after addition of the dendrimer conjugates. Upon exposure of cells to FITC-labeled amine-terminated dendrimer **1** for 5 min, a bright, punctuated green outline of the cells was observed, indicating adherence of FITC-dendrimer to the plasma membrane (Figure 4.7, DMR 1). Although imaged simultaneously, the origins of the PI and TMRM fluorescence are different. Here, imaging of PI and TMRM (both were excited using 543 nm laser line and red fluorescence was acquired through LP560 filter) was intended to demonstrate that the collapse of mitochondrial membrane potential (punctate structures within the cells) occurs before the increased characteristic PI fluorescence responsible for nuclear staining (large oval rings filled with fragmented red patches) as shown in Fig. 4.8, 30 min. The cellular interactions of fluorescently-labeled dendrimers **2** and **3** were also examined with the same protocols used for FITC-labeled dendrimer **1,** but no appreciable accumulation of the green fluorescence was observed on the membrane of HUVEC in culture (Figure 4.7, **DMR 2** & **DMR 3**). Thus, chemical conversion of cationic amines at the dendrimer surface to amides or sterically shielding the cationic surface via attached hydrophilic PEG chains resulted in substantial loss of the polymer's adhesion to the plasma membranes of HUVEC. Even at longer incubation times (>60 min) no significant accumulation at the membrane was observed for either the amide or PEG modified dendrimer conjugate.

To probe the effects of dendrimers on the membrane potential of intracellular mitochondria, cells were loaded with 100 nM TMRM dye prior to imaging. The cationic dye is retained in the mitochondria with high membrane potential indicative of cell viability. However, compromised cells undergo a characteristic loss of mitochondrial membrane potential and a disappearance of red fluorescent staining.[42] Confocal images of endothelial cells with TMRM-labeled mitochondria exposed to FITC-labeled dendrimers are shown in Figure 4.8. At early time points (5 min) of treatment with any of the dendrimer conjugates intracellular mitochondria retain TMRM dye in the matrix. After 15 min of exposure to dendrimer **1**, the plasma membrane of cultured cells no longer retained its integrity as indicated by the decrease in red mitochondrial fluorescence (white arrows) and a slow influx of extracellular PI into the cell nuclei (Fig. 4.8, **DMR 1**). Complete loss of TMRM fluorescence from mitochondria coincided with the staining of the nuclear envelope (white asterisks) and loss cell viability that occurred at 30 min of exposure to dendrimer **1**. In control experiments we demonstrated that TMRM, a mitochondria selective fluorescent dye, does not bind to cell nuclei, and vice versa, PI does not label mitochondria in cells with compromised plasma membranes (Figures 4.9 and 4.10).

Mitochondrial depolarization may be the result of a dramatic increase in cytosolic Ca^{2+} concentration due to the loss of plasma membrane integrity and influx of extracellular Ca^{2+}.[43] Correspondingly, no visible mitochondrial depolarization or PI staining of the nuclei was observed upon exposure of cultured cells to the FITC-labeled dendrimers **2** or **3** (Fig. 4.8, **DMR 2** & **DMR 3**). The TMRM fluorescence appeared to be unchanged over 30 min, indicating preservation of the mitochondrial membrane potential and minimal damage to the cellular plasma membrane. Despite the solvent accessible amines still available on

dendrimer conjugate **3**, the 2,000 MW PEG chains proved to be sufficient to block the cationic surface from interacting with the negatively charged membranes of endothelial cells.

| | 5 min | 30 min | 60 min | 90 min |

FITC (488 nm)

PI (543 nm)
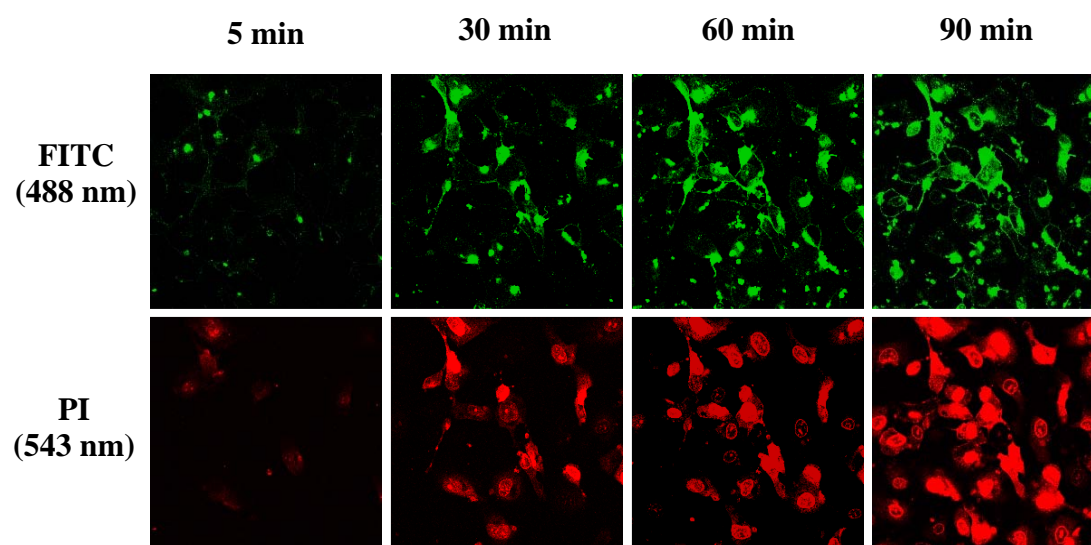
Figure 4.6   Confocal fluorescence microscopy images of the time dependent membrane permeability changes of HUVEC exposed to 3 μM amine containing dendrimer 1 in culture media containing 30 μM PI.
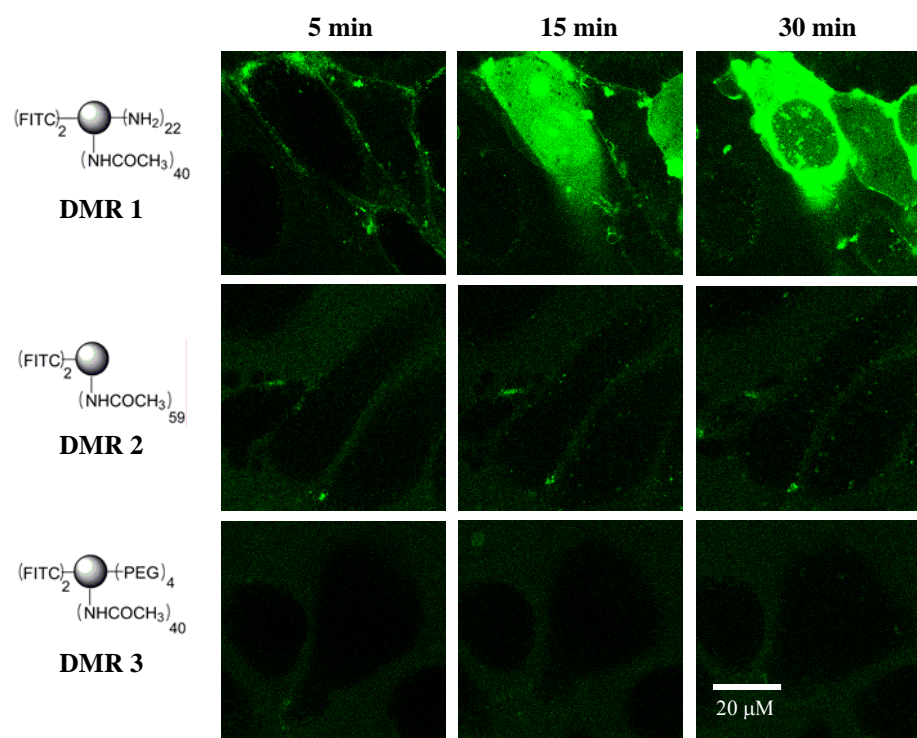
Figure 4.7   Confocal images of HUVEC treated with 3 µM fluorescent dendrimer conjugate (*green*) co-loaded with TMRM in KRH buffer supplemented with 30 µM of PI. Dendrimer **1** adhered and completely outlined the plasma membrane of most cells within 5 min followed by increasing green fluorescence over the 30 min of incubation. NO significant dendrimer adherence was observed with dendrimers **2** and **3**.

156
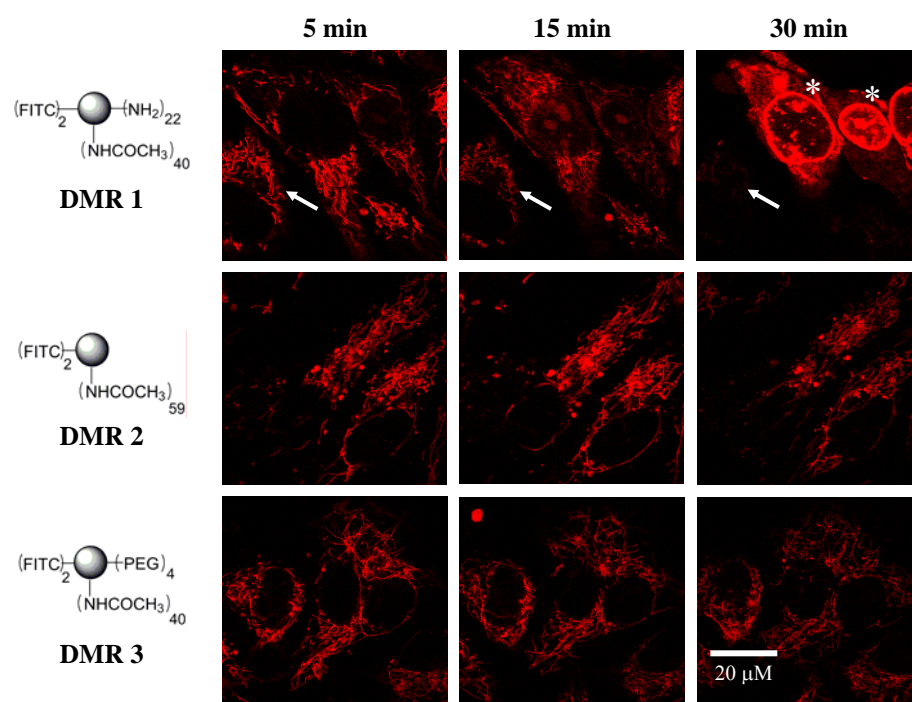
Figure 4.8   Confocal images of HUVEC treated with 3 µM fluorescent dendrimer conjugate co-loaded with TMRM in KRH buffer supplemented with 30 µM of PI. Dendrimer **1** resulted in a progressive loss of mitochondrial membrane potential (*decrease in TMRM fluorescence, white arrows*) and entrance of PI into the cells at 15 min and 30 min (*white asterisks denote typical red fluorescence of PI in the nuclei*).

	Green (DAB-Ac$_{40}$-FITC$_2$)	Red (TMRM dye)
0 min (Pre-Injection)		
5 min		
15 min		
30 min		
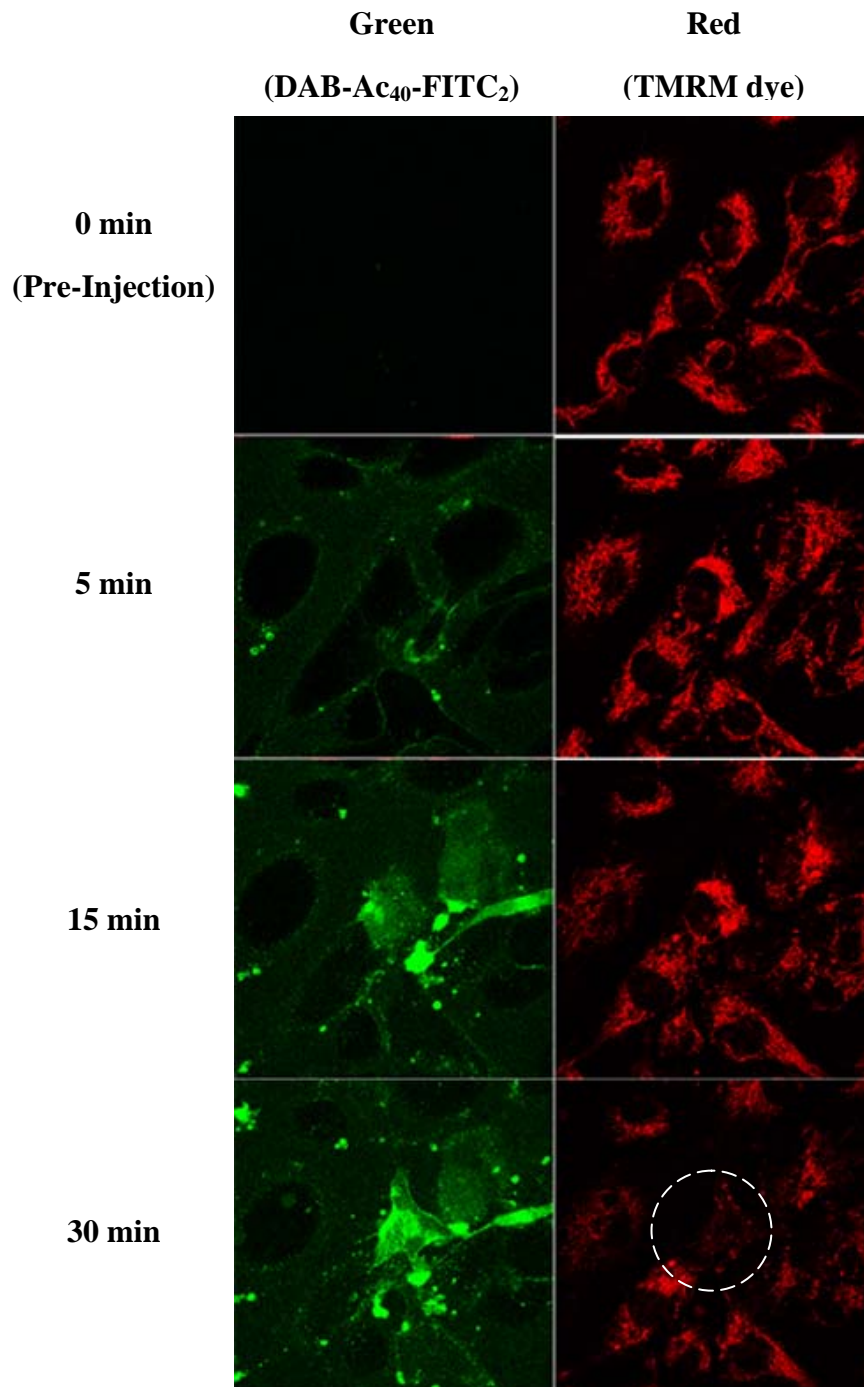
Figure 4.9   Time dependent mitochondrial depolarization as indicated via the diasapearance of TMRM (red) fluorescence. All cells indicate a gradual decrease in TMRM fluorescence over time but the affect is most pronounced in the indicated cell at 30 min. (dotted circle). These images serve as a control experiment, indicating no dark red staining of the nuclei without propidium iodide (PI) added to the incubation media.

	Green	**Red**
	(DAB-Ac$_{40}$-FITC$_2$)	**(PI dye)**
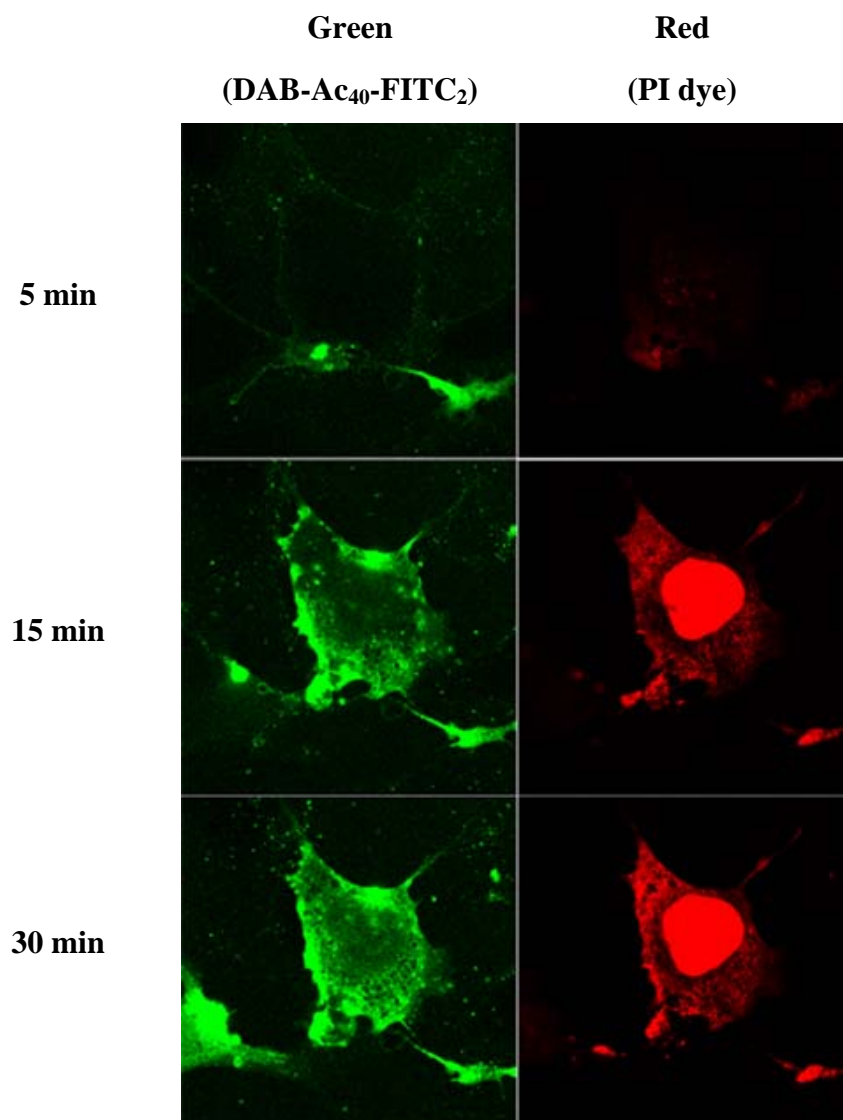
Figure 4.10   Time dependent membrane permeability toward propidium iodide (PI) as indicated via appearance of the bright red stained nuclei (red) fluorescence. The red fluorescence of skirting the nucleus of the cell is attributed to fluorescent staining of ribosomal RNA throughout the endoplasmic reticulum. These images serve as a control experiment, indicating the affect of dendrimer **2** on cells not previously stained with TMRM.
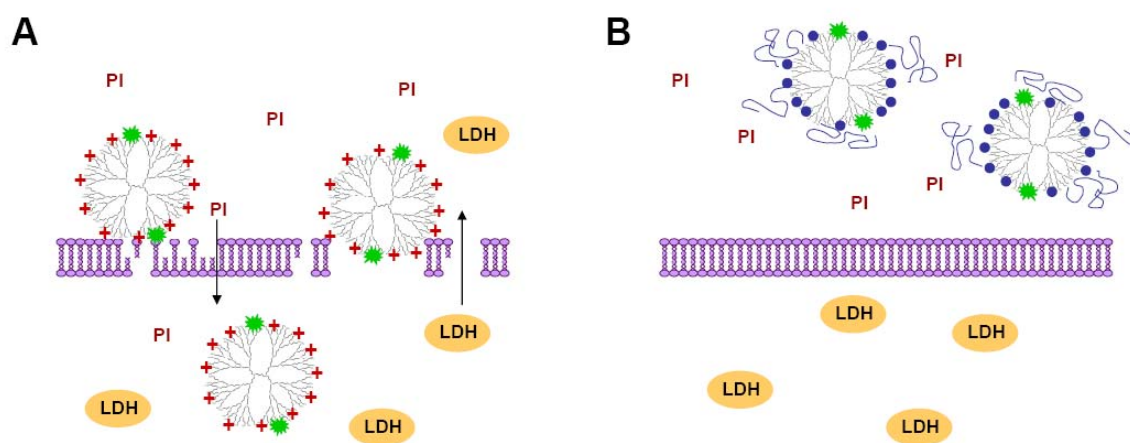
Figure 4.11   Illustration of dendrimers interacting with the plasma membrane of cultured cells. A) Primary amine containing dendrimer **1** (DAB-Ac$_{40}$-FITC$_2$) induces hole formation and allows the transport of dendrimer, PI, and LDH across the plasma membrane.   B) Amide/PEG modified dendrimer **3** (DAB-Ac$_{40}$-PEG$_4$-FITC$_2$) exhibits no membrane disruption or intracellular accumulation monitored via fluorescence based techniques.

4.4 Conclusion

Figure 4.11 summarizes our results obtained in the fluorescent viability assays and confocal microscopy experiments. Cationic amine residues at the surface of polypropylenimine dendrimers induced drastic and time-dependent changes in HUVEC membrane permeability toward cytosolic enzymes and PI (Fig. 4.11A). Rapid cellular uptake of PI, a low molecular weight dye, was detected as early as 15 min and the larger cytosolic proteins (e.g. LDH) were released from the cells at later time points. Alteration of amines to amides or covalent attachment of PEG resulted in dendrimer conjugates containing mixed functionalities with no acute toxicity profiles (Fig. 4.11B). The data presented herein are in agreement with the reported cytotoxicity of amine terminated dendrimers and strongly suggests that primary amine-terminated dendrimers should be avoided as drug delivery vehicles. In conclusion, the cytotoxicity and biocompatibility of dendrimer-vehicles is dependent on the surface composition, and it is essential that dendrimer-based drugs formulated for intravenous injection be tested for specific cytotoxicity toward endothelial cells.

4.5 References

1. Stiriba, S.-E.; Frey, H.; Haag, R. "Dendritic polymers in biomedical applications: from potential to clinical use in diagnostics and therapy." *Angew. Chem. Int. Ed.* **2002,** *41*, 1329-1334.

2. Svenson, S.; Tomalia, D. A. "Dendrimers in biomedical applications-reflections on the field." *Adv. Drug Deliv. Rev.* **2005,** *57*, 2106-2129.

3. Frechet, J. M. "Dendrimers and other dendritic macromolecules: from building blocks to functional assemblies in nanoscience and nanotechnology." *J. Polym. Sci. A: Poly. Chem.* **2003,** *41*, 3713-3725.

4. Boas, U.; Heegaard, P. M. H. "Dendrimers in drug research." *Chem. Soc. Rev.* **2004,** *33*, 43-63.

5. Gillies, E. R.; Frechet, J. M. "Dendrimers and dendritic polymers in drug delivery." *Drug Discovery Today* **2005,** *10*, 35-43.

6. Meijer, E. W.; Jansen, J.; Brabander-van den Berg, E. "Encapsulation of guest molecules into a dendritic box." *Science* **1994,** *266*, 1226-1229.

7. Morgan, M. T.; Carnahan, M. A.; Immoos, C. E.; Ribeiro, A. A.; Finkelstein, S.; Lee, S. J.; Grinstaff, M. W. "Dendritic molecular capsules for hydrophobic compounds." *J. Am. Chem. Soc.* **2003,** *125*, 15485-15489.

8. Patri, A. K.; Myc, A.; Beals, J.; Thomas, N. H.; Baker, J. R. "Synthesis and in vivo testing of J591 antibody-dendrimer conjugates for targeted prostate cancer therapy." *Bioconjug. Chem.* **2004,** *15*, 1174-1181.

9. Kukowska-Latallo, J. F.; Candido, K. A.; Cao, Z.; Nigavekar, S. S.; Majoros, I. J.; Thomas, T. P.; Balogh, L. P.; Khan, M.; Baker, J. R. "Nanoparticle targeting of anticancer drug improves therapeutic response in animal model of human epithelial cancer." *Cancer Res.* **2005,** *65*, 5317-5324.

10. Majoros, I. J.; Myc, A.; Thomas, T.; Mehta, C. B.; Baker, J. R. "PAMAM dendrimer-based multifunctional conjugate for cancer therapy: synthesis, characterization, and functionality." *Biomacromolecules* **2006,** *7*, 572-579.

11. Dufes, C.; Uchegbu, I. F.; Schatzlein, A. G. "Dendrimers in gene delivery." *Adv. Drug Deliv. Rev.* **2005,** *57*, 2177-2202.

12. Kubasiak, L. A.; Tomalia, D. A., Cationic dendrimers as gene transfection vectors: dendri-poly(amidoamines) and dendri-poly(propylenimines). In *Polymeric Gene Delivery*, Amiji, M. M., Ed. CRC Press LLC: Boca Raton, FL, 2005; pp 133-157.

13. Haensler, J.; Szoka, F. C., Jr. "Polyamidoamine cascade polymers mediate efficient transfection of cells in culture." *Bioconjug. Chem.* **1993,** *4*, 372-379.

14. Luo, D.; Haverstick, K.; Belcheva, N.; Han, E.; Saltzman, W. M. "Polyethylene glycol-conjugated PAMAM dendrimer for biocompatible, high efficiency DNA delivery." *Macromolecules* **2002,** *35*, 3456-3462.

15. Braun, C. S.; Vetro, J. A.; Tomalia, D. A.; Koe, G. S.; Koe, J. G.; Middaugh, C. R. "Structure/function relationships of polyamidoamine/DNA dendrimers as gene delivery vehicles." *J. Pharm. Sci.* **2005,** *94*, 423-436.

16. Bielinska, A. U.; Chen, C.; Johnson, J.; Baker, J. R., Jr. "DNA complexing with polyamidoamine dendrimers: implications for transfection." *Bioconjug. Chem.* **1999,** *10*, 843-850.

17. Bielinska, A. U.; Kukowska-Latallo, J. F.; Baker, J. R., Jr. "The interaction of plasmid DNA with polyamidoamine dendrimers: mechanism of complex formation and analysis of alterations induced in nuclease sensitivity and transcriptional activity of the complexed DNA." *Biochim. Biophys. Acta* **1997,** *1353*, 180-190.

18. Duncan, R.; Izzo, L. "Dendrimer biocompatibility and toxicity." *Adv. Drug Deliv. Rev.* **2005,** *57*, 2215-2237.

19. Hong, S.; Bielinska, A. U.; Mecke, A.; Keszler, B.; Beals, J. L.; Shi, X.; Balogh, L.; Orr, B. G.; Baker, J. R. "Interaction of poly(amidoamine) dendrimers with supported lipid bilayers and cells: hole formation and the relation to transport." *Bioconjug. Chem.* **2004,** *15*, 774-782.

20. Mecke, A.; Majoros, I. J.; Patri, A. K.; Baker, J. R. J.; Banaszak-Holl, M. M.; Orr, B. G. "Lipid bilayer disruption by polycationic polymers: the roles of size and chemical functional group." *Langmuir* **2005,** *21*, 10348-10354.

21. Lee, H.; Larson, R. G. "Molecular dynamics simulations of PAMAM dendrimer-induced pore formation in DPPC bilayers with a coarse-grained model." *J. Phys. Chem. B* **2006,** *110*, 18204-18211.

22. Fuchs, S.; Kapp, T.; Otto, H.; Schoneberg, T.; Franke, P.; Gust, R.; Schluter, A. D. "A surface-modified dendrimer set for potential application as drug delivery vehicles: synthesis, in vitro toxicity, and intracellular localization." *Chem. Eur. J.* **2004,** *10*, 1167-1192.

23. Jevprasesphant, R.; Penny, J.; Attwood, D.; McKeown, N. B.; D'Emanuele, A. "Engineering of dendrimer surfaces to enhance transepithelial transport and reduce cytotoxicity." *Pharm. Res.* **2003,** *20*, 1543-1550.

24. Tack, F.; Bakker, A.; Maes, S.; Dekeyser, N.; Bruining, M.; Elissen-Roman, C.; Janicot, M.; Brewster, M.; Janssen, H. M.; De Waal, B. F. M.; Fransen, P. M.; Lou,

X.; Meijer, E. W. "Modified poly(propylene imine) dendrimers as effective transfection agents for catalytic DNA enzymes (DNAzymes)." *J. Drug. Target.* **2006,** *14*, 69-86.

25.   Kojima, C.; Kono, K.; Maruyama, K.; Takagishi, T. "Synthesis of polyamidoamine dendrimers having poly(ethylene glycol) grafts and their ability to encapsulate anticancer drugs." *Bionconjug. Chem.* **2000,** *11*, 910-917.

26.   Sarin, V. K.; Kent, S. B. H.; Tam, J. P.; Merrifield, R. B. "Quantitative monitoring of solid-phase peptide synthesis by the ninhydrin reaction." *Anal. Biochem.* **1981,** *117*, 147-157.

27.   Puranam, K. L.; Boustany, R.-M., Assessment of cell viability and histochemical methods in apoptosis. In *Apoptosis in Neurobiology*, Hannun, Y. A.; Boustany, R.-M., Eds. CRC Press LLC: Boca Raton, Fl, 1998; pp 129-152.

28.   Hong, S.; Leroueil, P. R.; Janus, E. K.; Peters, J. L.; Kober, M.-M.; Islam, M. T.; Orr, B. G.; Baker, J. R., Jr.; Banaszak-Holl, M. M. "Interaction of polycationic polymers with supported lipid bilayers and cells: nanoscale hole formation and enhanced membrane permeability." *Bioconjug. Chem.* **2006,** *17*, 728-734.

29.   Majoros, I. J.; Keszler, B.; Woehler, S.; Bull, T.; Baker, J. R. "Acetylation of poly(amidoamine) dendrimers." *Macromolecules* **2003,** *36*, 5526-5529.

30.   Marano, R. J.; Toth, I.; Wimmer, N.; Brankov, M.; Rakoczy, P. E. "Dendrimer delivery of an anti-VEGF oligonucleotide into the eye: a long term study into inhibition of laser-induced CNV, distribution, uptake and toxicity." *Gene Ther.* **2005,** *12*, 1544-1550.

31.   Kim, T.; Seo, H. J.; Choi, J. S.; Jang, H.-S.; Baek, J.; Kim, K.; Park, J.-S. "PAMAM-PEG-PAMAM: Novel triblock copolymer as a biocompatible and efficient gene delivery vehicle." *Biomacromolecules* **2004,** *5*, 2487-2492.

32.   Chappey, O.; Wautier, M. P.; Wautier, J. L. "Endothelial cells in culture: a model to study in vitro vascular toxicity." *Toxic. in Vitro* **1995,** *9*, 411-419.

33.   Vane, J. R.; Anggard, E. E.; Botting, R. M. "Regulatory functions of the vascular endothelium." *N. Engl. J. Med.* **1990,** *323*, 27-36.

34.   Green, J. J.; Shi, J.; Chiu, E.; Leshchiner, E. S.; Langer, R.; Anderson, D. G. "Biodegradable polymeric vectors for gene delivery to human endothelial cells." *Bioconjug. Chem.* **2006,** *17*, 1162-1169.

35.   Gores, G. J.; Nieminen, A.-L.; Fleishman, K. E.; Dawson, T. L.; Herman, B.; Lemasters, J. J. "Extracellular acidosis delays onset of cell death in ATP-depleted hepatocytes." *Am. J. Physiol.* **1988,** *255*, 315-322.

36.   Lemasters, J. J.; DiGuiseppi, J.; Nieminen, A.-L.; Herman, B. "Blebbing, free Ca^{2+} and mitochondrial membrane potential preceding cell death in hepatocytes." *Nature* **1987,** *325*, 78-81.

37.   Becker, G. L.; Fiskum, G.; Lehninger, A. L. *J. Biol. Chem.* **1980,** *255*, 9009-9012.

38.   Jevprasesphant, R.; Penny, J.; Jalal, R.; Attwood, D.; McKeown, N. B.; D'Emanuele, A. "The influence of surface modification on the cytotoxicity of PAMAM dendrimers." *Int. J. Pharm.* **2003,** *252*, 263-266.

39.   Felgner, P. L.; Gadek, T. R.; Holm, M.; Roman, R.; Chan, H. W.; Wenz, M.; Northrop, J. P.; Ringold, G. M.; Danielsen, M. "Lipofection: A highly efficient, lipid-mediated DNA-transfection procedure." *Proc. Natl. Acad. Sci. USA* **1987,** *84*, 7413-7417.

40.   Horobin, R. W.; Weissig, V. "A QSAR-modeling perspective on cationic transfection lipids. 1. predicting efficiency and understanding mechansims." *J. Gene Med.* **2005,** *7*, 1023-1034.

41.   Kolhe, P.; Khandare, J.; Pillai, O.; Kannan, S.; Lieh-Lai, M.; Kannan, R. M. "Preparation, cellular transport, and activity of polyamidoamine-based dendritic nanodevices with a high drug payload." *Biomaterials* **2006,** *27*, 660-669.

42.   Kim, J.-S.; Ohshima, S.; Pediaditakis, P.; Lemasters, J. J. "Nitric oxide protects rat hepatocytes against reperfusion injury mediated by the mitochondrial permeability transition." *Hepatology* **2004,** *39*, 1533-1543.

43.   Sedova, M.; Dedkova, E. N.; Blatter, L. A. "Integration of rapid cytosolic Ca^{2+} signals by mitochondria in cat ventricular myocytes." *Am. J. Physiol. Cell Physiol.* **2006,** *291*, 840-850.

Chapter 5

Future Applications of Nitric Oxide Releasing Dendrimers

5.1 Introduction

The development of NO-releasing dendrimers via *N*-diazeniumdiolate and *S*-nitrosothiol chemistries enables new tools to study the role of NO in biomedical applications. Thus far the synthetic procedures to attach two of the most common organic NO donor functionalities to amine terminated dendrimers (e.g., PAMAM) have been established. Diazeniumdiolates and nitrosothiols both retained their characteristic NO-release behavior when attached to the dendrimer scaffolds and, in some cases, a "dendritic effect" was observed that may increase NO-releasing dendrimer utility. For example, alkyl diazeniumdiolates on the secondary amines of polypropylenimine dendrimers (Chapter 2) exhibited prolonged NO-release half-lives when compared to analogous diazeniumdiolate small molecules. The high local concentration of amines inside the dendrimer resulted in a dependence on pH and reduced proton initiated decomposition. The creation of the NO donor-modified dendrimers and full characterization of dendritic NO-release kinetics has laid the foundation for future discoveries.

As detailed in the previous chapters, dendrimers are attractive delivery vehicles for NO because the hyper-branched scaffold may be modified to contain a large number of NO donors per molecule. The most straightforward application of this technology is as polymer fillers to confer NO-release to biomedical grade polymers, similar to the strategies reviewed

in Chapter 1. In addition to storing micromolar quantities of NO per mg, the greatest attribute of dendrimers as macromolecular NO donors is the multivalent surface that may be functionalized with additional ligands. Expansion of the current work through conjugation of moieties capable of tissue specific targeting, attachment of molecular probes for imaging, and the synthesis of "pre-packaged" diazeniumdiolates for precise stoichiometric control of NO loading are the next steps toward creating *multi-functional* NO-releasing devices. As depicted in Figure 5.1, the proposed chemistry detailed in this chapter may allow for the fabrication of NO-releasing vehicles that may be targeted and tracked thereby harnessing the therapeutic potential of NO.

5.2 Dendrimer Doped Polymers for Wound Healing and other Biomedical Applications

Extensive research has been conducted on NO-releasing materials that have applications across a broad spectrum of medical device industries. For example, implants coated with NO-releasing polymers have been shown to reduce the incidence of infection[1] and aid in minimizing the foreign body response to implanted materials.[2] Sensors with sustained NO flux have led to more thromboresistant surfaces and improved sensor longevity.[3, 4] The NO-releasing dendrimers described in this thesis may also be incorporated into polymeric matrices. The ability to tailor the NO-release kinetics based on NO donor structure and increase the lipophilicity of the overall macromolecular framework to prevent leaching from the polymer, make dendrimers incredibly valuable tools for future sensor membrane research. The primary detriment to NO-releasing polymeric device coatings is that no system has an infinite reservoir of NO. As such, there is a limit to the amount of NO donor that may be loaded into the polymer before the polymer loses its desired mechanical properties. Nevertheless, storing large dendrimer-bound quantities of NO may extend NO-

167

release durations from days to weeks, and lengthen the experimental timescales for examining NO-dependent biological phenomena.

One setting where NO-releasing dendrimers may make the biggest impact is wound repair. Only recently has it been discovered that NO mediates many of the processes involved in wound closure including re-epithelialization, matrix remodeling, and tissue granulation.[5-7] However, maintaining sufficient levels of NO for prolonged periods at a wound site remains a challenge. Polyurethane barrier membranes have become a popular choice for wound closure devices because they facilitate adequate gas transport while maintaining a moist wound environment necessary to promote wound healing. Future studies aim to incorporate NO-releasing dendrimers into polyurethane sheets as wound dressings to treat infected wounds and promote normal wound healing. As shown in Figure 5.2, polyurethane dressings doped with NO-releasing dendrimers release NO gas only at the wound site. After use, the delivery vehicle may be discarded. In clinical settings where topical delivery is required, both diazeniumdiolate and nitrosothiol-modified dendrimers may prove useful. The lipophilicity of diazeniumdiolate-modified dendrimer and the water-uptake properties of the polymer may be tuned and used to create dressings that upon "soaking" exhibit high, rapid amounts of NO-release, or lower prolonged fluxes with extended release durations. Furthermore, polyurethane containing *S*-nitrosothiol modified dendrimers have the inherent ability to turn on and off the NO-release based on exposure to light.

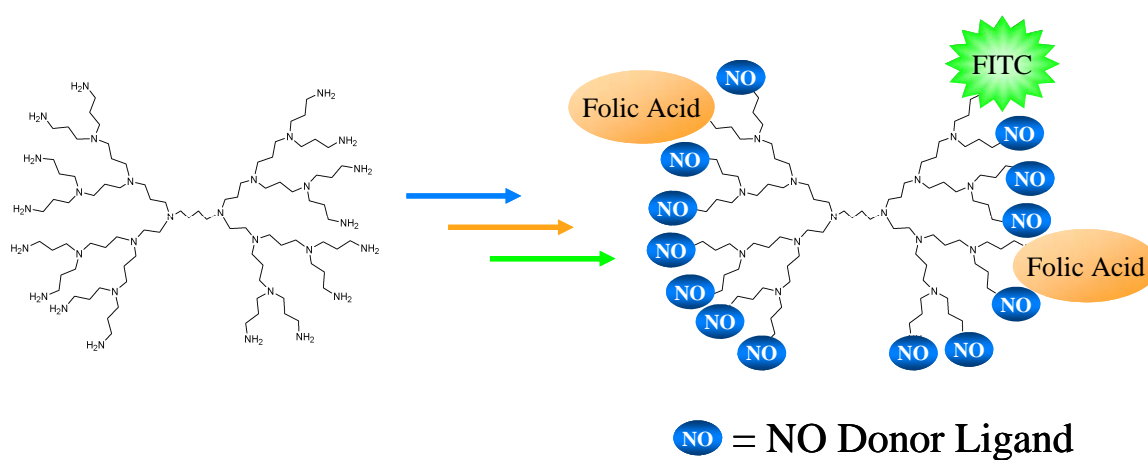Figure 5.1   Modification of a generation 3 polypropyleneimine dendrimer (DAB-Am-16) to possess a diaminobutane core and 16 primary amines functionalized with NO donor moieties, a fluorescent label for imaging (FITC), and folic acid residues for targeting cancer cells in vivo.
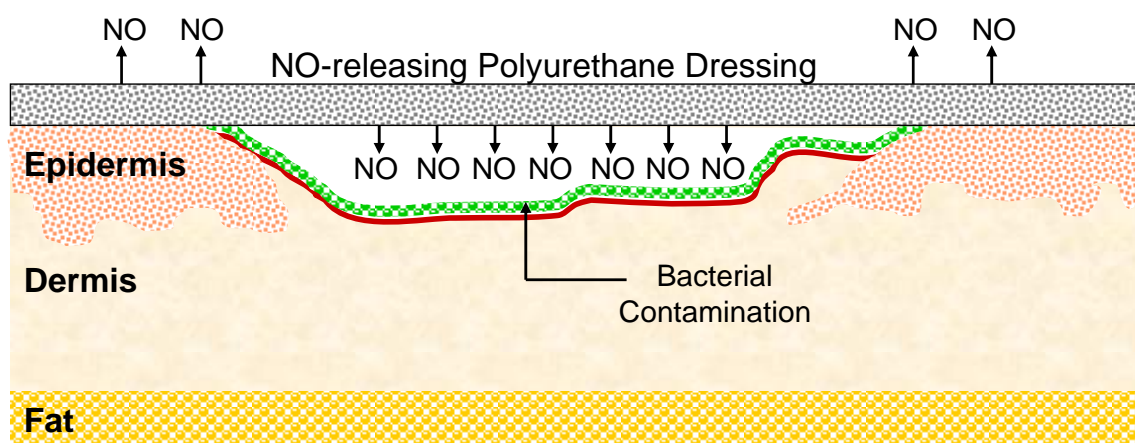
Figure 5.2   Diagram of a polyurethane wound dressing doped with NO-releasing dendrimers capable of delivering NO to infected wounds.

5.3 Strategies for Targeted NO Delivery

In addition to doping NO-donor functionalized dendrimers into polymers, the synthesis and use of *multifunctional* NO-releasing dendrimers may benefit the treatment of disease states known to be influenced by NO. The need for site specific delivery to realize the potential of NO as treatments for two such applications, cancer and ischemia/reperfusion injury, are discussed below.

5.3.1 Folic acid targeted anti-cancer therapeutics

Nitric oxide mediates multiple stages of cancer development. Unfortunately, the exact impact of NO on tumor cell biology remains unclear.[8-10] Petit et al. hypothesize that low levels of NO (pM) may mediate angiogenesis and enhance tumor cell proliferation while higher fluxes of NO (μM) may form reactive nitrogen species capable of killing cancer cells.[11] Several small molecule NO donors have shown efficacy against prostate, colon, and human breast cancers in vitro. Still, elucidating the mechanistic effects of NO on cancerous cells in vivo has been problematic due to *indiscriminate* NO release.[8, 12-16] Failure to deliver NO to specific cells and/or tissues of interest has limited its clinical development. [17-19] The primary obstacles impeding NO delivery to tumor tissue may be overcome through the development of multifunctional NO-releasing dendrimers.

The goal of targeted drug delivery is to maximize the concentration of a drug in specific organs or tissues of interest, while minimizing the drug's systemic distribution and toxicity to healthy cells. Active targeting involves the attachment of a target-specific ligand to the carrier system exterior that will interact preferentially with tumor cell surface receptors over healthy tissue.[20] For example, monoclonal antibodies target specific antigens on tumor cell surfaces and have been used to narrow the biodistribution and increase the efficacy of many pharmaceutical formulations.[21-24] In cancer research, small ligands such as folic acid have

171

been used as a successful method of active drug delivery, targeting the over-expression of folate receptors in solid tumors.[25-27] Up-regulation of the folate receptor has been observed in many human malignancies including ovarian, brain, kidney, endometrial and lung cancers, with minimal receptor expression in most normal tissues.[25, 28, 29] The over-expression of folate receptors on the tumor cell surface is due to the high demand for nutrients in rapidly dividing cells. The lack of folate receptors coupled with the high affinity of folate for the folate receptor allows folate conjugates to exhibit enhanced, pinpoint selectively for diseased tissue. [26, 27, 30 28] The small size, convenient availability, and facile attachment methods to the exterior of nanoparticles may make folic acid an ideal ligand for targeted NO-delivery systems.

An attractive feature of folic acid conjugated therapeutics is that folic acid retains its receptor binding properties when derivatized via its γ-carboxyl group.[25] Several procedures have been reported previously for attaching folic acid to nanoparticle constructs.[27, 30-32] A synthetic procedure modified from the one reported by Baker and co-workers is shown in Scheme 5.1.[33] The folic acid may first be activated with NHS/DCC in a DMSO solution and then added to a suspension of dendrimer in DMSO aiming to stoichiometrically convert 10 of the 64 exterior amines. The cyclized thiolactone of *N*-acetyl-D,L-penicillamine utilized in previous studies may also be added to convert the remaining amines to thiols. Conversion of the thiols to *S*-nitrosothiols in an acidified nitrite solution may result in the first folate targeted NO-releasing dendrimer conjugate. Direct conjugation of fluorophores for imaging, conversion of a portion of the amines to amides to reduce toxicity and increase vehicle solubility, or the attachment of poly(ethylene glycol) chains to improve biodistribution represent viable options for future conjugation to the dendritic framework (Figure 5.3). These chemistries may further unlock the power of dendrimers as NO-delivery vehicles.

172
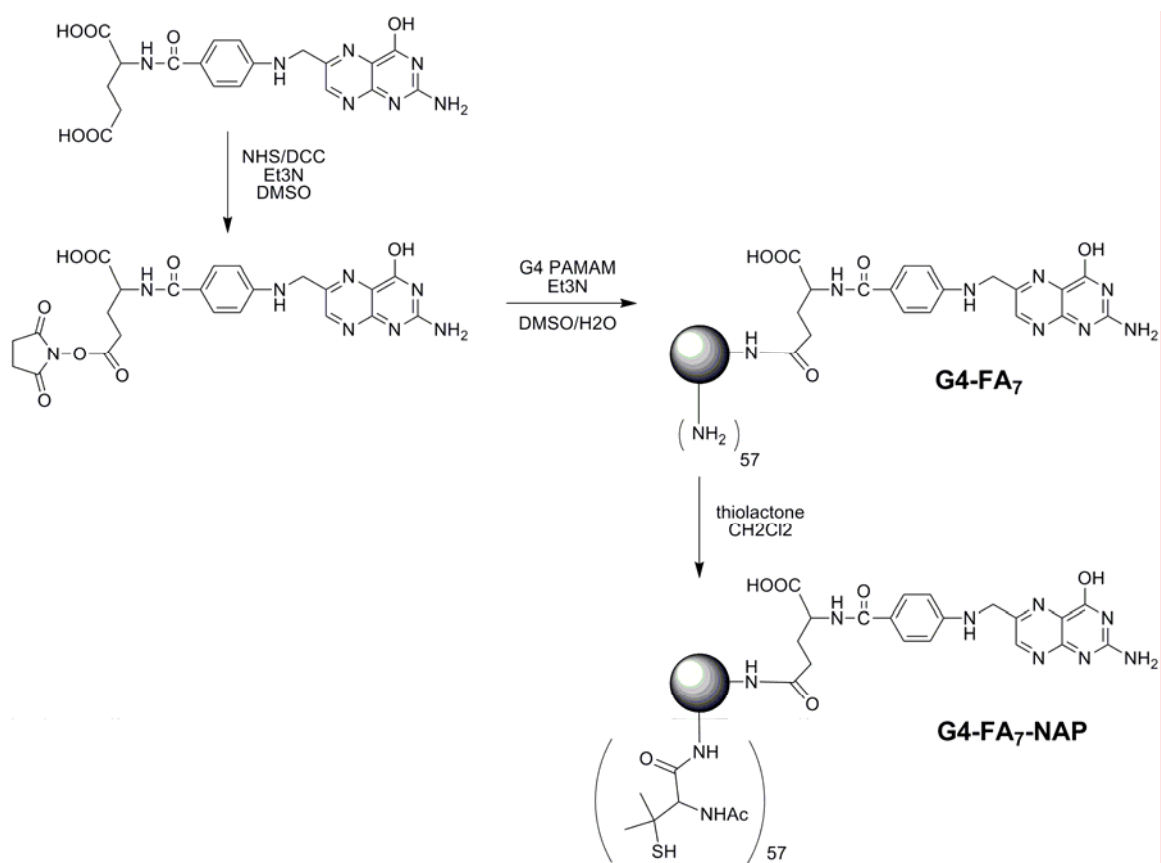
Scheme 5.1   Synthesis of folic acid dendrimer conjugate G4-FA$_7$ and thiolated dendrimer conjugate G4-FA$_7$-NAP.
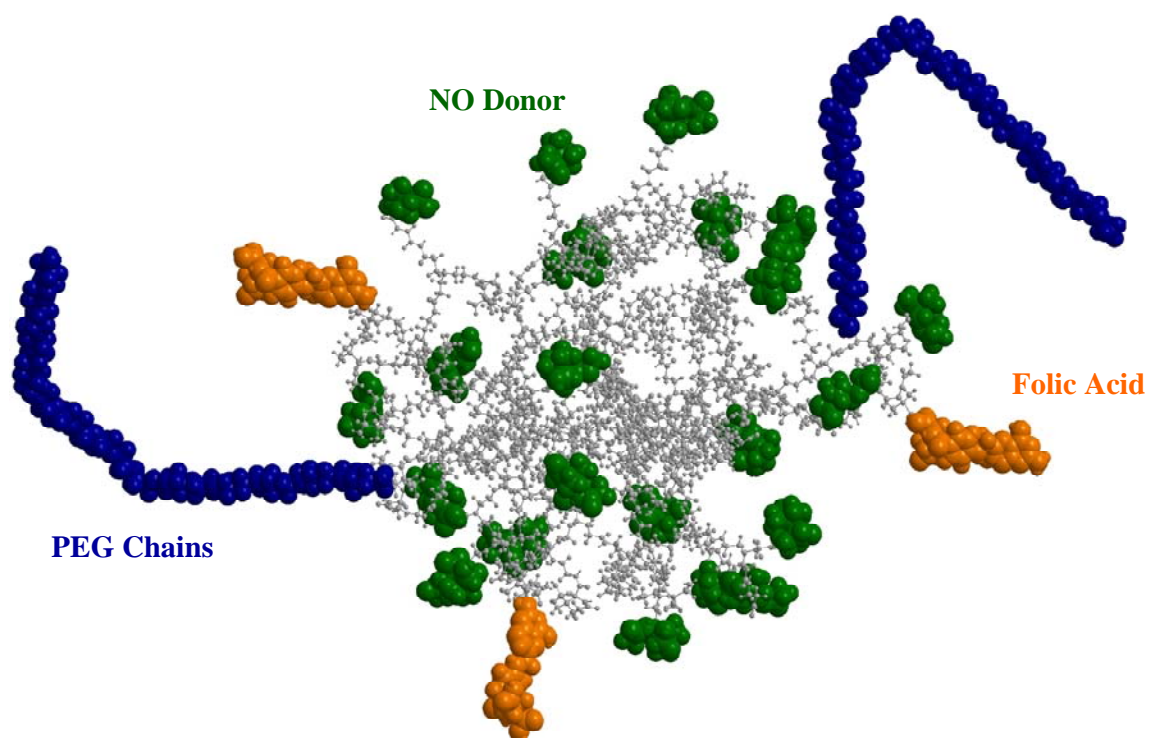
Figure 5.3   Multifunctional NO-releasing dendrimer delivery vehicle containing folate residues for tissue specific targeting and poly(ethylene glycol) chains to enhance vehicle biodistribution.

5.3.2 Targeted S-nitrosothiol dendrimers to treat ischemia/reperfusion injury

When an artery is clogged and blood flow through the heart is inhibited, heart tissue downstream of the blockage becomes deprived of oxygen and vital nutrients. This process is known as ischemia. Under such conditions, inflammation and other physiological changes occur to damage the heart muscle. When the blockage is removed through percutaneous intervention, the re-establishment of blood-flow and oxygenation leads to oxidative stress causing further cell death and an excessive inflammatory response, also known as "reperfusion injury." Ischemia/reperfusion (I/R) injury is a major complication with treatments for heart attack patients as it often results in the loss of heart muscle function and reoccurring heart attacks. To date, clinical trials have not identified an effective therapy for salvaging at-risk heart muscle after reperfusion therapy.[34]

Since the discovery of NO as the endothelial derived relaxation factor,[35] a number of studies have attempted to use NO to attenuate ischemia/reperfusion injury.[36,37, 38] Nitric oxide mediates many of the processes contributing to I/R injury including platelet activation, interaction of leukocytes with the vessel wall, inflammatory response, and cardiomyocyte apoptosis.[39] However, NO exhibits extremely sensitive and concentration dependent effects in models of I/R injury and has been reported to be both protective and detrimental, resulting in a controversy over the effects of experimental NO therapeutics.[34] To further elucidate NO's role in I/R injury, NO-releasing dendrimers with exterior residues for "sticking" the delivery vehicles to the vascular wall may be useful for creating a localized dose of NO in myocardial tissue.[40] Polylysine and PAMAM dendrimers have already been utilized to enhance the retention of delivery vehicle to the vessel wall by binding to the extracellular matrix after intravascular delivery.[41] As discussed in chapter 4, dendrimers like these possessing amine containing surfaces are highly cytotoxic toward endothelial cells that line

175

the vascular wall. Cationic amine terminated vehicles should thus be avoided to create vehicles with acceptable toxicity profiles. Ligands that show excellent specificity for targeting the endothelium should be employed like RGD peptide derivatives[42, 43] (arginine, glycine, aspartate) and sialyl-Lewis[x] tetrasaccharides.[44-46]

Sialyl Lewis[x] (sLe[x]) oligosaccharides are key ligands expressed on leukocyte and on endothelial cell surfaces that are recognized by L-selectin.[44] L-selectin belongs to a family of transmembrane glycoprotiens responsible for adhesion of leukocytes to the vascular endothelium in early cascade events of inflammation. Dendrimer conjugates of sLe[x] may exhibit excellent binding to the endothelium and provide prolonged NO-release during the inflammatory period of ischemia/reperfusion injury. Since synthesis and further derivatization of tetrasaccharides is challenging, future studies could make use of classic avidin-biotin conjugation to attach sLe[x] to G4-SNAP modified dendrimers to a protein delivery vehicle.[40] As shown in Scheme 5.2, biotin-*N*-hydroxysuccinimide could be reacted with G4-PAMAM in DMF to biotinylate approximately 25% of the exterior amines (16 of 64). Following conversion of the remaining amines to *S*-nitrosothiols, the biotin modified *S*-nitrosothiol dendrimer may be combined with commercially available sLe[x]-biotin (Glycotech, Gaithersburg, MD) and 1 equivalent of NeutrAvidin (Pierce, Rockford, IL) to create protein-based clusters of RSNO dendrimer and sLe[x] targeting ligand. The multimeric protein would be capable of targeting the endothelium with the pendant sLe[x] ligands and release NO via *S*-nitrosothiol chemistry.

Dendrimers tailored to specifically interact with the endothelium and accumulate at cell surfaces would produce "local" reservoirs of NO. Once exposed to the levels of glutathione present in blood or glutathione that may be added to reperfusion media NO-release will be intiated as described in Chapter 3. This chemistry presents a major advancement over using

well dispersed small molecule NO donors (e.g., SNAP) in solution that would not result in "dendritic pockets" of NO when stimulated with GSH.

5.4. Fluorescent Labeling and Near-IR Imaging

Dendrimers are an isolated class of nanoparticle drug delivery vehicles, but the entire field is subject to caution from regulatory agencies and skeptics of nanotechnology. As potential therapeutics that may end up saving human lives, each new drug delivery vehicle will be required to have a full exploration of its "nanotoxicology." One of the main concerns for nanoparticle drug delivery is the fate of the vehicle when it enters the body. Achievements made with NO-releasing dendrimers in the therapeutic areas described above will also endure the same scrutiny. Subsequent work will thus require creating vehicles containing molecular probes for imaging in combination with the therapeutic doses of NO. Fluorescein isothiocyanate (FITC, green) and rhodamine-B-isothiocyante (RITC, red) are two commercially available dyes (Sigma-Aldrich or Invitrogen) that possess a handle for rapid reaction with amine terminated dendrimers and may prove useful for imaging dendrimer in tissue biodistribution experiments with fluorescence microscopy. Fluorescently-labeled dendrimers are also vital for understanding cellular interactions in vitro as evidenced in Chapter 4. Near-infrared imaging will allow for imaging the biodistribution of IR dye-labeled dendrimers in whole rats, without harvesting individual organs. IRDye® 800 CW is prepared as the NHS-ester for direct covalent attachment with proteins and dendrimer based delivery vehicles. Dendrimers containing amines, amides, thiols, alcohols, PEG, or NO donors at the exterior may all be labeled with one or more of the dyes depicted in Figure 5.4 to monitor the systemic biodistribution after intravenous injection.

177

5.5 O^2-protected Diazeniumdiolates

In the future, O^2-protected diazeniumdiolates may be utilized to create stable dendrimer-NO adducts that exhibit enzymatic or pH triggered NO release. [47, 48] Saavedra and co-workers have reported a strategy to package protected diazeniumdiolates with a carboxylic acid handle for conjugation chemistry.[49] When coupling this chemistry to targeted delivery vehicles, concerns regarding the kinetics of ligand binding in vivo are paramount when deciding which O^2-protecting group to use.[50] For example, folic acid is metabolized by cells for essential cell functions, but the fate of the folate receptor-conjugate complex governs the potential therapeutic efficacy of the drug to be released. For NO-releasing dendrimers, the mechanism of NO donor decomposition must compensate for the rate of folate-receptor conjugate internalization (k_{int}), the rate of nanoparticle dissociation (k_{nd}), and the recycling of bound nanoparticle back to the tumor cell surface (k_r), requiring that folic acid and other ligand receptor targeted nanoparticle conjugates contain an active or "triggered" mechanism of NO release.

Sugar, acetal, vinyl, and photo-triggered protecting groups have all been utilized for the potential controlled release of NO from diazeniumdiolates.[51, 52] Attaching a protected NO donor as a ligand to the dendrimer scaffold has the following advantages: 1) exposure of dendrimers to harsh diazeniumdiolate synthesis conditions (i.e., strong base) will be eliminated; 2) simple isolation and chromatography of the NO donor–modified dendrimers which is currently inaccessible after loading NO; and, 3) greater control over the exact quantity of NO loaded on the nanoparticle scaffold.

5.5.1 Protected diazeniumdiolates with amine and carboxylic acid functionalities

178

Future studies should employ NO donor ligands for covalent modification of dendrimers via either -COOH or -NH$_2$ handles. The simplest model will contain a secondary amine for conversion to a diazeniumdiolate NO donor and a reactive carboxylic acid for NHS coupling to an amine terminated exterior of G4-PAMAM. Proline is an excellent example of such a precursor ligand. However, diazeniumdiolate formation often results in the sodium salt of the carboxyl anion that also has reactivity with alkylating agents (e.g, MOM-Cl) (Scheme 5.3A). To avoid "blocking" the carboxylic acid that will be used to couple the protected NO donor to the dendrimer, prolinol could be used as the starting material. Following charging under basic conditions and subsequent conversion to the MOM-ether, the alcohol could undergo a sharpless oxidation in a solution of RuCl$_3$ and NaIO$_4$ (Scheme 5.3B).[49]

Alternatively the O^2-protected ligand may consist of a polyamine containing one or more secondary amines for conversion to *N*-bound diazeniumdiolates. In this case, the primary amine termini could be coupled to carboxylic acid terminated half-generation dendrimers (e.g., G3.5 PAMAM). This approach poses an additional synthetic challenge as early work has shown some conversion of primary amines to diazeniumdiolates upon exposure to NO. To avoid trace quantities of primary amine diazeniumdiolate, selective protection of the primary amines on the polyamine ligands would be necessary before conversion of the secondary amines to NO donors. 2-acetyldimedone has been used previously to protect only the primary amines of polyamine chains.[53] Scheme 5.4 details the synthesis of a diethylenetriamine (DETA) functionalized ligand. The bis-*N*-[1-(4,4-dimiethyl-2,6-dioxocyclohexylidene)ethyl] (DDE) derivative could be converted to diazeniumdiolate via standard diazeniumdiolate formation conditions and protected utilizing previously reported strategies.[51, 52] The final step would require deprotection of the DDE protecting group with

2% hydrazine in DMF to yield the O^2-protected DETA/NO ligand for coupling with the carboxyl-terminated dendrimers.

5.5.2 pH sensitive acetals

Macromolecular drug formulations containing pH sensitive triggers have shown increased cellular delivery of doxorubicin and other anti-cancer therapeutics.[54-56] These carriers make use of the pH gradient of the endocytic pathway that begins with the physiological pH of the cell surface (e.g., pH 7.2-7.4), drops to a lower pH (5.5-6.0) within the endosomes, and approaches a relatively acidic pH in the lysosomal compartments (~5.0).[57] In the future, the chemistry of O^2-protected diazeniumdiolates may be expanded to provide triggered NO release chemistry utilizing the pH changes of intracellular components. Ideally, triggered on/off systems could be developed that turn the NO release "on" at or near endosomal pH and "off" at physiological pH.

Frechet and co-workers demonstrated that acetals are promising acid-sensitive linkages for conjugation to several alcohol functionalized therapeutics. They observed rapid hydrolysis and complete drug release at pH 5.0, while measuring minimal hydrolysis (10-20%) at pH 7.4.[58] The remarkable sensitivity of the alcohol protecting group to changes in pH makes this an attractive strategy for triggering NO release. Typically, the hydrolysis of acetal functionalized alcohols is first order relative to the concentration of hydronium ion (H_3O^+), making the expected rate of hydrolysis ten times faster with each unit of pH decrease.[59] Several acetal functionalities have also been utilized as O^2-protecting groups for diazeniumdiolate NO donors but have not been optimized for pH tunable NO-release.[51] The nucleophilic character of the terminal oxygen in the diazeniumdiolate zwitterion has allowed

its straightforward conversion to acetals. Initially reported by Saavedra et al., the methoxy methyl (MOM) protected diazeniumdiolate had a half life of >20 d at pH 7.4 and only 9 h in 1 M HCl.[52] Although this experiment required relatively harsh acidic conditions, it illustrates the stability of an NO donor at pH 7.4, but hydrolysis and NO release at a lower pH. Synthesis and testing of MOM-protected PYRRO/NO in our lab has confirmed these results (Figure 5.5). Current literature suggests that acetal-protected diazeniumdiolates are synthetically accessible. Potential variations of cyclic acetal structures are depicted in Figure 5.6. These protecting groups, commonly employed for alcohols, may confer a pH sensitive, triggered mechanism of NO release. Once an acceptable NO donor with the desired "on/off" pH behavior is obtained, this chemistry could be applied to dendrimer drug delivery vehicles through one of the previously described methods for O^2-protected diazeniumdiolate dendrimer modification.

5.6 Conclusion

The innovation to covalently attach NO to a dendrimer was a logical step in the evolution of diazeniumdiolate and nitrosothiol chemistry. Although previous small molecule NO donors have been optimized for desired NO-release kinetics, their therapeutic application falls short due to poor pharmacokinetics/biodistribution. Next generation NO-releasing dendrimers may overcome such issues and allow the use of NO as a therapeutic against a number of disease states previously unattainable with current techniques (e.g., cancer, ischemia/reperfusion injury). The preliminary data collected on some of the proposed future modifications to dendrimer scaffolds suggest that these chemistries are indeed feasible and may provide targeted, biocompatible drug delivery vehicles for NO.

Fluorescein isothiocyanate (FITC)

Rhodamine-B- isothiocyanate (RITC)
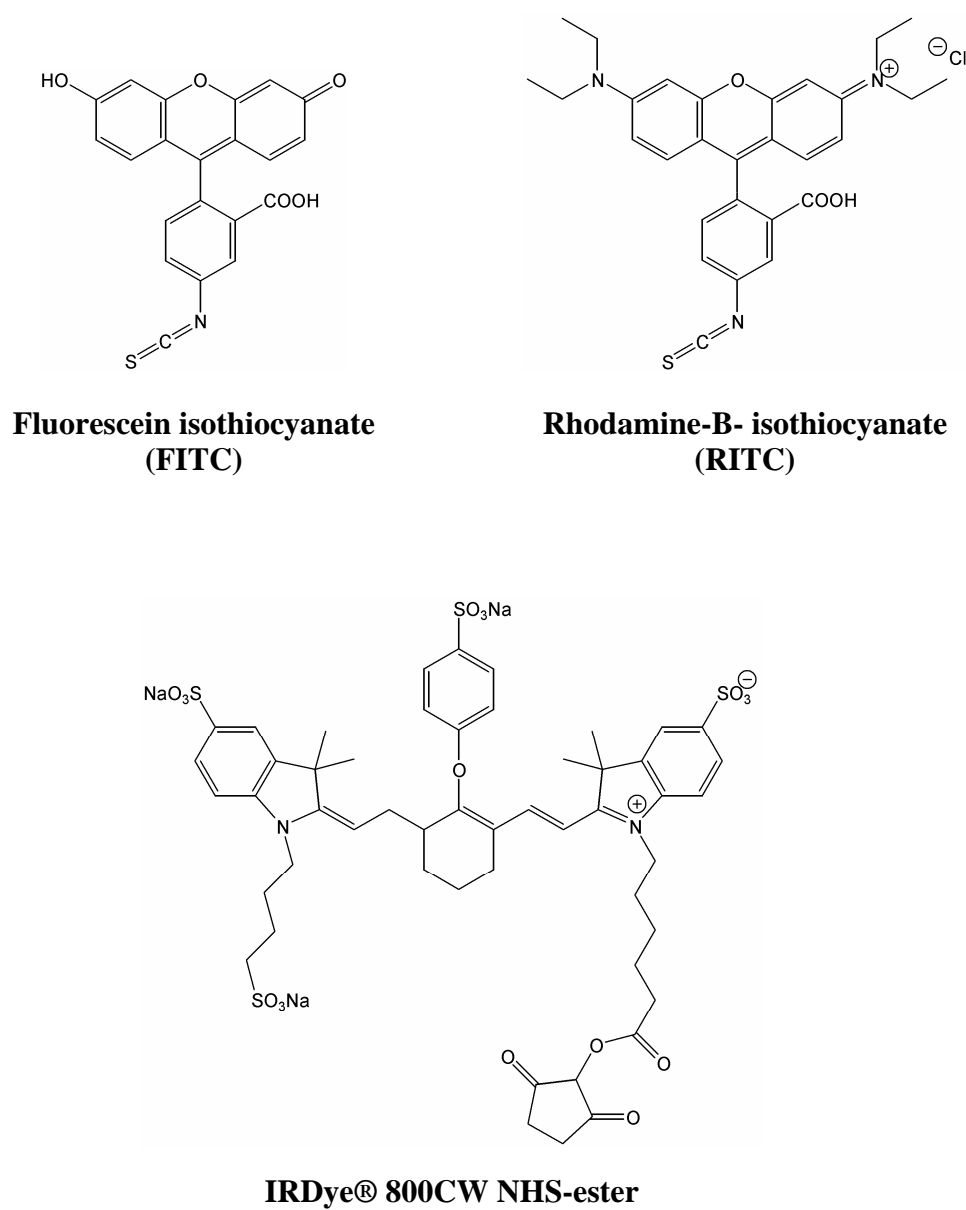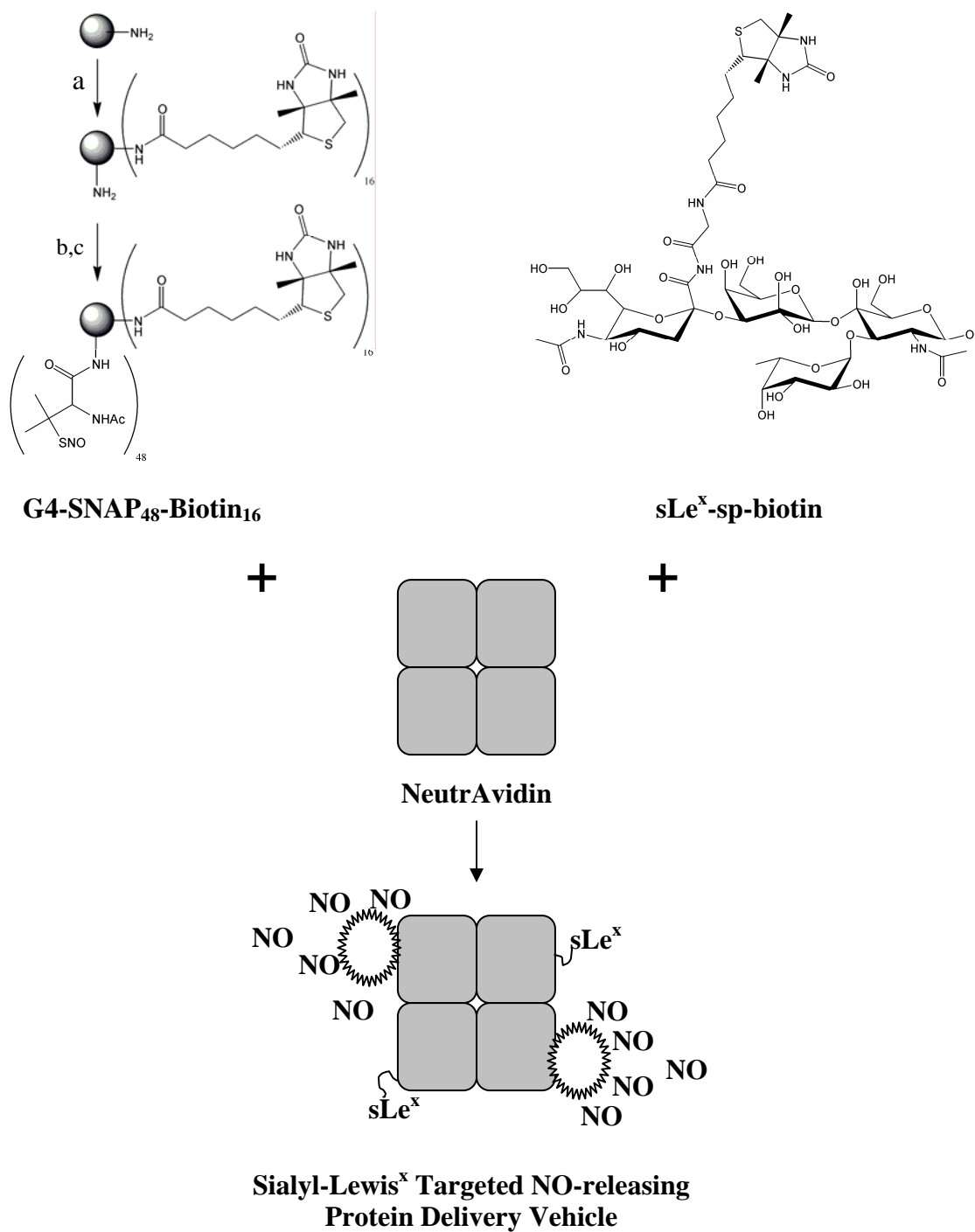
IRDye® 800CW NHS-ester

Figure 5.4   Molecular probes used for imaging G4-PAMAM conjugates with fluorescence and near-IR spectrocscopy.

G4-SNAP₄₈-Biotin₁₆

sLeˣ-sp-biotin

+

+

NeutrAvidin

**Sialyl-Lewisˣ Targeted NO-releasing
Protein Delivery Vehicle**

Scheme 5.2   Sialyl-Lewisˣ targeted NO-releasing protein delivery vehicle made from avidin conjugated G4-SNAP-Biotin and sLeˣ-sp-biotin. A) NHS-biotin, DMF; B) 3-acetamido-4,4-dimethylthietan-2-one, CH_2Cl_2; C) 1 M HCl, $NaNO_2$.

A

B
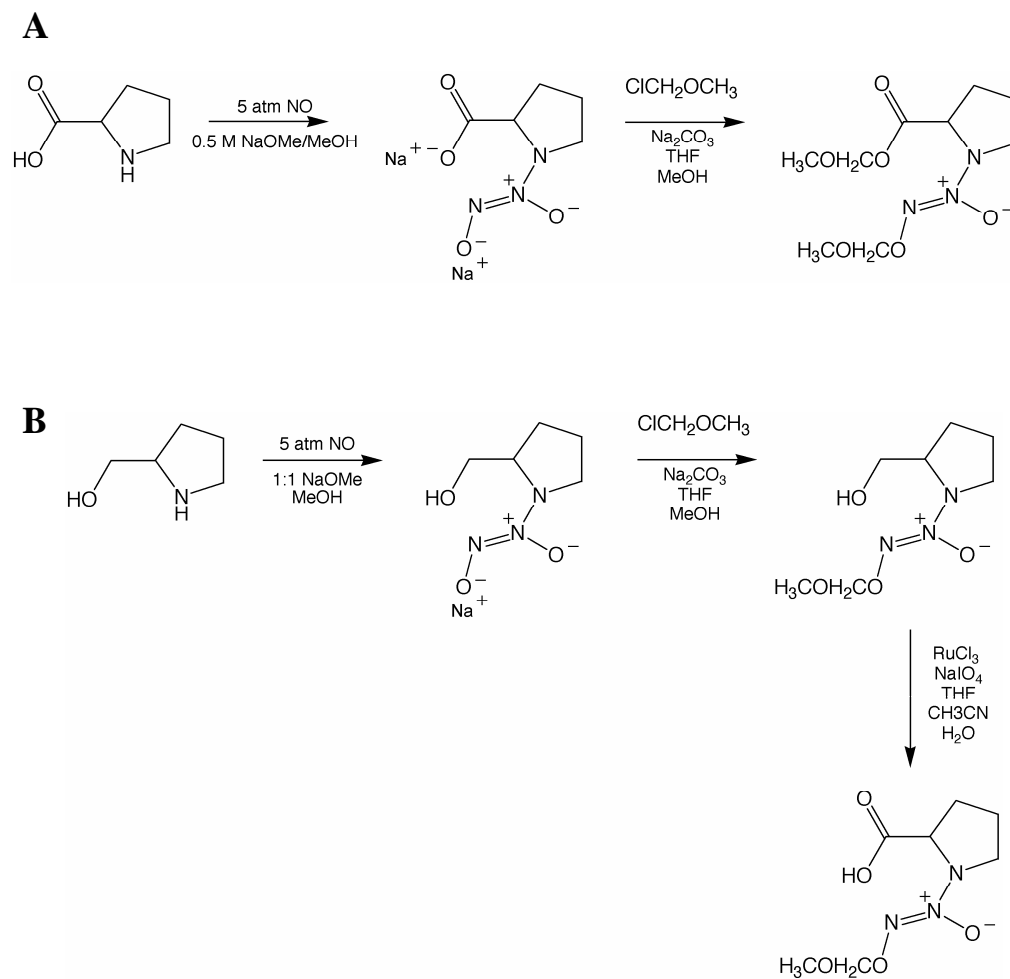
Scheme 5.3   A) Diazeniumdiolate formation of PROLI/NO and reaction with methoxymethyl chloride (MOM-Cl) to form the doubly protected MOM ether which eliminates the carboxylic acid functionality. B) Conversion of prolinol to the O^2-protected diazeniumdiolate which is oxidized up to the desired carboxylic acid residue for future coupling.
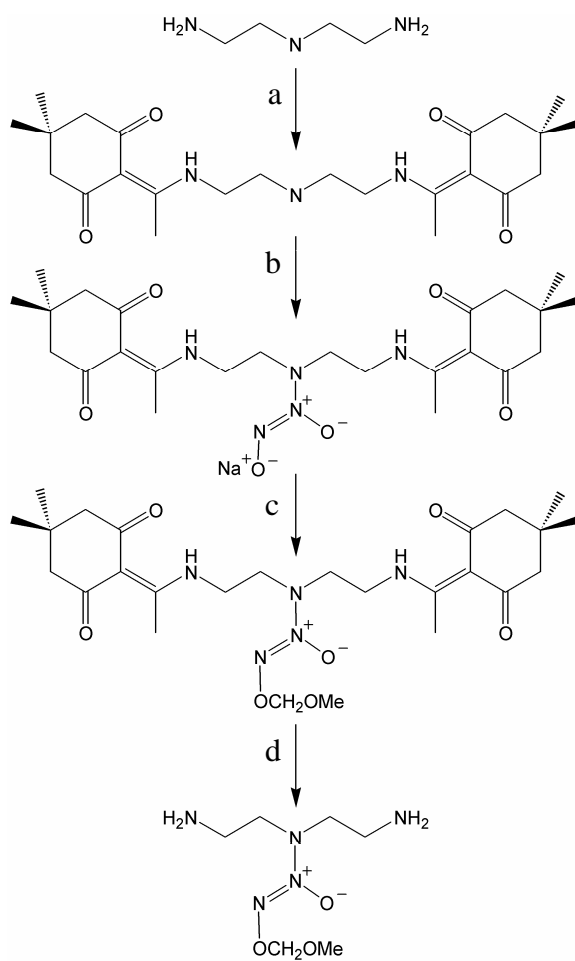
Scheme 5.4   Diazeniumdiolate modified polyamine ligand synthesis. A) 2-acetyldimedone, DMF; B) 0.1M NaOMe/MeOH, 5 atm NO; C) ClCH$_2$OMe, Na$_2$CO$_3$, THF; and d) 2% hydrazine in DMF.
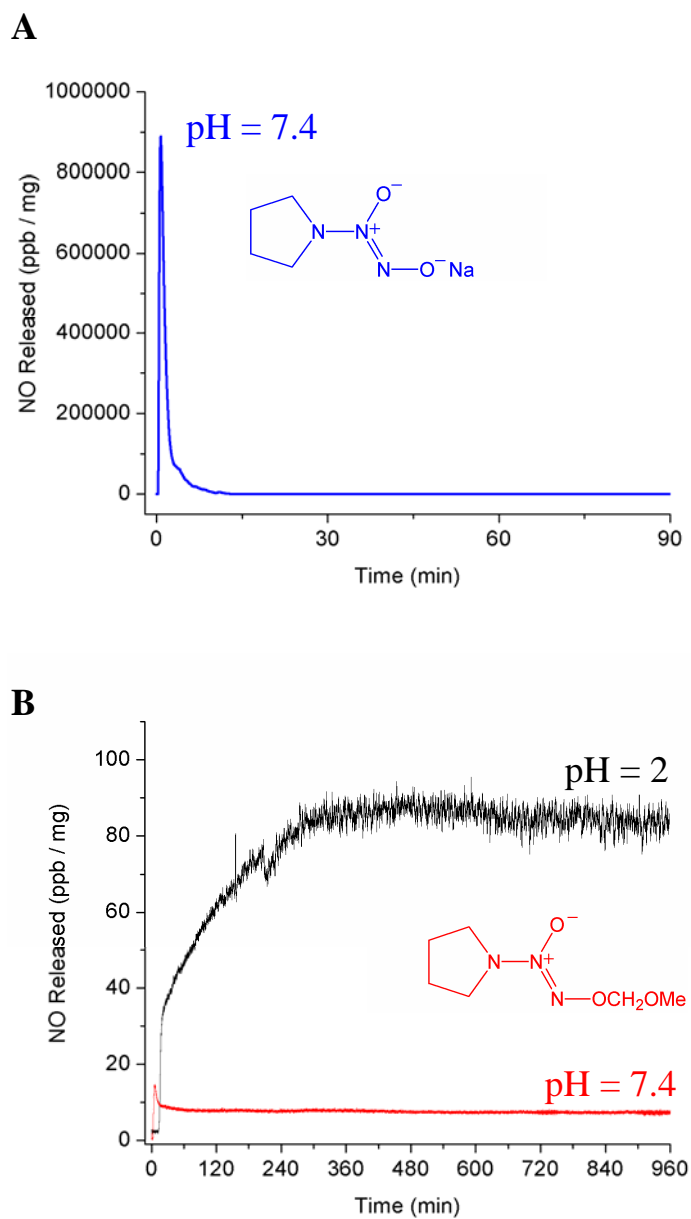
Figure 5.5   A) NO-release from PYRRO/NO at pH = 7.4. B) NO-release from O^2-MOM protected PYRRO/NO at pH = 2 and pH = 7.4.
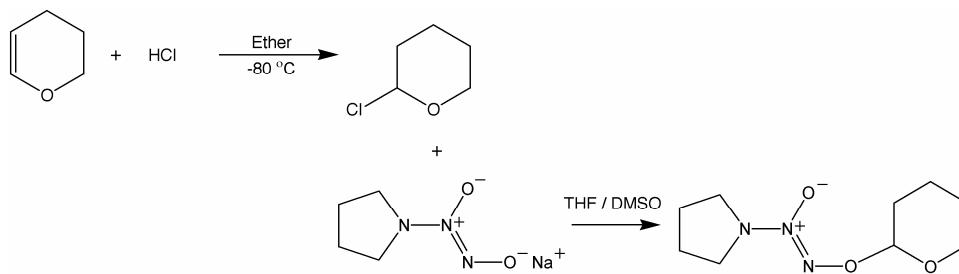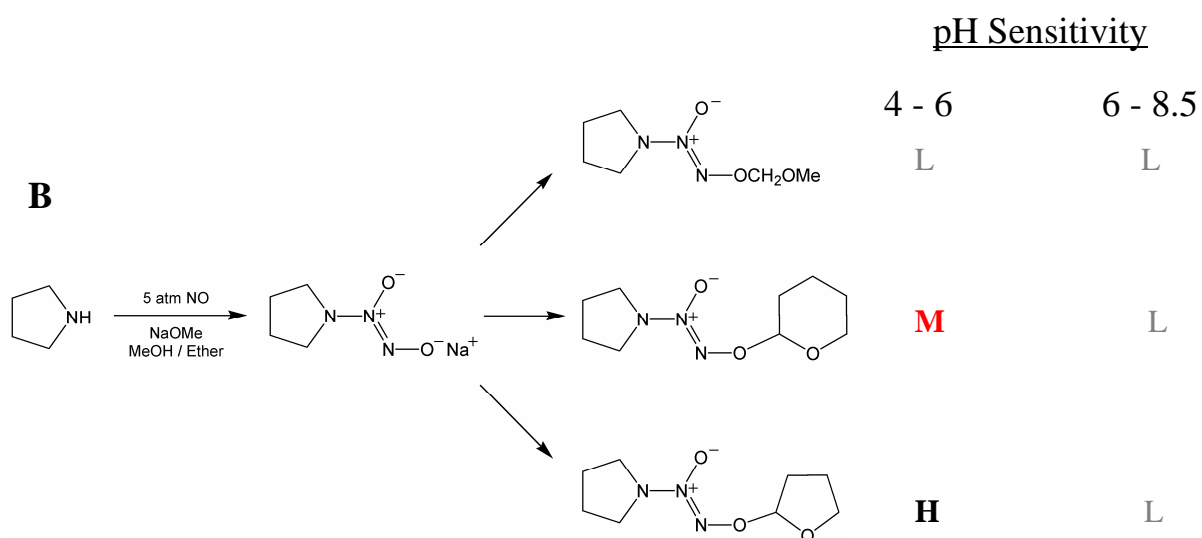
Figure 5.6   A) Synthesis of THP-protected PYRRO/NO from the halogenation of 2,3-dihydropyran to 2-chlorotetrahydropyran and reaction with PYRRO/NO diazeniumdioalte in THF/DMSO. B) The series of acetals proposed to study and their pH sensitivity as alcohol protecting groups. (H = high, M = medium, L = low)

5.7 References

1. Nablo, B. J.; Prichard, H. L.; Butler, R. D.; Klitzman, B.; Schoenfisch, M. H. "Inhibition of implant-associated infections via nitric oxide release." *Biomaterials* **2005,** *26*, 6984-6990.

2. Hetrick, E. M.; Prichard, H. L.; Klitzman, B.; Schoenfisch, M. H. "Reduced foregin body response at nitric oxide-releasing subcutaneous implants." *Biomaterials* **2007,** *28*, 4571-4580.

3. Frost, M. C.; Reynolds, M. M.; Meyerhoff, M. E. "Polymers incorporating nitric oxide-generating substances for improved biocompatibility of blood-contacting medical devices." *Biomaterials* **2005,** *26*, 1685-1693.

4. Reynolds, M. M.; Frost, M. C.; Meyerhoff, M. E. "Nitric oxide-releasing hydrophobic polymers: preparation, characterization, and potential biomedical applications." *Free Radical Biol. Med.* **2004,** *37*, 926-936.

5. Shekhter, A. B.; Serezhenkov, V. A.; Rudenko, T. G.; Pekshev, A. V.; Vanin, A. F. "Beneficial effect of gaseous nitric oxide on the healing of skin wounds." *Nitric Oxide* **2005,** *12*, 210-219.

6. Schwentker, A.; Vodovotz, Y.; Weller, R.; Billiar, T. R. "Nitric oxide and wound repair: role of cytokines?" *Nitric Oxide* **2002,** *7*, 1-10.

7. Luo, J.-d.; Chen, A. F. "Nitric oxide: a newly discovered function on wound healing." *Acta Pharmacologica Sinica* **2005,** *26*, 259-264.

8. Hofseth, L. J.; Hussain, S. P.; Wogan, G. N.; Harris, C. C. "Nitric oxide in cancer and chemoprevention." *Free Radical Biol. Med.* **2003,** *34*, 955-968.

9. Wink, D. A.; Mitchell, J. B. "Nitric oxide and cancer: an introduction." *Free Radical Biol. Med.* **2003,** *34*, 951-954.

10. Wink, D. A.; Vodovotz, Y.; Laval, J.; Laval, F.; Dewhirst, M. W.; Mitchell, J. B. "The multifaceted roles of nitric oxide in cancer." *Carcinogenesis* **1998,** *19*, 711-721.

11. Petit, J. F.; Nicaise, M.; Lepoivre, M.; Guissani, A.; Lemaire, G. "Protection by glutathione against the antiproliferative effects of nitric oxide. Dependence on kinetics of NO release." *Biochem. Pharmacol.* **1996,** *52*, 205-212.

12. Chopin, D. K.; Jaurand, M.-C.; Huguenin, S.; Vacherot, F.; Fleury-Feith, J.; Riffaud, J.-P.; Bolla, M. "Evaluation of the antitumoral potential of different nitric oxide-donating non-steroidal anti-inflammatory drugs (NO-NSAIDs) on human urological tumor cell lines." *Cancer Lett.* **2005,** *218*, 163-170.

13.   Mitchell, J. B.; Wink, D. A. "Nitric oxide and cancer: an introduction." *Free Radical Biol. Med.* **2003,** *34*, 951-954.

14.   Pervin, S.; Singh, R.; Chaudhuri, G. "Nitric oxide-induced cytostasis and cell cycle arrest of a human breast cancer cell line (MDA-MB-231): Potential role of cyclin D1." *Proc. Natl. Acad. Sci., U.S.A.* **2001,** *98*, 3583-3588.

15.   Waalkes, M. P.; Keefer, L. K.; Lui, J.; Saavedra, J. E. "Nitric oxide prodrugs and metallochemotherapeutics: JS-K and CB-3-100 enhance arsenic and cisplatin cytolethality by increasing cellular accumulation." *Mol. Cancer Ther.* **2004,** *3*, 709-714.

16.   Wang, P. G.; Braunschweiger, P. G. "Targeting nitric oxide to cancer cells: cytotoxicity studies of glyco-*S*-nitrosothiols." *Bioorg. Med. Chem. Lety.* **1999,** *9*, 2255-2258.

17.   Hanson, S. R.; Hutsell, T. C.; Keefer, L. K.; Mooradian, D. L.; Smith, D. J. "Nitric oxide donors: a continuing opportunity in drug design." *Adv. Pharmacol.* **1995,** *34*, 383-398.

18.   Wang, P. G.; Xian, M.; Tang, X.; Wu, X.; Wen, Z.; Cai, T.; Janczuk, A. J. "Nitric oxide donors: chemical activities and biological applications." *Chem. Rev.* **2002,** *102*, 1091-1134.

19.   Napoli, C.; Ignarro, L. J. "Nitric oxide-releasing drugs." *Ann. Rev. Pharmacol. Toxicol.* **2003,** *43*, 97-123.

20.   Mitra, A. K.; Duvvuri, S.; Majumdar, S. "Membrane transporter/receptor-targeted prodrug design: strategies for human and veterinary drug development." *Adv. Drug Delivery Rev.* **2004,** *56*, 1437-1452.

21.   Brannon-Peppas, L.; Blanchette, J. O. "Nanoparticle and targeted systems for cancer therapy." *Adv. Drug Delivery Rev.* **2004,** *56*, 1649-1659.

22.   Dinauer, N.; Balthasar, S.; Weber, C.; Kreuter, J.; Langer, K.; von Briesen, H. "Selective targeting of antibody-conjugated nanoparticles to leukemic cells and primary T-lymphocytes." *Biomaterials* **2005,** *26*, 5898-5906.

23.   Thomas, T. P.; Patri, A. K.; Myc, A.; Myaing, M. T.; Ye, J. Y.; Norris, T. B.; Baker, J. R. J. "In vitro targeting of synthesized antibody-conjugated dendrimer nanoparticles." *Biomacromolecules* **2004**.

24.   Wartlick, H.; Michaelis, K.; Balthasar, S.; Strebhardt, K.; Kreuter, J.; Langer, K. "Highly specific HER2-mediated dellular uptake of antibody-modified nanoparticles in tumour cells." *J. Drug Targeting* **2004,** *12*, 461-471.

25. Sudimack, J.; Lee, R. J. "Targeted drug delivery via the folate receptor." *Adv. Drug Delivery Rev.* **2000,** *41*, 147-162.

26. Lee, R. J.; Low, P. S. "Delivery of liposomes into cultured KB cells via folate receptor-mediated endocytosis." *J. Biol. Chem.* **1994,** *269*, 3198-3204.

27. Stella, B.; Arpicco, S.; Peracchia, M. T.; Desmaele, D.; Hoebeke, J.; Renoir, M.; D'Angelo, J.; Cattel, L.; Couvreur, P. "Design of folic acid-conjugated nanoparticles for drug targeting." *J. Pharm. Sci.* **2000,** *89*, 1452-1464.

28. Low, P. S. "Folate receptor-targeted drugs for cancer and inflammatory diseases." *Adv. Drug Delivery Rev.* **2004,** *56*, 1055-1058.

29. Parker, N.; Turk, M. J.; Westrick, E.; Lewis, J. D.; Low, P. S.; Leamon, C. P. "Folate receptor expression in carcinomas and normal tissues determined by a quantitative radio-ligand binding assay." *Anal. Biochem.* **2005,** *338*, 284-293.

30. Ni, S.; Stephenson, S. M.; Lee, R. J. "Folate receptor targeted delivery of liposomal daunorubicin into tumor cells." *Anticancer Res.* **2002,** *22*, 2131-2135.

31. Frechet, J. M. J.; Kono, K.; Liu, M. "Design of dendritic macromolecules containing folate or methotrexate residues." *Bioconjug. Chem.* **1999,** *10*, 115-1121.

32. Lu, Y.; Low, P. S. "Folate-mediated delivery of macromolecular anticancer therapeutic agents." *Adv. Drug Delivery Rev.* **2002,** *54*, 675-693.

33. Kukowska-Latallo, J. F.; Candido, K. A.; Cao, Z.; Nigavekar, S. S.; Majoros, I. J.; Thomas, T. P.; Balogh, L. P.; Khan, M.; Baker, J. R. "Nanoparticle targeting of anticancer drug improves therapeutic response in animal model of human epithelial cancer." *Cancer Res.* **2005,** *65*, 5317-5324.

34. Bolli, R.; Becker, L.; Gross, G.; Mentzer, R., Jr.; Balshaw, D.; Lathrop, D. A. "Myocardial protection at a crossroads: the need for translation into clinical therapy." *Circ. Res.* **2004,** *95*, 125-134.

35. Ignarro, L. J. "Nitric oxide: A unique endogenous signaling molecule in vascular biology." *Angew. Chem., Int. Ed.* **1999,** *38*, 1882-1892.

36. Schulz, R.; Kelm, M.; Heusch, G. "Nitric oxide in myocardial ischemia/reperfusion injury." *Cardiovasc. Res.* **2004,** *61*, 402-413.

37. Konorev, E. A.; Tarpey, M. M.; Joseph, J.; Baker, J. E.; Kalyanaraman, B. "S-nitrosoglutathione improves functional recovery in the isolated rat heart after cardioplegic ischemic arrest-evidence for a cardioprotective effect of nitric oxide." *J. Pharmacol. Exp. Ther.* **1995,** *274*, 200-206.

38. Bell, R. M.; Maddock, H. L.; Yellon, D. M. "The cardioprotective and mitochondrial depolarising properties of exogenous nitric oxide in mouse heart." *Cardiovasc. Res.* **2003,** *57*, 405-415.

39. Razavi, H. M.; Hamilton, J. A.; Feng, Q. "Modulation of apoptosis by nitric oxide: implications in myocardial ischemia and heart failure." *Pharmacol. Ther.* **2005,** *106*, 147-162.

40. Taite, L. J.; West, J. L. "Poly(ethylene glycol)-lysine dendrimers for targeted delivery of nitric oxide." *J. Biomater. Sci. Polymer Edn.* **2006,** *17*, 1159-1172.

41. Sakharov, D. V.; Jie, A. F. H.; Bekkers, M. E. A.; Emeis, J. J.; Rijken, D. C. "Polylysine as a vehicle for extracellular matrix-targeted local drug delivery, providing high accumulation and long-term retention within the vascular wall." *Arterioscler. Thromb. Vasc. Biol.* **2001,** *21*, 943-948.

42. Mitra, A.; Mulholland, J.; Nan, A.; McNeill, E.; Ghandehari, H.; Line, B. R. "Targeting tumor angiogenic vasculature using polymer-RGD conjugates." *J. Control. Release* **2005,** *102*, 191-201.

43. Dijkgraaf, I.; Rijnders, A. Y.; Soede, A.; Dechesne, A. C.; van Esse, G. W.; Brouwer, A. J.; Corstens, F. H. M.; Boerman, O. C.; Rijkers, D. T. S.; Liskamp, R. M. J. "Synthesis of DOTA-conjugated multivalent cyclic-RGD peptide dendrimers via 1,3-dipolar cycloaddition and their biological evaluation: implications for tumor targeting and tumor imaging purposes." *Org. Biomol. Chem.* **2007,** *5*, 935-944.

44. Palcic, M. M.; Li, H.; Zanini, D.; Bhella, R. S.; Roy, R. "Chemoenzymatic synthesis of dendritic sialyl Lewis^x." *Carbohydr. Res.* **1998,** *305*, 433-442.

45. Hanashima, S.; Castagner, B.; Esposito, D.; Nokami, T.; Seeberger, P. H. "Synthesis of a sialic acid a(2-3) galactose building block and its use in a linear synthesis of sialyl lewis X." *Org. Lett.* **2007,** *9*, 1777-1779.

46. Chervin, S. M.; Lowe, J. B.; Koreeda, M. "Synthesis and biological evaluation of a new sialyl lewis X mimetic derived from lactose." *J. Org. Chem.* **2002,** *67*, 5654-5662.

47. Hrabie, J. A.; Saavedra, J. E.; Roller, P. P.; Southan, G. J.; Keefer, L. K. "Conversion of proteins to diazeniumdiolate-based nitric oxide donors." *Bioconjug. Chem.* **1999,** *10*, 838-842.

48. Saavedra, J. E.; Booth, M. N.; Hrabie, J. A.; Davies, K. M.; Keefer, L. K. "Piperazine as a linker for incorporating the nitric oxide-releasing diazeniumdiolate group into other biomedically relevant functional molecules." *J. Org. Chem.* **1999,** *64*, 5124-5131.

49.   Chakrapani, H.; Showalter, B. M.; Kong, L.; Keefer, L. K.; Saavedra, J. E. "V-PROLI/NO, a prodrug of the nitric oxide donor, PROLI/NO." *Org. Lett.* **2007,** *9*, 3409-3412.

50.   Paulos, C. M.; Reddy, J. A.; Leamon, C. P.; Turk, M. J.; Low, P. S. "Ligand binding and kinetics of folate receptor recycling in vivo: impact on receptor-mediated drug delivery." *Mol. Pharmacol.* **2004,** *66*, 1406-1414.

51.   Hrabie, J. A.; Keefer, L. K. "Chemistry of the nitric oxide-releasing diazeniumdiolate functional group and its oxygen-substituted derivates." *Chem. Rev.* **2002,** *102*, 1135-1154.

52.   Saavedra, J. E.; Dunams, T. M.; Flippen-Anderson, J. L.; Keefer, L. K. "Secondary amine/nitric oxide complex ions, $R_2N[N(O)NO]^-$ O-functionalization chemistry." *J. Org. Chem.* **1992,** *57*, 6134-6138.

53.   Nash, I. A.; Bycroft, B. W.; Chan, W. C. "Dde - A selective primary amine protecting group: a facile solid phase synthetic approach to polyamine conjugates." *Tet. Lett.* **1996,** *37*, 2625-2628.

54.   Ulbrich, K.; Etrych, T.; Chytil, P.; Pechar, M.; Jelinkova, M.; Rihova, B. "Polymeric anticancer drugs with pH-controlled activation." *Int. J. Pharm.* **2004,** *277*, 63-72.

55.   Gillies, E. R.; Frechet, J. M. "Dendrimers and dendritic polymers in drug delivery." *Drug Discovery Today* **2005,** *10*, 35-43.

56.   Asokan, A.; Cho, M. J. "Exploitation of Intracellular pH Gradients in the cellular delivery of macromolecules." *J. Pharm. Sci.* **2002,** *91*, 903-913.

57.   Mellman, I.; Fuchs, R.; Helenius, A. "Acidification of the endocytic and exocytic pathways." *Ann. Rev. Biochem.* **1986,** *55*, 663-700.

58.   Gillies, E. R.; Goodwin, A. P.; Frechet, J. M. J. "Acetals as pH-Sensitive linkages for drug delivery." *Bioconjug. Chem.* **2004,** *15*, 1254-1263.

59.   Fife, T. H.; Jao, L. K. "Substituent effects in acetal hydrolysis." *J. Org. Chem.* **1965,** *30*, 1492-1495.